

CONTENTS

Foreword	iii
1. Introduction	1
1.1. Cosmic Rays	1
1.1.1. Discovery	1
1.1.2. Origin	2
1.2. Cosmic-Ray Nucleosynthesis	3
1.3. Importance of Lithium in the Big Bang Nucleosynthesis	3
1.4. Hadronic Gamma-Rays	4
1.5. ...And How It All Relates	5
2. Upper Limits to Diffuse Pionic Gamma Rays	8
2.1. Overview	8
2.2. Data	10
2.3. A Simple Model for Pionic Gamma-Rays	12
2.4. Procedure	14
2.5. Results	15
2.5.1. Galactic Spectrum	15
2.5.2. Extragalactic Spectrum	16
3. The Lithium–Gamma-Ray Connection	18
3.1. Overview	18
3.2. The Gamma-Ray – Lithium Connection: Formalism	19
3.3. Observational Inputs	23
3.3.1. The Observed Gamma-Ray Background and Limits to the Pionic Contribution	23
3.3.2. Lithium Abundances	24
3.4. ${}^6\text{Li}$ and Gamma-Rays From Galactic Cosmic Rays	25
3.4.1. Solar ${}^6\text{Li}$ and Gamma-rays	25
3.4.2. The Observed EGRB and Non-Primordial Lithium	28
3.5. ${}^6\text{Li}$ and Gamma-Rays From Cosmological Cosmic Rays	31
4. Is There a Solar ${}^6\text{Li}$ Problem?	34
4.1. Overview	34
4.2. Cosmic-Ray Spectrum	35
4.3. Pionic Gamma-ray Spectrum	36
4.4. Estimates of GCR-Produced ${}^6\text{Li}$	38
5. Diffuse TeV Gamma-Ray Observations	41
5.1. Overview	41

5.2. High-Energy Gamma-Ray Data	45
5.3. Analysis of the Data	47
5.3.1. Diffuse Components	47
5.3.2. Unresolved Sources	50
5.4. Implications and Observational Strategy.....	52
5.4.1. Point Source Spectral Break: Implications	53
5.4.2. “GeV Excess” Explained by Dark Matter?	53
5.4.3. Answering the Questions: Observations	53
5.5. TeV Excess: Possible Outcomes	56
6. Probing Primordial and pre-Galactic Lithium with High Velocity Clouds	59
6.1. Overview	59
6.2. High-Velocity Clouds.....	60
6.3. Lithium in HVC: Expectations	61
6.4. Lithium in HVC: Observability.....	62
7. Discussion	64
Appendices	67
A1. Notation and Normalization Conventions	67
A2. Cosmic Gamma-Radiation Transfer	68
A3. CNO Reaction Rates.....	70
References	72

FOREWORD

This book is an adaptation of the doctoral thesis titled "Probing and Raising the Lithium Problems with Hadronic Gamma Rays and Cosmic-Ray Nucleosynthesis", which was defended in June 2006 at the Department of Astronomy, University of Illinois at Urbana-Champaign (Urbana, USA). I have kept most of the original text, with the exception of the Introduction chapter which has been broadened to include a very brief introduction into cosmic rays and problematics and importance of lithium in the big bang nucleosynthesis. For a more detailed review, throughout the introduction I refer the reader to the key texts relevant for a certain topic. The purpose of this monography is to present a current state of affairs and some new, fresh approaches to solving and probing the *lithium problem(s)* whose resolution, in the light of precision cosmology, can potentially lead to a major turning point for modern day physics and cosmology. Though related to a very specific topic, most of the work and key ideas presented in this text are based on the fundamental physical principles, and it is my strong belief that the reader will find them quite straightforward. One can easily get lost in the details of some very complicated models, which, though important, can often obscure the view to the big picture and how all the pieces fit together. Thus, one of the key points that I will try to present to the reader throughout this text is how quite simple models if **used together**, can be very powerful tools in science.

I would like to thank my advisor, Brian Fields, for his guidance, and I am especially grateful for his support, patience, encouragement and understanding, not just in my work, but in my teaching and surviving the grad school in general. I am thankful for enlightening scientific discussions which enhanced the content of this dissertation with John F. Beacom, Rich Cyburt, Vasiliki Pavlidou and Charles Dermer. I am especially grateful to my friend and colleague Zarija Lukić for all scientific and not so scientific discussions we had, for his support during our undergrad and grad years, for looking after me and being there for me. I wish to extend special thanks to my family and my friends, Slobodan, Ivana and Vera Prodanović, Jelena Jokić, Mirjana Ninkov and Jelena Pilipović for their support, encouragement and not letting me quit, even if they all know that astrology is where the real money is.

Parts of this work were already published in refereed journals. This work was partially supported by the Ministry of Science within the project Nuclear Spectroscopy and Rare Processes No 141002B, and by the Provincial Secretariat for Science and Technological Development.

January 2007, Novi Sad, Serbia
Tijana Prodanović

Chapter 1

INTRODUCTION

1.1. COSMIC RAYS

Cosmic rays are energetic (most often relativistic - with energies larger than their masses) charged particles that originate in *astrophysical*, collisionless shocks (as opposed to e.g. planetary “bow shocks”). Mostly they are ionized nuclei, where about 90% of them are cosmic-ray protons, 9% are alpha particles and the rest are heavier nuclei.

The importance of cosmic rays is immediately evident when the energy density of CR protons in the interstellar medium $\epsilon_{\text{ISM}} \sim 0.83 \text{ eV/cm}^3$ is compared with the energy density of the average Galactic magnetic field ($B \sim 3 \mu\text{Gauss}$) $\epsilon_{\text{mag}} \sim 0.25 \text{ eV/cm}^3$ (Gaisser 1990). Thus it is obvious that cosmic rays are important source energy and pressure, as well as non-thermal radiation. They are important probes of acceleration sites – supernovae, as the most common and dominant acceleration site, but also more exotic ones as cosmological shocks that arise during the process of large-scale structure formation. Moreover, cosmic rays have been measured to have energies up to $\sim 10^{20} \text{ eV}$ (e.g. Fly’s Eye (Bird et al. 1994)) which provides us with a unique probe of physics beyond the reach of modern day accelerators. The origin of these ultra-high energy cosmic rays still remains a mystery.

1.1.1. DISCOVERY

The origin of cosmic-rays and their history has been a subject of intensifying interest for almost a century. The notion of cosmic radiation surfaced in 1912 when Victor Hess, in a series of balloon experiments, measured atmospheric ionization up to 5 km. His experiment revealed that somewhere above 1.5 km the flux of the ionizing radiation becomes greater than at the sea level (where it is due to natural radioactivity) and keeps increasing with height (Hess 1912). This discovery of “penetrating radiation” was the first evidence for an extraterrestrial source of ionizing radiation. However, the nature of cosmic rays (as they were named by Millikan in 1925), was not yet evident at the time since high-energy gamma rays were also speculated to be the sources of this ionizing radiation. The corpuscular nature of cosmic rays was discovered in 1929 in an experiment done by Bothe and Kolhörster where they measured the absorption coefficient of “penetrating radiation” which along with the use of coincidence technique allowed them to rule out high-energy gamma-rays (Bothe

and Kolhorster 1929). Nevertheless, the connection between cosmic rays and gamma rays turns out to be a deep one, which we will explore in detail later in this book. The work of Baade and Zwicky (1934) presented one of the first evidences for supernovae as the source of cosmic rays.

1.1.2. ORIGIN

Cosmic rays originate from collisionless shocks (mean free path between collisions of particles is much larger than the width of the shock), where the presence of at least a weak magnetic field is crucial. The standard acceleration mechanism through which bulk of cosmic rays gain their energy is known as the (first order) Fermi acceleration mechanism, or diffusive shock acceleration. There, we have a plane shock front coming into unshocked gas and leaving behind shocked gas. Particles in the unshocked gas, once they enter the shock, start diffusing by scattering off the irregularities in the magnetic field. This scattering can lead them back to the unshocked region, where soon enough a shock front will pass and thus you get a situation where particles of gas go back and forth across the shock front. With each crossing of the shock front, a particle gains some fixed energy which basically depends on the strength of the shock. This way of gaining the energy in steps naturally produces a power-law cosmic-ray spectrum which is what is observed (for a detailed review of cosmic-ray acceleration we refer the reader to Gaisser (1990)). For instance, cosmic-ray spectrum, in a strong shock limit, is $\propto E^{-2}$. Of course, the longer the shock lasts, the more crossing can occur, and thus the more energy a particle can gain. However, at some point, for a given magnetic field B , a particle will have sufficient total momentum p to stop diffusing, that is, a particle will stop responding to magnetic field irregularities that are smaller than Larmor radius of the particle $r_L = pc/(ZqB)$, where q is the particle charge. Thus, maximum energy that a particle can be accelerated to will be higher for a longer lasting shocks, and stronger magnetic fields.

Bottom line is that any site where shocks are produced (with magnetic field present) is the place where cosmic rays are accelerated. But what in the universe is a common enough occurrence, with enough power to produce such energetic cosmic rays with such fluxes that we observe? The first obvious answer to this question are *supernovae remnants*. Supernova explosions produce strong shocks, that are long lived and have sufficient power (efficiency of only few percent is enough) to produce a cosmic ray population that we call *galactic cosmic rays* and observe¹ up to energies ~ 100 TeV.

As mentioned at the beginning of this Chapter, even more energetic cosmic rays are observed (up to energies $\sim 10^{20}$ eV), though their origin is most likely extragalactic, the exact mechanism and source(s) are not yet known, and will thus not be further discussed in this text.

Beside the well known galactic cosmic-ray population, recently a lot of attention has been given to a cosmological component of cosmic rays. This as-yet putative cosmic-ray population would originate in shocks (Miniati et al. 2000, Keshet et al. 2003, Ryu et al. 2003) associated with baryonic infall and merger events during the growth

¹Note that the observed cosmic-ray spectrum is somewhat steeper $\propto E^{-2.7}$ due to cosmic-ray propagation through galaxy where the more energetic cosmic-rays are, the more of them escape the galactic magnetic field and the spectrum steepens.

of large-scale cosmic structures. Diffusive shock acceleration (e.g. Blasi 2004, Kang et al. 2002, Jones and Ellison 1991, Furlanetto and Loeb 2004) would then generate a population of relativistic ions and electrons, that would basically fill the universe, unlike the standard galactic cosmic rays, which are mostly "random-walking" through galaxies. The existence of this structure-formation cosmic-ray population would have important implication and will thus be further explored in this text.

1.2. COSMIC-RAY NUCLEOSYNTHESIS

Cosmic rays play a crucial role in the synthesis of light elements - lithium, beryllium and boron (LiBeB). In the famous paper by Burbidge, Burbidge, Fowler and Hoyle (1957), the origin of LiBeB synthesis was described as "the x -process", since there was no known site for production of these light elements that could explain their observed stellar abundances at that time. Eventually it was shown (Reeves et al. 1970) that Galactic cosmic ray (GCR) interactions with the interstellar medium (ISM) can successfully explain the observed LiBeB abundances.

LiBeB nuclei encode the history of cosmic ray exposure in local matter. In the past 15 years or so, measurements of LiBeB in the Sun and in Galactic disk have been joined by LiBeB observations in halo stars; these offer particularly valuable information about cosmic-ray origins and interactions in Galactic and proto-Galactic matter. In particular, different scenarios for cosmic ray origin lead to different LiBeB trends, which have been modeled and compared with observations (see, e.g. Vangioni-Flam and Cassé (2001), Fields and Olive (1999a), Ramaty et al. (2000), and references therein). For the purposes of this work, the details of these models are less important than the following basic distinction: *all* LiBeB species are produced as cosmic rays interact with interstellar gas and fragment—"spall"—heavy nuclei, e.g. $p + O \rightarrow {}^9\text{Be}$. However, the fusion processes $\alpha + \alpha \rightarrow {}^6,7\text{Li}$ yield lithium isotopes exclusively, and indeed dominate the cosmic-ray production of Li (Steigman and Walker 1992, Montmerle 1977c). This makes cosmic-ray lithium production particularly "clean" since its evolution depends uniquely on its exposure to cosmic rays, and unlike Be and B, does *not* depend on the ambient heavy element abundances.

However, the story is more complex for ${}^{11}\text{B}$, which can also be produced in core-collapse supernovae by the "neutrino process" (e.g. Woosley et al. 1990, Yoshida et al. 2004). Finally, ${}^7\text{Li}$ has the most diverse lineage, to which we now turn.

1.3. IMPORTANCE OF LITHIUM IN THE BIG BANG NUCLEOSYNTHESIS

Standard big bang nucleosynthesis (BBN) theory relies essentially on only one parameter, the baryon-to-photon ratio, to predict H, D, ${}^3\text{He}$, ${}^4\text{He}$ and ${}^7\text{Li}$ primordial abundances. The concordance between predictions and observations of these elements has been the key to success of the BBN theory (for a review of the BBN theory and comparison with observations we refer the reader to the classic paper by Olive et al. (2000)) and a powerful tool for determining the baryon density of the universe, Ω_b . Although all LiBeB species are produced in the big bang nucleosynthesis only ${}^7\text{Li}$ has

primordial abundance that is not negligible compared its GCR nucleosynthesis. In the early Galaxy, and hence in halo stars, ${}^7\text{Li}$ is dominated by the contribution from primordial nucleosynthesis (e.g. Cyburt et al. 2003b, and references therein), with a small contribution from cosmic-ray fusion as well as the neutrino process (Ryan et al. 2000). Moreover, observations of Li in low-metallicity stars show flatness with respect to the metallicity (“Spite plateau”; Spite and Spite 1982), indicating that such observed pre-Galactic ${}^7\text{Li}$ abundance is apparently the primordial.

However, recent determination of the Ω_b with high precision made by the *WMAP* (Spergel et al. 2003), resulted in a primordial ${}^7\text{Li}$ abundance predicted by the BBN theory, which is now substantially higher (at least a factor of ~ 2) than the plateau ${}^7\text{Li}$ abundance inferred from halo stars (Cyburt et al. 2003b). This represents a serious discrepancy which we will be referring to as “*the ${}^7\text{Li}$ problem*”. In this era of precision cosmology brought to us by *WMAP* measurements, any such discrepancy between theory and observations may be a potential indicator of a new physics that is beyond the standard BBN model. But before such major claims can be made, a more conventional potential causes, such as observational or nuclear input systematics, have to be explored. This was the main motivation behind the research presented in this text, where the goal was to present a fresh approach to testing the origin of both lithium isotopes.

1.4. HADRONIC GAMMA-RAYS

Cosmic-ray interactions with interstellar gas produce not only LiBeB, but also inevitably produce γ -rays. Cosmic rays in the Galactic disk today lead to pronounced emission seen in the Galactic plane (Hunter et al. 1997). Thus, cosmic ray populations in (and between!) external galaxies contribute to a diffuse extragalactic γ -ray background (hereafter the EGRB). The existence of an EGRB was already claimed by some of the first γ -ray observations (Fichtel et al. 1973). The most recent high-energy (i.e. roughly in the 30 MeV – 30 GeV range) γ -ray observations are those of the EGRET experiment on the Compton Gamma-Ray Observatory, and the EGRET team also found evidence for a EGRB (Sreekumar et al. 1998). The intensity, energy spectrum, and even the existence of an EGRB are not trivial to measure, as this information only arises as the residual after subtracting the dominant Galactic foreground from the observed γ -ray sky. The procedure for foreground subtraction is thus crucial, and different procedures starting with the same EGRET data have arrived at an EGRB with a lower intensity and different spectrum (Strong et al. 2004b), or have even failed to find evidence for an EGRB at all (Keshet et al. 2004). Despite these uncertainties, we will see that the EGRB (or limits to it) and Li abundances are mutually very constraining.

Whether or not an EGRB has yet been detected, at some level it certainly should exist. EGRET detections of individual active galactic nuclei (blazars) as well as the Milky Way and the LMC together guarantee that unresolved blazars (e.g. Stecker and Salamon 1996, Mukherjee and Chiang 1999), and to a lesser extent normal galaxies (Pavlidou and Fields 2002), will generate a signal at or near the levels claimed for the EGRB. Many other EGRB sources have been proposed, but one of the promising has

been a subject of intense interest recently: namely, γ -rays originating from structure-formation cosmic rays. Gamma-ray emission would follow from inverse Compton scattering of these cosmological electrons off of the ambient photon backgrounds and from decay of π^0 produced in hadronic collisions ($pp \rightarrow pp\pi^0 \rightarrow \gamma\gamma$; Loeb and Waxman 2000). The most recent semi-analytical and numerical calculations (Gabici and Blasi 2003b, Miniati 2002) suggest that this “structure forming” component to the EGRB is likely below the blazar contribution, but the observational and theoretical uncertainties here remain large; upcoming γ -ray observations by GLAST (Gehrels and Michelson 1999) will shed welcome new light on this problem.

Studies of structure formation cosmic rays (hereafter SFGRs) have focused primarily on their γ -ray signatures. However, recently Suzuki and Inoue (2002) also proposed using ${}^6\text{Li}$ as a diagnostic of shock activity in the Local Group. These authors note that the resulting ${}^6\text{Li}$ abundances in halo stars could be used to probe the shocks and resulting cosmic rays in proto-Galactic matter. We also will draw on this idea, with an emphasis on the fact that pre-Galactic Li production would be (by itself) difficult to distinguish observationally from the primordial ${}^7\text{Li}$ production from big bang nucleosynthesis. Cosmic rays created during cosmic structure formation would lead to pre-Galactic Li production, which would act as a “contaminant” to the primordial ${}^7\text{Li}$ content of metal-poor halo stars. Given the already existing problem of establishing the concordance between ${}^7\text{Li}$ observed in halo stars and primordial ${}^7\text{Li}$ as predicted by the *WMAP*, it is crucial to set limits to the level of “contamination” by the SFGR population.

Cosmic-ray interactions provide the *only* known source for the nucleosynthesis of ${}^6\text{Li}$, ${}^9\text{Be}$, and ${}^{10}\text{B}$, making these species ideal observables of cosmic ray activity.² For more than a decade, a large body of work has focused on the light elements Li, Be, and B (LiBeB) as signatures of cosmic-ray interactions with the diffuse gas (for a recent review see Cassé et al. 2001). LiBeB abundances in Galactic halo stars have been used to probe the history of cosmic rays in the (proto-)Galaxy, where the isotope ${}^6\text{Li}$ is a particularly powerful probe of *any* cosmic-ray population, since unlike Be and B, it does *not* depend on the ambient heavy element abundances. More recently, a great deal of attention has been focused on high-energy γ -rays also produced in interactions during cosmic-ray propagation. Here, we draw attention to the tight connection between these observables, particularly between γ -rays and ${}^6\text{Li}$.

1.5. ...AND HOW IT ALL RELATES

The link between the nucleosynthesis and γ -ray signatures of cosmic-ray history has been pointed out by others in multiple contexts. We note in particular the prescient work of Montmerle (1977a,b,c), who in a series of papers considered the implications of a hypothetical population of “cosmological cosmic rays” in addition to the usual Galactic cosmic rays. Montmerle’s analysis is impressive in its foresight and

²In fact, a pre-Galactic component of ${}^6\text{Li}$ can be produced in some scenarios in which dark matter decays via hadronic (Dimopoulos et al. 1988) or electromagnetic (Jedamzik 2000, Kawasaki et al. 2001, Cyburt et al. 2003a) channels. Such scenarios are constrained via their effects on the other light elements, but some level of ${}^6\text{Li}$ production is hard to rule out completely.

its breadth. Montmerle (1977a) develops the formalism for a homogeneous population of cosmological cosmic rays (assumed to be created instantaneously at some redshift), and describes their propagation in an expanding universe, as well as their light-element and γ -ray production. He identifies the tight connection between ${}^6\text{Li}$ and extragalactic γ -rays, and exploits this connection to use the available EGRB data to constrain Li production for a variety of different assumptions. A particularly pertinent case involves an EGRB near the levels discussed today (“normalization 2” in Montmerle’s parlance), coupled with a cosmic baryon density close to modern values (e.g. Spergel et al. 2003, Cyburt et al. 2003b). Under these conditions, Montmerle (1977b) finds that cosmological cosmic-ray activity at a level sufficient to explain the EGRB also leads to a present ${}^6\text{Li}$ abundance that is about an order of magnitude smaller than the solar abundance. This result foreshadows an important conclusion we will find: if the solar ${}^6\text{Li}$ abundance is produced by Galactic cosmic rays, then the associated pionic γ -ray production exceeds the *entire* EGRB by about a factor of 2.

Our work thus follows these pioneering efforts, further emphasizing and formally exploring the intimate connection between cosmic-ray nucleosynthesis and high-energy γ -ray astrophysics. We will build on the work of Suzuki and Inoue (2002) to point out the possible importance of another, *pre-Galactic*, source of cosmic-ray ${}^7\text{Li}$ and ${}^6\text{Li}$, which could confound attempts to identify the pre-Galactic Li abundance with the primordial component. We cannot rule out (or in!) this possible source, but we will constrain it using observations of γ -rays (Fields and Prodanović 2005). Moreover, we apply the Li–gamma-ray connection to test the standard assumption that the solar ${}^6\text{Li}$ abundance originates from interactions of galactic cosmic rays (hereafter GCRs) with the interstellar medium (hereafter ISM). However, this gave rise to an alarming result that although under extreme assumptions, the pionic γ -ray intensity that accompanies GCR production of the solar ${}^6\text{Li}$ will not saturate the observed EGRB, when implementing more realistic ones the observed EGRB allows for only $\approx 60\%$ of the solar ${}^6\text{Li}$ abundance to be produced by standard GCRs. Thus, our result represents a strong hint for the need of a new ${}^6\text{Li}$ source. We will be referring to this as “*the ${}^6\text{Li}$ problem*”. Recent suggestions such as dark matter and low-energy cosmic rays are discussed. Upcoming gamma-ray observations by *GLAST* (Gehrels and Michelson 1999) will better constrain (or determine!) the pionic γ -ray fraction of the EGRB and will thus be the key in determining the severity of this problem.

Because the uncertainties in gamma-ray observations are still large to resolve these lithium problems, we also propose additional observational tests: 1) observations of lithium in low-metallicity high-velocity clouds could provide an independent test of the severity of the ${}^7\text{Li}$ problem as well as test the potential exposure to this cosmological cosmic-ray population; 2) we demonstrate how observations of the diffuse Galactic Plane gamma-ray emission over a wide energy range GeV–TeV–PeV could be used to disentangle the hadronic from the electron component of the gamma-ray observations, which would eliminate one uncertainty in the Li–gamma-ray connection and constrain the potential ${}^6\text{Li}$ problem.

This book is organized as follows: in Chapter 2 we (Prodanović and Fields 2004a) demonstrate a model-independent way of constraining the pionic component of the diffuse Galactic Plane gamma-ray emission as well as the pionic component of the

EGRB where those pionic gamma-rays would originate from SFCR interactions; in Chapter 3 (Fields and Prodanović 2005) we formally show and discuss the generality and tightness of the ${}^6\text{Li}$ - γ connection and use it to constrain the SFCR contribution to pre-Galactic ${}^7\text{Li}$ production and to test the allowed ${}^6\text{Li}$ production with GCR fusion reaction with the ISM where the standard single power-law cosmic-ray spectrum was assumed; in Chapter 4 (Prodanović and Fields 2006) we refine our analysis by employing a carefully propagated cosmic-ray spectrum, and also estimating the spallation ($p, \alpha + \text{CNO} \rightarrow {}^6\text{Li}$) contribution to the solar ${}^6\text{Li}$ abundance; in Chapter 5 (Prodanović et al. 2007) we demonstrate how GeV–TeV–PeV gamma-ray observations can be used to determine the Galactic pionic gamma-ray component and thus eliminate one uncertainty that is relevant for determining the potential ${}^6\text{Li}$ problem; in Chapter 6 (Prodanović and Fields 2004b) we identify a new site for measuring the pre-Galactic lithium production and testing the ${}^7\text{Li}$ problem as well as the SFCR population. Finally, our results are discussed in Chapter 7.

Chapter 2

UPPER LIMITS TO DIFFUSE PIONIC GAMMA RAYS

2.1. OVERVIEW

The prominence of diffuse emission in the γ -ray sky above $\gtrsim 50$ MeV has been known since the earliest days of γ -ray astronomy itself (Fichtel et al. 1973). These diffuse photons carry unique and direct information about some of the most energetic sites and processes in nature. Diffuse γ -ray observations thus provide a powerful tool both (1) to test specific models of known or postulated astrophysical sources, and (2) to constrain, in a model-independent way, known physical processes which might occur in one or more sources. In this Chapter³ we take the latter approach, focusing in particular on the γ -ray spectrum and the constraints it places on the contribution of hadronic interactions to the overall diffuse background.

The diffuse γ -ray sky is dominated by emission from the Galactic plane (Hunter et al. 1997), but the presence of emission even at the Galactic poles already suggests that an extragalactic component is present as well Sreekumar et al. (1998). The spectra of these two components are each remarkable both for what they show and what they do not show. Namely, in neither spectrum is there a strong indication of hadronic interactions, which are dominated by proton collisions with interstellar matter, which yield γ -rays predominantly through pion production and decay: $pp \rightarrow pp\pi^0 \rightarrow \gamma\gamma$. The pionic spectrum is symmetric about a peak at $m_\pi/2$. This feature, the “pion bump,” is notably inconspicuous in the γ -ray data.

As we will see in detail below, the Galactic spectrum is well-described by a simple broken power law, with a break at ~ 0.77 GeV. No strong pion bump is observed. Hunter et al. (1997) do note that there is as a $\sim 2\sigma$ deviation in the 60 – 70 MeV energy bin, but this region in the spectrum is otherwise well-fit by a smooth power law. If real, this feature is remarkably narrow. Intriguingly, detailed models of known Galactic processes run into difficulties explaining this spectrum (and its simplicity). The model of Strong et al. (2000) includes a sophisticated 2-D model of the cosmic-ray, gas, and photon fields in the Galaxy, and includes hadronic interactions, electron bremsstrahlung and inverse Compton scattering of starlight. However, when using only known cosmic ray populations and spectra, this model is unable to account for

³Parts of this were already published in a refereed journal (Prodanović and Fields 2004a)

the observed γ -ray spectrum. The spectrum above about 1 GeV is flatter than the prediction of pionic emission, so other sources seem to be required as well. Proposed explanations for this “GeV excess” include modifications to the proton spectrum, and additional inverse Compton radiation due to an extended halo of cosmic ray electrons (Strong et al. 2000). The main goals of this Chapter is to quantify the portion that can be pionic.

Information about the extragalactic component of diffuse γ -rays is more difficult to obtain, as one must first subtract the Galactic foreground, which is large at low– and possibly even high–Galactic latitudes. As we will see, the nature of the extragalactic spectrum depends on the method used to subtract the Galactic foreground. Different techniques have recently emerged, leading to different results for the shape and amplitude of the spectrum. Sreekumar et al. (1998) find a single power-law, while Strong et al. (2003) find a smaller but “convex” spectrum. In either case, no pion bump is seen.

Many astrophysical sites have been proposed to explain the extragalactic emission. These necessarily include “guaranteed” sources, namely, active (Stecker and Salamon 1996, Mukherjee and Chiang 1999) and normal (Pavlidou and Fields 2002) galaxies. These are the classes of objects which have been directly detected in nearby objects, but which would be unresolved when at large distances. These sources certainly contribute to (and possibly dominate) the diffuse γ -ray sky, and thus must be removed from any extragalactic signal before any additional sources can be identified.

Indeed, many other sources have been proposed to contribute to (and possibly dominate) the extragalactic γ -ray sky. Chief among these are γ -rays produced in the formation of large scale structures. There is a growing consensus that structure formation leads to shocks in the baryonic gas (Miniati et al. 2000, Keshet et al. 2003, Totani and Inoue 2002, Furlanetto and Loeb 2004, Gabici and Blasi 2003a), and thus to particle acceleration (Miniati 2002, Berrington and Dermer 2003, Kang and Jones 2002, Ryu et al. 2003, Gabici and Blasi 2003b). The resulting “cosmological cosmic rays” have recently become the subject of intense interest, and the initial estimates of Loeb and Waxman (2000) suggested that the inverse Compton radiation from the relativistic electron component would be sufficient to explain the entire diffuse γ -ray background. Later work showed (Gabici and Blasi 2003b, Berrington and Dermer 2003, Miniati 2002) that the structure formation contribution is likely smaller, of order $\sim 10\%$ of the (Sreekumar) background.⁴ Nevertheless, determining the nature of the γ -ray signature of SFCRs remains as a key observational and theoretical goal.

In this Chapter we will place model-independent constraints on hadronic and thus pionic emission mechanisms, as shown in Prodanović and Fields (2004a). We focus on this component because it is the key ingredient that we will use in Chapter 3 in order to constrain the cosmic-ray nucleosynthesis of Li. Moreover, detection of this component would finally confirm observationally the theoretical expectation that the same astrophysical acceleration processes which give rise to non-thermal electrons (and associated inverse Compton radiation) also give rise to non-thermal ions. We exploit the well-defined properties of the pion decay spectrum, that is, its symmetry

⁴Though it should be kept in mind that the true background level could well be smaller than the Sreekumar estimate, in which case the structure formation component could still be significant.

about $m_{\pi^0}/2$, to quantify the maximal pionic fraction of the observed γ -ray intensity. We (Prodanović and Fields 2004a) find that the Galactic spectrum above 30 MeV can be at most about 50% pionic. The maximum pionic contribution to the extragalactic spectrum is energy dependent; it also depends on the redshift range over which the sources are distributed, ranging from as low as about 20% for pions generated very recently, to as much as 90% if the pions are generated around redshift 10.

2.2. DATA

We will consider the Galactic and extragalactic emission in turn. For the Galactic spectrum, we adopt the EGRET data (Hunter et al. 1997) for the inner Galaxy ($300^\circ < \ell < 60^\circ$, $|b| \leq 10^\circ$). We find that the flux density can be well-fit by a broken power law, with index -1.52 below 0.77 GeV, and index -2.25 above:

$$I_{\text{obs}}(\epsilon) = \begin{cases} 4.66 \times 10^{-5} \epsilon_{\text{GeV}}^{-1.52} \text{ cm}^{-2} \text{ s}^{-1} \text{ sr}^{-1} \text{ GeV}^{-1} & \epsilon_{\text{GeV}} < 0.77 \\ 3.86 \times 10^{-5} \epsilon_{\text{GeV}}^{-2.25} \text{ cm}^{-2} \text{ s}^{-1} \text{ sr}^{-1} \text{ GeV}^{-1} & \epsilon_{\text{GeV}} > 0.77. \end{cases} \quad (2.1)$$

This simple fit somewhat overestimates the flux in the region within about ± 100 MeV of the break, but this region will not strongly affect our results.

Although diffuse emission from the Galactic plane dominates the γ -ray sky, the emission is nonzero even at the Galactic poles, which suggests that there *is* an extragalactic component. However, it is already clear that careful subtraction will be crucial in obtaining the extragalactic gamma-ray spectrum. Several schemes have been proposed for subtraction of the Galactic foreground. The basic approach of the EGRET team (Sreekumar et al. 1998) is to correlate the γ -ray sky with tracers of Galactic γ -ray sources. The dominant source is the hydrogen column, itself derived from observations of neutral H at 21 cm, H₂ as traced by CO, and H II as probed by pulsar dispersion studies. The interstellar photon field, which is up-scattered by inverse Compton processes, is also estimated. Sreekumar et al. (1998) find evidence for a statistically significant isotropic component, with flux $I(> 100 \text{ MeV}) = (1.45 \pm 0.05) \times 10^{-5} \text{ photons cm}^{-2} \text{ s}^{-1} \text{ sr}^{-1}$ and a spectrum consistent with a single power law of index 2.1 ± 0.03 :

$$I_{\text{obs}} = I_0 \left(\frac{E}{E_0} \right)^{-2.1 \pm 0.03} \quad (2.2)$$

where $E_0 = 0.451 \text{ GeV}$ and $I_0 = 7.32 \times 10^{-6} \text{ cm}^{-2} \text{ sr}^{-1} \text{ s}^{-1} \text{ GeV}^{-1}$.

Recently, Strong et al. (2003) have taken a different approach in subtracting the Galactic foreground, based on their sophisticated and detailed model of the spatial and energetic content of the Galaxy. They used the GALPROP model for cosmic ray propagation to predict the Galactic component and give the new estimate of the EGRB from EGRET data. Strong et al. (2003) also find evidence for an EGRB, but with a different spectral shape, and in general a lower amplitude than that of Sreekumar et al. (1998). The Strong et al. (2003) Galactic foreground estimates also includes the Strong et al. (2000) estimate of the pionic contribution. This model-based constraint will serve as an important consistency check of our model-independent

results. We used the least square method to fit their data with a cubic logarithmic function for the energy range 0.05-10 GeV:

$$\ln(I_{\text{obs}}E^2) = -13.9357 - 0.0327 \ln E + 0.1091(\ln E)^2 + 0.0101(\ln E)^3. \quad (2.3)$$

In this fit energy E is understood to be in the units of GeV and I in units of photons $\text{cm}^{-2} \text{s}^{-1} \text{sr}^{-1} \text{GeV}^{-1}$.

Indeed, the latest analysis of EGRET data done by Keshet et al. (2004) also implies that Galactic foreground was underestimated in previous work. They find that Galactic foreground in fact dominates the sky and that only an upper limit on the EGRB can be placed. However, Keshet et al. (2004) analysis did not contain spectral information which is why it could not be further investigated in this work, being that our procedure is based on the spectral shapes. The data used in this Chapter along with the fits are shown in Fig. 2.1 (Galactic component) and Fig. 2.2 (EGRB).

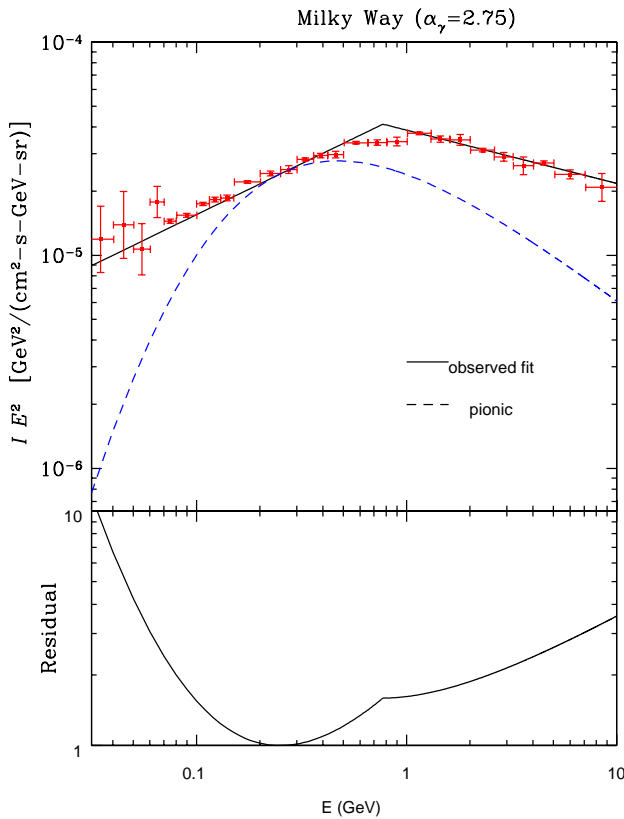


Figure 2.1: In this figure we present the maximal pionic contribution to the Galactic γ -ray spectrum. EGRET data points are taken from Hunter et al. (1997). The lower panels represent the residual, that is, $\log[(IE^2)_{\text{obs}}/(IE^2)_{\pi^0}] = \log(I_{\text{obs}}/I_{\pi^0})$. Note that the kink at 0.77 GeV is unphysical and just due to the overshooting of the simple broken power-law fit.

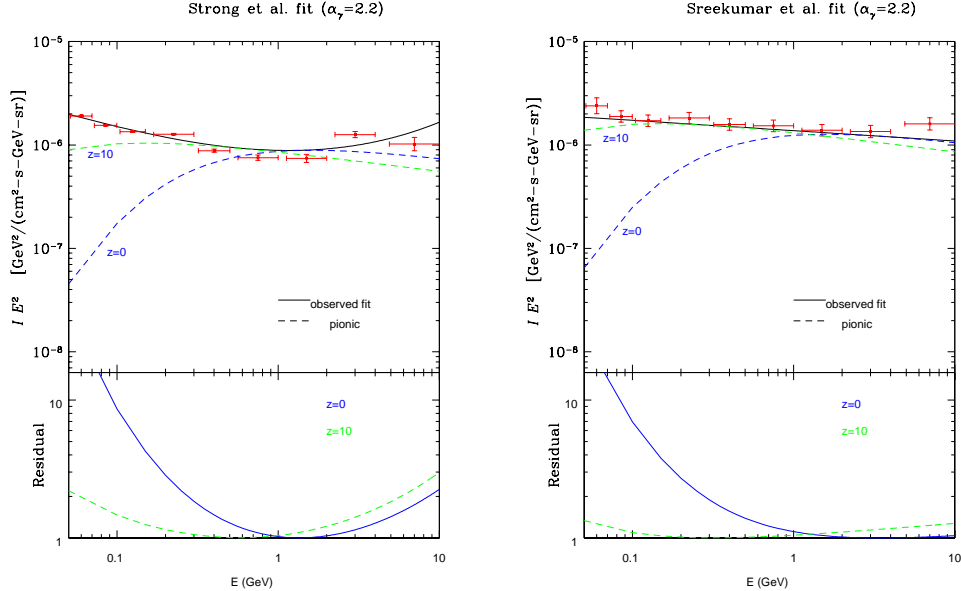


Figure 2.2: The maximal pionic contribution to the extragalactic γ -ray spectrum, computed by assuming that pionic γ -rays originated at a single redshift, namely at $z_* = 0$ and $z_* = 10$. EGRET data points for both fits taken from Strong et al. (2003). Lower panels represent the residual function as in Fig. 2.1.

2.3. A SIMPLE MODEL FOR PIONIC GAMMA-RAYS

The general expression for the γ -ray intensity spectrum at energy ϵ in a particular direction is given by the line-of-sight integral

$$I(\epsilon) = \frac{1}{4\pi} \int_{\text{los}} q(\epsilon, \vec{r}) ds = \frac{1}{4\pi} \int_{\text{los}} \Gamma(\epsilon) n_H(\vec{r}) ds \quad (2.4)$$

where we have ignored absorption and scattering processes which are negligible for $\epsilon \lesssim 20$ GeV (e.g. Madau and Phinney 1996, Salamon and Stecker 1998). In Eq. (2.4) we write the γ -ray emissivity (production rate per unit volume) in terms of the local hydrogen density n_H and the production rate per H-atom (e.g. Stecker 1970, Dermer 1986)

$$\Gamma(\epsilon) = \int_{\epsilon+m_\pi^2/4\epsilon}^{\infty} \frac{dE_\pi}{\sqrt{E_\pi^2 - m_\pi^2}} \int dE_p \phi(E_p) \frac{d\sigma(E_p, E_\pi)}{dE_\pi}. \quad (2.5)$$

Note that if the *shape* of the cosmic ray spectrum $\phi(E)$ is the same everywhere along the line of sight, then $I(\epsilon) = \Gamma(\epsilon) N_H$, where N_H is the hydrogen column density, and thus the shape of the observed γ -ray spectrum $I(\epsilon)$ is the same as that of the source $\Gamma(\epsilon)$. This is the case of interest to us.

The production rate Γ reflects the production and decay of neutral pions (with cross section σ) due to a cosmic ray flux spectrum ϕ . The shape of $\Gamma(\epsilon)$ has well-known

properties that reflect the symmetry of the decay photons in the pion rest frame. As described in detail by Stecker (1970, 1971), the underlying isotropic nature of the rest-frame emission and the cosmic-ray beam is encoded in the emissivity spectrum, whose only photon energy dependence is through the lower limit in Eq. (2.5). This can be written as $\epsilon_0(\epsilon/\epsilon_0 + \epsilon_0/\epsilon)$ which clearly has a minimum at $\epsilon_0 = m_\pi/2$, and is invariant under $\epsilon/\epsilon_0 \rightarrow \epsilon_0/\epsilon$; these properties guarantee that the spectrum is peaked at $\epsilon_0 = 69$ MeV (the pion bump) and falls off symmetrically on a $\log I - \log \epsilon$ plot.

The other key property of emissivity is found in the isobar+scaling model, which provides a good fit to accelerator data (Dermer 1986). Namely, at high energies $\epsilon \gg m_\pi/2$, the emissivity goes to the power law $\Gamma(\epsilon) \sim \epsilon^{-\alpha_p}$ (and thus by symmetry it goes at low energies as $\epsilon^{+\alpha_p}$). This simple asymptotic power-law dependence is what allows us to constrain the pionic contribution of γ -ray spectra.

Note that the region of the spectrum immediately around the pion bump depends most sensitively on the details of the pion production cross section $d\sigma(E_p, E_\pi)/dE_\pi$ and thus on the shape of the proton spectrum $\phi_p(E)$ with which it is convolved. Consequently, a detection of the pion bump, and its width, would not only unambiguously identify a hadronic source, but would also constrain the spectrum of source particles. In this case, our constraints, which are based on the absence of a pion bump and the asymptotic behavior of the pion spectrum, become superfluous. We look forward to this obsolescence, due to the eventual detection of the pion bump by GLAST or its successors. But until then our results remain relevant.

A convenient semi-analytic fit to the pionic γ -ray source-function was recently presented by Pfrommer and Enßlin (2004). Using Dermer's model (Dermer 1986) for the production cross section, they arrive at the form:

$$\Gamma(\epsilon) = \xi^{2-\alpha_\gamma} \frac{n(r)_{p,CR}}{\text{GeV}} \frac{4}{3\alpha_\gamma} \left(\frac{m_{\pi^0}}{\text{GeV}}\right)^{-\alpha_\gamma} \left[\left(\frac{2\epsilon}{m_{\pi^0}}\right)^{\delta_\gamma} + \left(\frac{2\epsilon}{m_{\pi^0}}\right)^{-\delta_\gamma} \right]^{-\alpha_\gamma/\delta_\gamma} \sigma_{pp}. \quad (2.6)$$

The spectral index α_γ determines the shape parameter $\delta_\gamma = 0.14\alpha_\gamma^{-1.6} + 0.44$. The effective cross section σ_{pp} they modeled to the form $\sigma_{pp} = 32 \times (0.96 + e^{4.4-2.4\alpha_\gamma})$ mbarn. Following Dermer (1986) we take the pion multiplicity to be $\xi = 2$. The cosmic ray projectile number density is $n_p(r)$. This source function peaks at half the pion rest energy. In Dermer's model the γ -ray spectral index α_γ is equivalent to the cosmic ray spectral index i.e. $\alpha_\gamma = \alpha_p$ (Dermer 1986). Note that in our limits on the dimensionless *fraction* of observed emission that is due to pion decay, only the energy dependence (i.e. the *shape*) of the emissivity in Eq. (2.6) is important.

For the case of extragalactic emission, these pionic γ -rays can come from different redshifts. Thus, for extragalactic origin Eq. (2.4) becomes

$$I(\epsilon) = \frac{1}{H_0} \int dz \frac{n_{H,com}(z) \Gamma[(1+z)\epsilon, z]}{(1+z)\mathcal{H}(z)} \quad (2.7)$$

where the dimensionless expansion rate $\mathcal{H}(z) = H(z)/H_0$ takes the form $\mathcal{H}(z) = \sqrt{\Omega_m(1+z)^3 + \Omega_\Lambda}$ in a flat universe. The redshift dependence of the source-function Γ depends on the nature of the emission site (galaxies, cosmological shocks, etc.). For

purposes of illustration, we will use a single-redshift approx $n(z) = n_0\delta(z - z_*)$. In this approximation different z_* amount to the shift of the pionic γ -ray flux in log-log plot. Thus in this simplistic view the form of the source-function would stay the same as in Eq. (2.6) but ϵ_γ would be substituted with $E_\gamma(1+z)$ where E_γ is now the observed gamma-ray energy. Note that in this case, any pion bump would be redshifted, and thus would appear at energies $< m_{\pi^0}/2$. Thus it is clear that this feature is not apparent in the extragalactic spectrum, which is flat or even convex at these energies.

Of course, any realistic case will include contributions from a range of redshifts. However, one can view this distribution as an ensemble of delta functions, which will be an averaging over our simple cases, with a redshift-dependent weighting which scales as $(1+z)^{-1}n_{\text{H,com}}(z)\mathcal{H}(z)^{-1}$ (c.f. Eq. 2.7).

2.4. PROCEDURE

The main goal of this Chapter is to place a constraint to the maximal pionic contribution to diffuse gamma-ray flux based on the shape of the pionic spectrum, and fact that the pion bump is not observed. The way to obtain this upper limit is to see how much can we increase the pionic contribution by changing the parameters that it depends on so that it always stays at or below the observed values at all energies. The parameters that we change are the projectile and target number densities that enter in cosmic ray production of pions and the redshift from where we assume all pionic gamma rays originate. The condition of matching logarithmic slopes

$$\frac{d \log I_{\text{obs}}(E)}{dE} = \frac{d \log I_{\pi^0}(E)}{dE} \quad (2.8)$$

of theoretical pionic gamma-ray flux and the fit to the observed gamma-ray flux guarantees that the ratio I_{π^0}/I_{obs} is extremized (and in fact maximized for the spectra we consider). Here $I_{\pi^0}(E) = n_H(\vec{r})\Gamma(E)$ and is given in units of $\text{GeV}^{-1} \text{s}^{-1} \text{cm}^{-2}$. The energy which satisfies Eq. (2.8) thus sets the values of our parameters that maximize pionic flux.

Since the energy of pionic gamma-rays depends on the redshift as stated in the previous section, the slope of this theoretical flux will be the following function of observed energy E and the redshift z :

$$\frac{d \log I_{\pi^0}}{d \log E} = -\alpha_\gamma \frac{(2E(1+z)/m_{\pi^0})^{\delta_\gamma} - (2E(1+z)/m_{\pi^0})^{-\delta_\gamma}}{(2E(1+z)/m_{\pi^0})^{\delta_\gamma} + (2E(1+z)/m_{\pi^0})^{-\delta_\gamma}}. \quad (2.9)$$

Of course, for the Galactic spectrum we take $z = 0$.

The choice of α_γ depends on the origin of cosmic rays. In the case of Galactic cosmic rays we will be using the classic observed–i.e. *propagated*–value $\alpha_\gamma = 2.75$ (confirmed recently by, e.g. Boezio et al. 2003, Alcaraz et al. 2000, Sanuki et al. 2000). For extragalactic γ -rays, the sources are not known, but both blazars and shocks in cosmological structure formation have received considerable attention. For the case of blazars, it is not clear whether the emission is due to hadronic or leptonic

processes. Blazar γ -ray spectral indices have a distribution which averages give to a diffuse flux with index $\alpha_\gamma \sim 2.2$ (Stecker and Salamon 1996); if the emission is pionic this would be the proton index as well. Also, it is well known that the spectral index of cosmic rays accelerated in fairly strong shocks is $\alpha \approx -2$ (Blandford and Eichler 1987, Jones and Ellison 1991) which is expected to be the case with the cosmic rays from structure formation. Although the spectrum of structure-formation cosmic rays is not very well known for this purpose we will adopt the value $\alpha_\gamma = 2.2$, which is near the strong-shock limiting value of 2, and consistent with the Galactic *source* value (see discussion in, e.g. Fields et al. 2001), as well as that of blazars.

Now we have to match the slopes of the observed gamma-ray spectra to the slope of the theoretical pionic flux that was given in Eq. (2.9). This amounts to equating (2.9) with to the appropriate expressions for the spectra: Eqs. (2.12) or (2.13) for extragalactic, and Eq. (2.10) for Galactic. We then solve for $E_\gamma(z)$, where we put $z = 0$ for the Galactic case, and $z = z_*$ for the extragalactic case.

2.5. RESULTS

2.5.1. GALACTIC SPECTRUM

As described in Section 2.2, we fit the EGRET data for the Galactic spectrum with a broken power-law (Eq. 2.1), and we use the emissivity for a proton spectrum $\alpha_p = \alpha_\gamma = 2.75$. In order to set up an upper limit to the pionic contribution we match the low-energy index -1.52 to the slope of pionic γ -rays; fitting to the higher energy portion of the spectrum would lead to an unobserved excess in the low-energy portion. The logarithmic slope of Galactic spectrum is then just

$$\frac{d \log I_{\text{obs}}}{d \log E} = -1.52. \quad (2.10)$$

We now equate this with pionic slope given in Eq. (2.9) and solve for $E_\gamma(z = 0)$. This sets up the maximal normalization to the pionic spectrum which is plotted in the Fig. 2.1 along with the observed Galactic spectrum. Also plotted is the logarithmic residual function.

After integration over energies up to 10 GeV we can finally obtain the maximal pionic fraction of the Galactic γ -ray flux based on the shape of the pion decay spectrum as well as the lack of as strong detection of the pion bump:

$$f_{\pi^0, \text{MW}}(> \epsilon) = \frac{I_{\pi^0, \text{max}}(> \epsilon)}{I_{\text{obs}}(> \epsilon)} \quad (2.11)$$

where $I(> \epsilon) = \int_\epsilon I(E) dE$. We find pionic fraction to be $f_{\pi^0, \text{MW}}(> 30 \text{MeV}) = 53\%$ and $f_{\pi^0, \text{MW}}(> 200 \text{MeV}) = 81\%$. While this integral constraint provides a diagnostic of the hadronic “photon budget,” we stress that the lesson of the residual plot in Fig. 2.1 is that the deficit is not at all uniform across energies, but is very large at both high and low energies.

2.5.2. EXTRAGALACTIC SPECTRUM

By going through the slope-matching procedure described in the previous section we can fix the parameters that maximize the pionic contribution to the different extragalactic γ -ray spectra we consider. For the Sreekumar et al. (1998) spectrum (Eq. 2.2), the logarithmic slope is just a constant

$$\frac{d \log I_{\text{obs}}}{d \log E} = -2.1. \quad (2.12)$$

On the other hand, for Eq. (2.3) (Strong et al. 2003), we have

$$\frac{d \ln I_{\text{obs}}}{d \ln E} = -2 + \frac{d \ln(I_{\text{obs}} E^2)}{d \ln E} \quad (2.13)$$

$$= -2.0327 + 0.2182 \ln E + 0.0305(\ln E)^2. \quad (2.14)$$

In our simplistic picture we assume that all of the pionic γ -rays originated at a single redshift. Thus we go through this procedure for a set of redshifts ranging from $z = 0$ up to $z = 10$. Fig. 2.2 shows our maximized pionic contribution for the two extreme redshifts, along with the fits to the observed γ -ray spectrum and the actual EGRET data points (Strong et al. 2003). We also present the residual, which is what is left after pionic flux contribution is subtracted from the observed γ -ray spectrum. Here we see that for both EGRB spectra, the residual is large at low energies. However, the different shapes of the two EGRB candidate spectra lead to qualitatively different behavior at high energies ($\gtrsim 1$ GeV): the residual remains substantial (\gtrsim a factor of 2) for the Strong et al. (2003) fit, suggesting the need for other component(s) to dominate both high and low energies. But for the Sreekumar et al. (1998) fit, the residual is small, and thus the pionic contribution can be dominant above 1 GeV. This difference highlights the current uncertainty of our knowledge of the EGRB spectrum (and even its existence, Keshet et al. 2004). Our analysis thus underscores the need for a secure determination of the Galactic foreground and the extragalactic background.

To finally obtain the upper limit for the γ -rays that originated from pion decay, we integrate pionic and the observed (for both fits) flux. Then the ratio of these energy-integrated fluxes is the maximal fraction of pionic γ -rays for a given redshift.

$$g(z) = \frac{\int_{E_0}^{10 \text{ GeV}} d\epsilon I_{\pi}(\epsilon, z)}{\int_{E_0}^{10 \text{ GeV}} d\epsilon I_{\text{obs}}(\epsilon)}. \quad (2.15)$$

In Fig. 2.3 we plot this ratio as a function of redshift for three different integration ranges and for both Strong et al. (2003) and Sreekumar et al. (1998) fits to EGRET data. Note that the results asymptotically approach unity. A glance at Fig. 2.2 suggests the reason for this: the effect of increasing the emission redshift z_* to “slide” the pionic spectrum leftward, toward lower energies. As a result, the peak and low-energy falloff are redshifted out of the fit regime, and the remaining high-energy power-law tail of the pionic emission then provides a good fit to the observations.

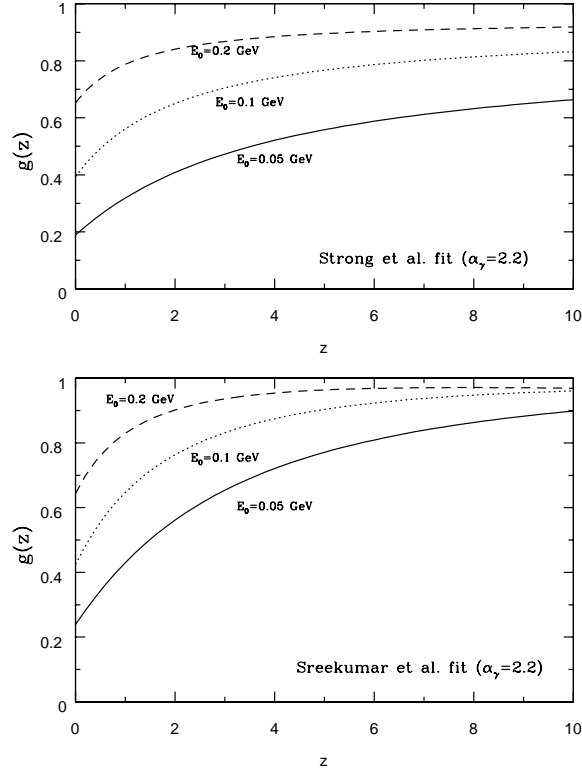


Figure 2.3: In this figure we see the maximal fraction of pionic energy-integrated flux. It is given as a function of the redshift of origin for the pionic γ -rays. Fluxes were integrated from E_0 up to 10 GeV.

Chapter 3

THE LITHIUM–GAMMA-RAY CONNECTION

3.1. OVERVIEW

The rare isotope ${}^6\text{Li}$ is made only by cosmic rays, dominantly in $\alpha\alpha \rightarrow {}^6\text{Li}$ fusion reactions with ISM helium. Consequently, this nuclide provides a unique diagnostic of the history of cosmic rays in our Galaxy. The same hadronic cosmic-ray interactions also produce high-energy γ rays (mostly via $pp \rightarrow \pi^0 \rightarrow \gamma\gamma$). Thus, hadronic γ -rays and ${}^6\text{Li}$ are intimately linked. Specifically, ${}^6\text{Li}$ directly encodes the local cosmic-ray fluence over cosmic time, while extragalactic hadronic γ rays encode an average cosmic-ray fluence over lines of sight out to the horizon. In this Chapter ⁵ we quantify and examine this link, as demonstrated in Fields and Prodanović (2005), and show how ${}^6\text{Li}$ and γ -rays can be used together to place important model-independent limits on the cosmic-ray history of our Galaxy and the universe. We first constrain γ -ray production from ordinary Galactic cosmic rays, using the local ${}^6\text{Li}$ abundance. We find that the solar ${}^6\text{Li}$ abundance demands an accompanying extragalactic pionic γ -ray intensity which exceeds that of the *entire* observed EGRB by a factor of 2–6 (Fields and Prodanović 2005). We then constrain Li production using recent determinations of extragalactic γ -ray background (EGRB). As noted in Chapter 1 of this book, cosmic rays created during cosmic structure formation would lead to pre-Galactic Li production, which would act as a “contaminant” to the primordial ${}^7\text{Li}$ content of metal-poor halo stars. In this Chapter we use the EGRB to place an upper limit on this contamination if we attribute the entire EGRB pionic contribution to structure forming cosmic rays (SFCRs). Unfortunately, the uncertainties in the determination of the EGRB are so large that the present γ -ray data cannot guarantee that the pre-Galactic Li is small compared to primordial ${}^7\text{Li}$; thus, an improved determination of the EGRB will shed important new light on this issue. Our limits and their more model-dependent extensions will improve significantly with additional observations of ${}^6\text{Li}$ in halo stars, and with improved measurements of the EGRB spectrum by GLAST.

⁵Parts of this were already published in a refereed journal (Fields and Prodanović 2005)

3.2. THE GAMMA-RAY – LITHIUM CONNECTION: FORMALISM

Before doing a detailed calculation let us first establish a simple, back of the envelope, connection between γ -rays and lithium. We know that low energy ($\sim 10 - 100$ MeV/nucleon) hadronic cosmic rays produce lithium through $\alpha\alpha \rightarrow {}^6,7\text{Li} + \dots$. But higher-energy (> 280 MeV/nucleon) cosmic rays also produce γ -rays via neutral pion decay: $pp \rightarrow \pi^0 \rightarrow \gamma\gamma$. Because they share a common origin in hadronic cosmic-ray interactions, we can directly relate cosmic ray lithium production to “pionic” γ -rays. The cosmic-ray production rate of ${}^6\text{Li}$ per unit volume is $q({}^6\text{Li}) = \sigma_{\alpha\alpha \rightarrow {}^6\text{Li}} \Phi_\alpha n_\alpha$, where Φ_α is the net cosmic ray He flux, n_α is the interstellar He abundance, and $\sigma_{\alpha\alpha \rightarrow {}^6\text{Li}}$ is the cross section for ${}^6\text{Li}$ production, appropriately averaged over the cosmic-ray energy spectrum (detailed definitions and normalization conventions appear in Appendix 1). Thus, the ${}^6\text{Li}$ mole fraction $Y_6 = n_6/n_b$ is just $Y({}^6\text{Li}) \sim \int \frac{dt}{n_b} q({}^6\text{Li}) \sim y_{\alpha,\text{cr}} Y_{\alpha,\text{ism}} \sigma_{\alpha\alpha \rightarrow {}^6\text{Li}} \Phi_p t_0$ where $y_{\alpha,\text{cr}} = \Phi_\alpha/\Phi_p \approx (\text{He}/\text{H})_{\text{ism}}$.

On the other hand, the cosmic-ray production rate of pionic γ -rays is just the pion production rate times a factor of 2, that is, $q_\gamma = 2\sigma_{pp \rightarrow \pi^0} \Phi_{p,\text{cr}} n_{p,\text{ism}}$. Integrated over a line of sight towards the cosmic particle horizon, this gives a EGRB intensity $I_\gamma \sim c \int dt q_\gamma / 4\pi \sim 2\sigma_{pp \rightarrow \pi^0} c \Phi_p t_0$. Thus we see that both the ${}^6\text{Li}$ abundance and the γ -ray intensity have a common factor of the (time-integrated) cosmic-ray flux, and so we can eliminate this factor and express each observable in terms of the other:

$$Y({}^6\text{Li}) \sim y_{\alpha,\text{cr}} Y_{\alpha,\text{gas}} \frac{2\pi}{n_b c} \frac{\sigma({}^6\text{Li})^{\alpha\alpha}}{\sigma_{\pi^0}^{pp}} I_\gamma. \quad (3.1)$$

From Eq. (3.1) we see that the connection between cosmic-ray lithium production and pionic γ -ray flux is straightforward.

This rough argument shows the intimacy of the connection between ${}^6\text{Li}$ and pionic γ -rays. However, this simplistic treatment does not account for the expansion of the universe, nor for time-variations in the cosmic cosmic-ray flux, nor for the inhomogeneous distribution of sources within the universe. We now include these effects in a more rigorous treatment.

For Li production at location \vec{x} , the production rate per unit (physical) volume is

$$q_{\text{Li}}(\vec{x}) = \sigma_{\alpha\alpha} \Phi_\alpha^{\text{cr}}(\vec{x}) n_{\alpha,\text{gas}}(\vec{x}) = y_{\alpha,\text{cr}} Y_\alpha^{\text{ism}} \sigma_{\alpha\alpha} \Phi_p^{\text{cr}}(\vec{x}) n_{b,\text{gas}}(\vec{x}) \equiv \mu(\vec{x}) \Gamma_{\text{Li}}(\vec{x}) n_b(\vec{x}). \quad (3.2)$$

Here, $y_{\alpha,\text{cr}} = (\alpha/p)_{\text{cr}}$ is the cosmic-ray He/H ratio, and is assumed to be constant in space and time.⁶ The target density of (interstellar or intergalactic) helium is $n_{\alpha,\text{gas}}$, which we write in terms of its ratio $Y_\alpha^{\text{ism}} = n_{\text{He}}/n_b$ to the baryon density. We take $Y_\alpha^{\text{ism}} \approx 0.06$ to be constant in space and time, but we do not assume this for the baryon density $n_b(\vec{x})$. The baryonic gas fraction

$$\mu = n_{b,\text{gas}}/n_b \quad (3.3)$$

accounts for the fact that not all baryons need to be in a diffuse form. Finally, we will find it convenient to write $q_{\text{Li}}(\vec{x})$ in terms of the local baryon density and the local Li production rate $\Gamma_{\text{Li}}(\vec{x})$ per baryon.

⁶That is, we ignore the small non-primordial ${}^4\text{He}$ production by stars, and we neglect any effects of H and He segregation. Both of these should be quite reasonable approximations.

With these expressions, we have

$$\frac{d}{dt} Y_{\text{Li}}(\vec{x}) = \mu(\vec{x}) \Gamma_{\text{Li}}(\vec{x}) \quad (3.4)$$

which we can solve to get

$$Y_{\text{Li}}(\vec{x}, t) = \int_0^t dt' \mu(\vec{x}, t') \Gamma_{\text{Li}}(\vec{x}, t') \quad (3.5)$$

$$= y_{\alpha, \text{cr}} Y_{\alpha}^{\text{ism}} \sigma_{\alpha\alpha} \int_0^t dt' \mu(\vec{x}, t') \Phi_p^{\text{cr}}(\vec{x}, t') \quad (3.6)$$

$$= y_{\alpha, \text{cr}} Y_{\alpha}^{\text{ism}} \sigma_{\alpha\alpha} F_p(\vec{x}, t) \quad (3.7)$$

where $F_p(\vec{x}, t) = \int_0^t dt' \mu(\vec{x}, t') \Phi_p^{\text{cr}}(\vec{x}, t')$ is the local proton fluence (time-integrated flux), weighted by the gas fraction. Thus we see that Li (and particularly ${}^6\text{Li}$) serves as a “cosmic-ray dosimeter” which measures the net local cosmic-ray exposure.

We now turn to γ rays from hadronic sources, most of which come from neutral pion production and decay: $pp \rightarrow \pi^0 \rightarrow \gamma\gamma$. The extragalactic background due to these process is expected to be isotropic (at least to a good approximation). In this case, the total γ -ray intensity $I_{\gamma} = dN_{\gamma}/dA dt d\Omega$, integrated over all energies, is given by an integral

$$I_{\gamma}(t) = \frac{c}{4\pi} \int_0^t dt' q_{\gamma}^{\text{com}}(t') \quad (3.8)$$

of the sources over the line of sight to the horizon. We are interested in particular in the case of hadronic sources, so that $q_{\text{com}} = a^3 q$ is the total (energy-integrated) comoving rate of hadronic γ -ray production per unit volume; here a is the usual cosmic scale factor, which we normalize to a present value of $a_0 = a(t_0) = 1$. A formal derivation of Eq. (3.8) appears in Appendix 2, but one can arrive at this result from elementary considerations. Namely, note that the comoving number density of photons produced at any point is just $n_{\gamma, \text{com}} = \int_0^t q_{\gamma}^{\text{com}} dt'$. We neglect photon absorption and scattering processes, and thus particle number conservation along with homogeneity and isotropy together demand that the comoving number density of ambient photons at any point is the same as the comoving number density of photons produced there. Furthermore, the total (energy-integrated) photon intensity is also isotropic and thus by definition is $I_{\gamma} = n_{\gamma, \text{com}} c/4\pi$, which is precisely what we find in Eq. (3.8).

The comoving rate of pionic γ -ray production per unit volume at point \vec{s} is

$$q_{\gamma\pi}^{\text{com}}(\vec{s}, t) = \sigma_{\gamma} \Phi_p(\vec{s}, t) n_{\text{H, gas}}^{\text{com}}(\vec{s}, t) = \mu(\vec{s}, t) \sigma_{\gamma} \Phi_p(\vec{s}, t) n_{\text{H}}^{\text{com}}(\vec{s}, t) \quad (3.9)$$

where n_{H} is the (comoving) hydrogen density, and $\Phi_p = 4\pi \int I_p(\epsilon) d\epsilon$ is the total (integrated over energy ϵ) omnidirectional cosmic-ray proton flux. The flux-averaged pionic γ -ray production cross section is

$$\sigma_{\gamma} \equiv 2\xi_{\alpha} \zeta_{\pi} \sigma_{\pi^0} = 2\xi_{\alpha} \frac{\int d\epsilon I_p(\epsilon) \zeta_{\pi} \sigma_{\pi^0}(\epsilon)}{\int d\epsilon I_p(\epsilon)} \quad (3.10)$$

where the factor of 2 counts the number of photons per pion decay, σ_{π^0} is the cross section for pion production and ζ_{π} is the pion multiplicity, and the factor $\xi_{\alpha} = 1.45$ accounts for $p\alpha$ and $\alpha\alpha$ reactions (Dermer 1986).

Then we have

$$I_{\gamma\pi}(t) = \frac{n_{b,0}c}{4\pi} Y_H \sigma_{\gamma} \int_0^t dt \mu(\vec{s}) \frac{n_b^{\text{com}}(\vec{s})}{n_{b,0}} \Phi_p(\vec{s}, t) = \frac{n_{b,0}c}{4\pi} \sigma_{\gamma} Y_H^{\text{ism}} F_p(t) \quad (3.11)$$

where

$$F_p(t) = \int_0^t dt \mu(\vec{s}) \frac{n_b^{\text{com}}(\vec{s})}{n_{b,0}} \Phi_p(\vec{s}) \quad (3.12)$$

is a mean value of the cosmic-ray fluence along the line of sight, where the average is weighted by the gas fraction and the ratio $n_b^{\text{com}}(\vec{s})/n_{b,0}$ of the local baryon density along the photon path. Note that the γ -ray sources are sensitive to the overlap of the cosmic-ray flux with the diffuse hydrogen gas density, and thus need not be homogeneous. Even so, we still assume the ERGB intensity to be isotropic, which corresponds to the assumption that the line-of-sight integral over the sources averages out any fluctuations.

One further technical note: $I_{\gamma\pi} \equiv I_{\gamma\pi}(> 0) = \int_0^{\infty} d\epsilon_{\gamma} I_{\gamma\pi}(\epsilon_{\gamma})$ represents the total pionic γ -ray flux, integrated over photon energies. While this quantity is well-defined theoretically, real observations have some energy cutoff, and thus report $I_{\gamma}(> \epsilon_0) = \int_{\epsilon_0}^{\infty} d\epsilon_{\gamma} I_{\gamma}(\epsilon_{\gamma})$, typically with $\epsilon_0 = 100$ MeV. But the spectrum of pionic γ -rays will be shifted towards lower energies if they originate from a nonzero redshift. Thus it is clear that γ -ray intensity I_{γ} , integrated above some energy $\epsilon_0 \neq 0$, will be redshift-dependent. A way to eliminate this z -dependence is to include *all* pionic γ -rays, that is to take $I_{\gamma\pi} \equiv I_{\gamma\pi}(> 0 \text{ GeV})$, i.e. to take $\epsilon_0 = 0$. As discussed in more detail in Appendix 2, the ${}^6\text{Li}$ - γ proportionality is only exact for $I_{\gamma\pi}(> 0)$, as this quantity removes photon redshifting effects which spoil the proportionality for $\epsilon_0 \neq 0$. Thus we will have to use information on the pionic spectrum to translate between $I_{\gamma\pi}(> \epsilon_0)$ and $I_{\gamma\pi}(> 0)$; these issues are discussed further in §3.3.1.

Thus we see that the lithium abundance and the pionic γ -ray intensity (spectrum integrated from 0 energy) arise from very similar integrals, which we can express via the ratio

$$\frac{I_{\gamma}(t)}{Y_i(\vec{x}, t)} = \frac{n_b c}{4\pi y_{\alpha, \text{cr}} y_{\alpha, \text{ism}}} \frac{\sigma_{\gamma}}{\sigma_{\alpha\alpha}^i} \frac{F_p(t)}{F_p(\vec{x}, t)} \quad (3.13)$$

where i denotes ${}^6\text{Li}$ or ${}^7\text{Li}$. Note that this “ γ -to-lithium” ratio has its only significant space and time dependence via the ratio $F_p(t)/F_p(\vec{x}, t)$ of the line-of-sight baryon-averaged fluence to the local fluence.⁷

The relationship expressed in Eq. (3.13) is the main result of this Chapter, and we will bring this tool to bear on Li and γ -ray observations, using each to constrain the

⁷In fact, the ratio also depends on the shape of the cosmic-ray spectrum (assumed universal), which determines the ratio of cross sections. We will take this into account below when we consider different cosmic-ray populations.

other. To do this, it will be convenient to write Eq. (3.13) in the form

$$I_{\gamma\pi}(t) = I_{0,i} \frac{Y_i(\vec{x}, t)}{Y_{i,\odot}} \frac{F_p(t)}{F_p(\vec{x}, t)} \quad (3.14)$$

where the scaling factor

$$I_{0,i} = \frac{n_b c}{4\pi y_{\alpha,cr} y_{\alpha,ism}} \frac{\sigma_\gamma}{\sigma_{\alpha\alpha}^i} Y_{i,\odot} \quad (3.15)$$

is independent of time and space, and only depends, via the ratio of cross sections, on the shape of the cosmic-ray population considered. Table 3.1 presents the values of $I_{0,i}$ for the different spectra that will be considered in the following sections. Values of the scaling factor were obtained by using photon multiplicity $\xi_\gamma = 2$, $\zeta_\alpha = 1.45$, baryon number density $n_b = 2.52 \times 10^{-7} \text{ cm}^{-3}$, CR and ISM helium abundances $y_\alpha^{\text{cr}} = y_\alpha^{\text{ism}} = 0.1$ and solar abundances as in §3.3.2. For the π^0 and lithium production cross-sections, we used the fits taken from Dermer (1986) and Mercer et al. (2001), and from that obtained the ratios of flux-averaged cross-sections for different spectra, and these are also presented in Table 3.1.

Table 3.1: Lithium and γ -ray Scalings and Production Ratios

Cosmic-Ray Population	$I_{0,6}$	$I_{0,7}$	$\sigma_{6\text{Li}}^{\alpha\alpha}/\sigma_\pi^{pp}$	$\sigma_{7\text{Li}}^{\alpha\alpha}/\sigma_\pi^{pp}$	${}^7\text{Li}/{}^6\text{Li}$
	[$\text{cm}^{-2}\text{s}^{-1}\text{sr}^{-1}$]				
GCR	9.06×10^{-5}	8.36×10^{-4}	0.21	0.28	1.3
SFCR	1.86×10^{-5}	1.15×10^{-4}	1.02	2.03	2.0

Table 3.1 shows that the different cosmic-ray spectra lead to very different Li-to- γ ratios. For example, the ${}^6\text{Li}$ -to- γ ratio $\sigma_{6\text{Li}}^{\alpha\alpha}/\sigma_\pi^{pp}$ is almost a factor of 5 higher in the SFCR case than in the GCR case. The reason for this stems from the different threshold behaviors and energy dependences of the Li and π^0 production cross sections. Li production via $\alpha\alpha$ fusion has a threshold around 10 MeV/nucleon, above which the cross section rapidly rises through some resonant peaks. Then beyond ~ 15 MeV/nucleon, the cross section for ${}^6\text{Li}$ drops exponentially as $e^{-E/16}$ MeV/nucleon (Mercer et al. 2001), rapidly suppressing the importance of any projectiles with $E \gg 16$ MeV/nucleon. Thus, as has been widely discussed, Li production is a low-energy phenomenon for which the important projectile energy range is roughly 10–70 MeV/nucleon.

On the other hand, $pp \rightarrow \pi^0$ production has a higher threshold of 280 MeV, and the effective cross section $\zeta_\pi \sigma_{pp}^\pi$ rises with energy up to and beyond 1 GeV. Neutral pion production is thus a significantly higher-energy phenomenon.

These different cross section behaviors are sensitive to the differences in the two cosmic-ray spectra we adopt. On the one hand, we adopt a GCR spectrum that is a power law in *total* energy: $\phi_p(E) \propto (m_p + E)^{-2.75}$, a commonly-used (e.g. Dermer 1986) approximation to the locally observed (i.e. *propagated*) spectrum. This

spectrum is roughly constant for $E < m_p$. Thus, there is no reduction in cosmic-ray flux between the Li and π^0 thresholds. Furthermore the flux only begins to drop far above the π^0 threshold at 280 MeV, so that there is significant pion production over a large range of energies, in contrast to the intrinsically narrow energy window for Li production. As a result of the effects, $\sigma_{6\text{Li}}^{\alpha\alpha}/\sigma_{\pi}^{pp} \ll 1$ for the GCR case.

In contrast, the SFCR flux is taken to be the standard result for diffusive acceleration due to a strong shock: namely, a power law in momentum $\phi(E) \propto p(E)^{-2}$. This goes to $\phi \propto E^{-1}$ at $E \lesssim m_p$, and $\phi \propto E^{-2}$ at higher energies. This spectrum thus drops by a factor of 28 between the Li and π^0 thresholds, and continues to drop above the π^0 threshold, offsetting the rise in the pion cross section. This behavior thus suppresses π^0 production relative to the GCR case, and thus we have a significantly higher $\sigma_{6\text{Li}}^{\alpha\alpha}/\sigma_{\pi}^{pp}$ ratio. As we will see, these ratios—and the differences between them—will be critical in deriving quantitative constraints.

3.3. OBSERVATIONAL INPUTS

We have seen that the EGRB intensity and lithium abundances are closely linked. Here we collect information on both observables.

3.3.1. THE OBSERVED GAMMA-RAY BACKGROUND AND LIMITS TO THE PIONIC CONTRIBUTION

Ever since γ -rays were first observed towards the Galactic poles as well as in the plane (Fichtel et al. 1973), the existence of emission at high Galactic latitudes has been regarded as an indication of an EGRB. However, any information regarding the intensity, energy spectrum, and even the existence of the EGRB is only as reliable as the procedure for subtracting the Galactic foreground. Such procedures are unfortunately non-trivial and model-dependent. The EGRET team (Sreekumar et al. 1998) used an empirical model for tracers of Galactic hydrogen and starlight, and found evidence for an EGRB which dominates polar emission. Other groups have recently presented new analyses of the EGRET data. In a semi-empirical approach using a model of Galactic γ -ray sources, Strong et al. (2004b) also find evidence for an EGRB, but with a different energy spectrum and a generally lower intensity than the Sreekumar et al. (1998) result. Finally, Keshet et al. (2004) find that the Galactic foreground is sufficiently uncertain that its contribution to the polar emission can be significant, possibly saturating the observations. Consequently, the Keshet et al. (2004) analysis is unable to confirm the existence of an EGRB in the EGRET data; instead, they can only to place upper limits on the EGRB intensity.

As shown in Chapter 2 (Prodanović and Fields 2004a) a model-independent limit on the fraction of EGRB flux that is of pionic origin (γ -rays that originate from π^0 decay) can be placed. For the pionic γ -ray source-function we use Eq. (2.6). A key feature of the pionic γ -ray spectrum is that it approaches a power law at both high and low energies, going to ϵ^{α_γ} for $\epsilon \ll m_\pi/2$ and to $\epsilon^{-\alpha_\gamma}$ for $\epsilon \gg m_\pi/2$. In Dermer's model, the γ -ray spectral index α_γ is equal to the cosmic-ray spectral index. As in Chapter 2 (Prodanović and Fields 2004a) we adopt the value $\alpha_\gamma = 2.2$ for pionic extragalactic γ -rays, which is consistent with blazars and structure-forming cosmic

rays as their origin, and assume a single-redshift approximation, that is, we assume that these γ -rays are all coming from one redshift, and thus our limit on the maximal pionic fraction is a function of z .

To obtain the EGRB spectrum from EGRET data, a careful subtraction of Galactic foreground is needed. In Chapter 2 we (Prodanović and Fields 2004a) considered two different EGRB spectra and obtained the following limit: for the Sreekumar et al. (1998) spectrum we found that the pionic fraction of the EGRB (integrated spectra above 100 MeV) can be as low as about 40% for cosmic rays that originated at present, to about 90 % for $z = 10$; for the more shallow spectrum of Strong et al. (2004b) we found that pionic fraction can go from about 40% for $z = 0$ up to about 80% for $z = 10$. However, the Keshet et al. (2004) analysis of the EGRET data implies that the Galactic foreground dominates the γ -ray sky so that only an upper limit on the EGRB can be placed, namely $I_\gamma(> 100\text{MeV}) \leq 0.5 \times 10^{-5} \text{ cm}^{-2} \text{ s}^{-1} \text{ sr}^{-1}$. Thus, in this case, we were not able to obtain the pionic fraction.

However, to be able to connect the pionic γ -ray intensity $I_{\gamma\pi}$ with lithium mole fraction Y_i as shown in (3.13), $I_{\gamma\pi}$ must include all of the pionic γ -rays, that is, the spectrum has to be integrated from energy $\epsilon_0 = 0$. The upper limit to the pionic γ -ray intensity above energy ϵ_0 for a given redshift can be written as

$$I_{\gamma\pi}(> \epsilon_0) = f_\pi(> \epsilon_0, z) I_\gamma^{\text{obs}}(> \epsilon_0) \quad (3.16)$$

$$= \mathcal{N}_{\text{max}} \int_{\epsilon_0} \varphi[\epsilon(1+z)] d\epsilon \quad (3.17)$$

where $f_\pi(> \epsilon_0, z)$ is the upper limit to the fraction of pionic γ -rays (Prodanović and Fields 2004a), $I_\gamma^{\text{obs}}(> \epsilon_0)$ is the observed intensity above some energy, while $\varphi[\epsilon(1+z)]$ is the semi-analytic fit for pionic γ -ray spectrum given in Eq. (2.6) (Pfrommer and Enßlin 2004) which is maximized with \mathcal{N}_{max} normalization constant. An upper limit to the pionic γ -ray intensity that covers all energies $I_{\gamma\pi}(> 0, z)$, follows immediately from the above equations:

$$I_{\gamma\pi}(> 0, z) = f_\pi(> \epsilon_0, z) I_\gamma^{\text{obs}}(> \epsilon_0) \frac{\int_0 \varphi[\epsilon(1+z)] d\epsilon}{\int_{\epsilon_0} \varphi[\epsilon(1+z)] d\epsilon}. \quad (3.18)$$

Now this is something that is semi-observational and can be easily obtained from γ -ray intensity observed above some energy, and from procedure described in Chapter 2 (Prodanović and Fields 2004a) and Eq. (2.6) (Pfrommer and Enßlin 2004).

3.3.2. LITHIUM ABUNDANCES

Given the EGRB intensity, we will infer the amount of associated lithium production. It will be of interest to compare this to the solar abundance, and also to the primordial abundance of ${}^7\text{Li}$. We take the solar Li isotope abundances from Anders and Grevesse (1989): $({}^6\text{Li}/\text{H})_\odot = 1.53 \times 10^{-10}$ and $({}^7\text{Li}/\text{H})_\odot = 1.89 \times 10^{-9}$. These are derived from meteoritic data, and thus reflect conditions in the pre-solar nebula and in particular are not plagued by the well-known deficit of Li in the solar photosphere. However, it is worth noting that the galactic chemical evolution history of Li includes not only

the sources we have mentioned, but also sinks. Main sequence stars destroy both Li isotopes in all but their outermost layers, and for stars in the mass range $1 - 4M_{\odot}$ and $6 - 10M_{\odot}$, there may be no additional Li production (Romano et al. 2001). These stars thus act as Li sinks, and contribute to Galactic astration of Li, similar to but less severe than the astration of deuterium. Consequently, the solar Li isotopic abundances are strictly speaking a *lower limit* to the total Galactic production, with some additional production (up to a factor ~ 2 higher, using deuterium as a guide; Cyburt et al. 2003b) being hidden by astration.

Metal-poor halo stars (extreme Population II) serve as a “fossil record” of pre-Galactic lithium. Ryan et al. (2000) find a pre-Galactic abundance

$$\left(\frac{\text{Li}}{\text{H}}\right)_{\text{pre-Gal,obs}} = (1.23_{-0.16}^{+0.34}) \times 10^{-10} \quad (3.19)$$

based on an analysis of very metal-poor halo stars. On the other hand, one can use the WMAP (Spergel et al. 2003) baryon density and BBN to predict a “theoretical” (or “CMB-based”) primordial ${}^7\text{Li}$ abundance (Cyburt et al. 2003b):

$$\left(\frac{{}^7\text{Li}}{\text{H}}\right)_{\text{BBN,thy}} = (3.82_{-0.60}^{+0.73}) \times 10^{-10}. \quad (3.20)$$

These abundances are clearly inconsistent. Possible explanations for this discrepancy include unknown or underestimated systematic errors in theory and/or observations or new physics; these are discussed thoroughly elsewhere (see e.g. Cyburt et al. 2004 and references therein). For our purposes, we will acknowledge this discrepancy by comparing pre-Galactic lithium production by cosmic rays with both the observed and CMB-based Li abundances.

3.4. ${}^6\text{Li}$ AND GAMMA-RAYS FROM GALACTIC COSMIC RAYS

We have shown that ${}^6\text{Li}$ abundances and extragalactic γ -rays are linked because both sample cosmic-ray fluence. We now apply this formalism to γ -ray and ${}^6\text{Li}$ data. In this section we turn to the hadronic products of Galactic cosmic rays, which are believed to be the dominant source of ${}^6\text{Li}$, but a sub-dominant contribution to the EGRB.

3.4.1. SOLAR ${}^6\text{Li}$ AND GAMMA-RAYS

We place upper limits on the lithium component of GCR origin by using the formalism established in earlier sections. To be able to find $I_{\gamma}/Y_{6\text{Li}}$ from Eq. (3.13) we assume that ratio of cosmic-ray fluence along the line of sight (weighted by gas fraction) to the local cosmic-ray fluence is $F_p(t)/F_p(\vec{x}, t) \approx 1$. That is, we assume that the Milky Way fluence is typical of star forming galaxies, i.e. that the γ -luminosities are comparable: $L_{\text{MW}} \approx \langle L \rangle_{\text{gal}}$. Note that in the most simple case of a uniform approximation (cosmic-ray flux and gas fraction the same in all galaxies), the two fluences would indeed be exactly equal.

Taking the solar ${}^6\text{Li}$ abundance and $\langle \sigma_{6\text{Li}}^{\alpha\alpha} \rangle / \langle \sigma_{\pi}^{pp} \rangle = 0.21$ for the ratio of GCR flux averaged cross-sections, we now use Eq. (3.14) to find $I_{\gamma_{\pi}^0}(\epsilon > 0) = 9.06 \times$

$10^{-5} \text{cm}^{-2} \text{s}^{-1} \text{sr}^{-1}$ is the hadronic γ -ray intensity that is required if all of the solar ${}^6\text{Li}$ is made via Galactic cosmic-rays.

We wish to compare this ${}^6\text{Li}$ -based pionic γ -ray flux to the observed EGRB intensity $I_\gamma^{\text{obs}}(\epsilon > \epsilon_0)$. However, Eq. (3.14) gives the hadronic γ -ray intensity integrated over all energies, whereas the observed one is above some finite energy. Thus we have to compute

$$I_{\gamma\pi}^0(\epsilon > \epsilon_0) = I_{\gamma\pi}^0(\epsilon > 0) \frac{\int_{\epsilon_0} d\epsilon I_{\epsilon,\pi}}{\int_0 d\epsilon I_{\epsilon,\pi}} \quad (3.21)$$

$$= 9.06 \times 10^{-5} \text{cm}^{-2} \text{s}^{-1} \text{sr}^{-1} \frac{\int_{\epsilon_0} d\epsilon I_{\epsilon,\pi}}{\int_0 d\epsilon I_{\epsilon,\pi}}. \quad (3.22)$$

We follow the model of Pavlidou and Fields (2002) to calculate the GCR emissivity over the history of the universe. The source function q_γ^{com} (equivalent to Eq. (3.9)) is given by a coarse-graining over galactic scales, so that

$$q_{\gamma,\text{gcr}}^{\text{com}}(z, \epsilon) = L_\gamma(\epsilon) n_{\text{gal}}^{\text{com}}(z) \quad (3.23)$$

where L_γ is the average galactic γ -ray luminosity (by photon number), and $n_{\text{gal}}^{\text{com}}(z)$ is the mean comoving number density of galaxies. The key assumptions for the luminosity L_γ are: (1) that supernova explosions provide the engines powering cosmic-ray acceleration, so that the cosmic-ray flux $\Phi \propto \psi$ scales with the supernova rate and thus the star formation rate ψ ; (2) that the targets come from the gas mass which evolves following the ‘‘closed box’’ prescription; and (3) that the Milky Way luminosity represents that of an average galaxy. With these assumptions we have that $L_\gamma \propto \mu\psi$, and thus that $q_\gamma^{\text{com}} \propto \mu\dot{\rho}_\star$, where $\dot{\rho}_\star$ is the cosmic star formation rate.

Following Pavlidou and Fields (2002), the specific form of $I_{\epsilon,\pi}$ is expressed in terms of the present day Milky Way gas mass fraction $\mu_{0,\text{MW}}$, cosmic star-formation rate $\dot{\rho}_\star(z)$, Milky Way γ -ray (number) luminosity $L_{\gamma,\text{MW}}(z, E)$, cosmology Ω_Λ and Ω_m , and integrated up to z_* , the assumed starting redshift for star formation. For this calculation we adopt the following values: $\mu_{0,\text{MW}} = 0.14$, $\Omega_\Lambda = 0.7$, $\Omega_m = 0.3$ and $z_* = 5$. For the cosmic star formation rate we use the dust-corrected analytic fit from Cole et al. (2001). Finally we need the (number) luminosity of pionic γ -rays which we can write as

$$L_{\gamma,\text{MW}}(z, E) = \Gamma_\gamma N_p = \frac{q_{\gamma\pi}}{n_p} N_p \propto \Phi M_{\text{gas}} \quad (3.24)$$

where n_p is the proton number density in the Galaxy, N_p is the total number of protons in the Galactic ISM, while $q_{\gamma\pi} [\text{s}^{-1} \text{GeV}^{-1} \text{cm}^{-3} \text{sr}^{-1}]$ is the source function of γ -rays that originate from pion decay adopted from Pfrommer and Enßlin (2004). Notice that in Eq. (3.21) we have the ratio of two integrals where integrands are identical, thus normalizations and constants will cancel out. Therefore, instead of using the complete form of $L_{\gamma,\text{MW}}(z, E)$ we need only use the spectral shape of the pionic γ -ray source function (Pfrommer and Enßlin 2004), that is, only the part that is energy- and redshift-dependent.

Finally then, we find

$$I_{\gamma\pi}^0(\epsilon > 0.1 \text{GeV}) = 3.22 \times 10^{-5} \text{cm}^{-2} \text{s}^{-1} \text{sr}^{-1} \quad (3.25)$$

Table 3.2: Upper limit on Li of SFCR origin

EGRB [$\text{cm}^{-2}\text{s}^{-1}\text{sr}^{-1}$]	z	$I_{\gamma,\pi}(> 0)$	$(\text{Li}/\text{H})_{\text{SFCR}}^{\text{max}}$	$\frac{\text{Li}_{\text{SFCR}}^{\text{max}}}{\text{Li}_{\text{p}}^{\text{theo}}}$	$\frac{\text{Li}_{\text{SFCR}}^{\text{max}}}{\text{Li}_{\text{p}}^{\text{obs}}}$	f_{π}
(Sreekumar et al. 1998)	0	8.78×10^{-6}	2.19×10^{-10}	0.57	1.78	0.91
$I_{\gamma,\text{obs}}(> 0.1) = 1.57 \times 10^{-5}$	10	1.22×10^{-4}	3.04×10^{-9}	7.95	24.7	0.15
(Strong et al. 2004a)	0	4.59×10^{-6}	1.14×10^{-10}	0.30	0.93	1.29
$I_{\gamma,\text{obs}}(> 0.1) = 1.11 \times 10^{-5}$	10	6.27×10^{-5}	1.56×10^{-9}	4.09	12.69	0.21
(Keshet et al. 2004)	0	$< 6.5 \times 10^{-6}$	$< 1.62 \times 10^{-10}$	0.42	1.32	2.86
$I_{\gamma,\text{obs}}(> 0.1) < 0.5 \times 10^{-5}$	10	$< 4.03 \times 10^{-5}$	$< 1.00 \times 10^{-9}$	2.63	8.16	0.46

which we can now compare to the observed EGRB values $I_{\gamma}^{\text{obs}}(\epsilon > 0.1\text{GeV})$ that are given in the first column of Table 3.2. As one can see, our *pionic* EGRB γ -ray intensity is between 2 and 6 times larger than the *entire* observed value! Moreover, the total observed high-latitude ($b > 30^\circ$) emission (Kniffen 1996) is $I_{\gamma}^{\text{obs,hi-lat}}(> 0.1\text{ GeV}) = 1.5 \times 10^{-5} \text{ cm}^{-2} \text{ s}^{-1} \text{ sr}^{-1}$, consistent with the Sreekumar et al. (1998) value. Thus the GCR-based ${}^6\text{Li}$ demand for pionic γ -rays exceeds the entire observed high-latitude signal by a factor of 2, independent of any prescription for Galactic foreground subtraction. The discrepancy is thus model-independent.

Here it is noteworthy to compare our ${}^6\text{Li}$ -based estimate of the galactic EGRB contribution to the work of Pavlidou and Fields (2002). That calculation adopted the same model for the redshift history of cosmic-ray flux and interstellar gas, and so only differed from the present calculation in the normalization to Galactic values. Pavlidou and Fields (2002) normalized to the *present* Galactic γ -ray luminosity. This amounts to a calibration not to the time-integrated cosmic-ray *fluence*, but rather to the instantaneous cosmic ray *flux*, as determined by the Dermer (1986) emissivity, a Galactic gas mass of $10^{10}M_{\odot}$, and an estimate of the present Galactic star formation rate. This normalization gave a galactic EGRB component which at all energies lies *below* the total Sreekumar et al. (1998) background. Our calculation is normalized to solar ${}^6\text{Li}$, which is a direct measure of Galactic (or at least solar neighborhood) cosmic-ray *fluence*, and which contains fewer uncertainties than the factors entering in the Pavlidou and Fields (2002) result. Yet surprisingly, the ${}^6\text{Li}$ -based fluence result gives a high pionic EGRB, while the more uncertain normalization gives an acceptable result.

Our surprising result can have important consequences for GCRs and Li nucleosynthesis in general. Thus, it deserves a more careful investigation. Namely, we have assumed that ${}^6\text{Li}$ is produced solely by $\alpha\alpha$ fusion processes. However, we note that spallation processes of the kind $p, \alpha + \text{CNO}$ also produce ${}^6\text{Li}$. By ignoring these processes thus far, we have overestimated the $\alpha\alpha$ contribution to ${}^6\text{Li}$ and in turn overestimated its inferred EGRB contribution. Though, the spallation processes are negligible at low metallicities, and are even sub-dominant for an ISM with solar metallicity, in a more detailed calculation this channel must be accounted for. Another important change in our result might come from adopting a more carefully propagated cosmic-ray spectrum. In this section we have been using a standard, single power-law spectrum, which is a good approximation for CR energies above $\sim 100\text{ GeV}$ where

energy losses are dominated by CR escape. However, because of sharply declining cross-section, ${}^6\text{Li}$ production via $\alpha\alpha$ fusion reaction is dominated by CR energies close to the threshold (~ 10 GeV), where ionization energy losses become important, and the CR spectrum becomes less steep. Thus, taking a carefully propagated CR spectrum will increase GCR ${}^6\text{Li}$ production as allowed by the EGRB observations. Finally we note that if the astration of ${}^6\text{Li}$ is taken into consideration (c.f. §3.3.2), one might use ${}^6\text{Li}$ abundance larger than solar. In that case one would find that the accompanying *pionic* EGRB γ -ray intensity is even more constraining. These effects will be taken into account in Chapter 4 where we present a thorough investigation of this potential but crucial ${}^6\text{Li}$ problem.

3.4.2. THE OBSERVED EGRB AND NON-PRIMORDIAL LITHIUM

We can exploit Eq. (3.14) in both directions. Here we use the observed EGRB spectrum to constrain the ${}^6\text{Li}$ abundance produced via Galactic cosmic rays. By comparing this Galactic ${}^6\text{Li}$ component to the observed solar abundance we can then place an upper limit on the *residual* ${}^6\text{Li}$ which (presumably) was produced by SFCR. As described in §3.3.1, with the observed EGRB spectrum in hand we can place an upper limit on its fraction of pionic origin. In the case of SFCR-produced pionic γ -rays, we can place constraints directly only in the presence of a model for the SFCR redshift history. Since a full model is unavailable, below (Section 3.5) we adopt the “single-redshift approximation.” However, in the case of galactic cosmic rays we have a better understanding of the redshift history of the sources. Therefore, we will follow Pavlidou and Fields (2002) to calculate the pionic differential γ -ray intensity for some set of energies

$$I_{\gamma_\pi, E} = \frac{c}{4\pi H_0 \psi_{\text{MW}}} \int_0^{z_*} dz \frac{\dot{\rho}_*(z) L_{\gamma_\pi} [(1+z)E]}{\sqrt{\Omega_\Lambda + \Omega_M (1+z)^3}} \times \left[\frac{1}{\mu_{0, \text{MW}}} - \left(\frac{1}{\mu_{0, \text{MW}}} - 1 \right) \frac{\int_{z_*}^z dz (dt/dz) \dot{\rho}_*(z)}{\int_{z_*}^0 dz (dt/dz) \dot{\rho}_*(z)} \right] \quad (3.26)$$

where I_{γ_π} is in units of $\text{s}^{-1} \text{cm}^{-2} \text{GeV}^{-1}$, and ψ_{MW} is the present Milky Way star formation rate. For the pionic γ -ray luminosity L_{γ_π} we will, as before, use the pionic γ -ray source function adopted from Pfrommer and Enßlin (2004) (Eq. 2.6, $\alpha_\gamma = 2.75$ for GCR spectrum), however we will let the normalization be determined by maximizing the pionic contribution to the EGRB. The adopted parameters, cosmology, and cosmic star formation rate we keep the same as in previous subsection.

Once we obtain the spectrum we can then fit it with

$$\ln(I_{\gamma_\pi} E^2) = -14.171 - 0.546 \ln E - 0.131 (\ln E)^2 + 0.032 (\ln E)^3 \quad (3.27)$$

where E is in GeV and I_{γ_π} is in photons $\text{cm}^{-2} \text{s}^{-1} \text{sr}^{-1} \text{GeV}^{-1}$. The free leading term in the above equation is set by requiring that $I_{\gamma_\pi} = I_{\gamma, \text{obs}}$ at the energy $E = 0.44$ GeV which maximizes pionic contribution by demanding that the pionic γ -ray spectrum always stays below the observed one (since the feature of pionic peak is not observed).

We also fit the Strong et al. (2004b) data with

$$\ln(I_{\gamma,\text{obs}}E^2) = -14.003 - 0.144 \ln E - 0.097(\ln E)^2 + 0.017(\ln E)^3 \quad (3.28)$$

in the same units.

By going through the procedure described in Chapter 2 (Prodanović and Fields 2004a) we can now obtain an upper limit to the fraction of pionic γ -ray compared to the Strong et al. (2004b) observed EGRB spectrum. This maximized pionic (green dashed line), as well as the observed, γ -ray spectrum is presented in Fig. 3.1. We find the upper limit to pionic fraction to be $f_{\pi}(> 0.1\text{GeV}) \equiv \int_{0.1} dE I_{\gamma\pi} / \int_{0.1} dE I_{\gamma,\text{obs}} = 0.75$. We note in passing that a maximal pionic fraction as appears in Fig. 3.1 gives a poor fit at energies both above and below the matching near 0.4 GeV, suggesting the presence of other source mechanisms. This mismatch reflects a similar problem in the underlying Galactic γ -ray spectrum, and suggests that the pionic contribution to the EGRB is in fact sub-maximal.

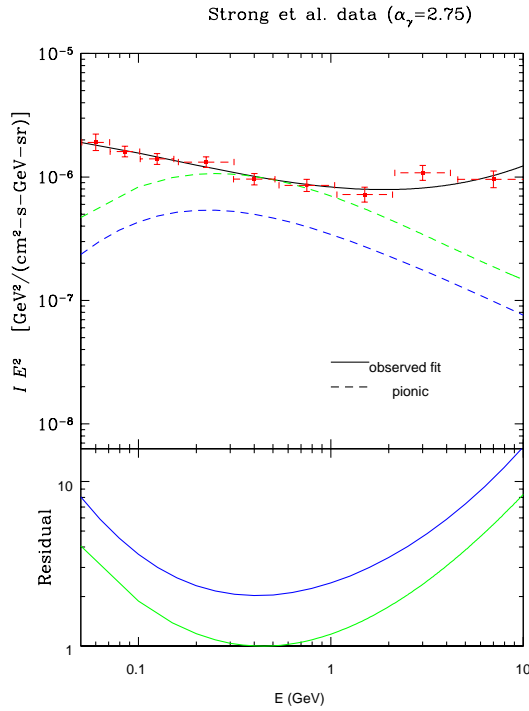


Figure 3.1: In the upper panel of this figure, we plot the pionic (dashed lines: green-maximized, blue-normalized to the Milky Way) EGRB spectrum, where decaying pions are of GCR origin, compared to the observed EGRB spectrum (solid line, fit to data); for purposes of illustration, we use the Strong et al. (2004b) data points, which are given in red crosses. The bottom panel represents the residual function, that is, $\log[(IE^2)_{\text{obs}}/(IE^2)_{\pi}] = \log(I_{\text{obs}}/I_{\pi})$.

Thus, the pionic γ -ray flux above 0.1 GeV is $I_{\gamma\pi}(> 0.1) = 0.83 \times 10^{-5} \text{ cm}^{-2} \text{ s}^{-1} \text{ sr}^{-1}$. From Eq. (3.21) it now follows that the total flux is $I_{\gamma\pi}(> 0) = 2.31 \times 10^{-5} \text{ cm}^{-2} \text{ s}^{-1} \text{ sr}^{-1}$. As before, we can now use Eq. (3.14) to find the GCR ${}^6\text{Li}$ mole fraction

$$\left(\frac{Y_{6\text{Li}}}{Y_{6\text{Li}_\odot}} \right)_{\text{GCR}} = \frac{I_{\gamma\pi}(> 0)}{9.06 \times 10^{-5} \text{ photons cm}^{-2} \text{ s}^{-1} \text{ sr}^{-1}} = 0.25 \quad (3.29)$$

and thus, SFCCR-produced ${}^6\text{Li}$ can be at most (neglecting the ${}^6\text{Li}$ astration) the residual ${}^6\text{Li}$

$$\begin{aligned} \left(\frac{Y_{6\text{Li}}}{Y_{6\text{Li}_\odot}} \right)_{\text{SFCCR}} &= 1 - \left(\frac{Y_{6\text{Li}}}{Y_{6\text{Li}_\odot}} \right)_{\text{GCR}} \\ &= 0.75. \end{aligned} \quad (3.30)$$

With the appropriate scaling between ${}^7\text{Li}$ and ${}^6\text{Li}$ as given in Table 3.1, we can then determine the total elemental Li = ${}^7\text{Li} + {}^6\text{Li}$ abundance and compare it to the primordial values from (3.19) and (3.20):

$$\left(\frac{\text{Li}}{\text{H}} \right)_{\text{SFCCR}} = 3.45 \times 10^{-10} = 0.90 \left(\frac{{}^7\text{Li}}{\text{H}} \right)_{\text{p,thy}} = 2.81 \left(\frac{{}^7\text{Li}}{\text{H}} \right)_{\text{p,obs}}.$$

So far we have been determining the maximized pionic fraction of the EGRB based only on the shape of the pionic spectrum. However, in the case of normal galaxies we have a better understanding of what that fraction should be. That is, we can normalize pionic spectrum to the one of the Milky Way, and then integrate over the redshift history of sources. Following Pavlidou and Fields (2002) (and references therein) we set up the normalization by requiring that $\int_{0.1 \text{ GeV}} dEL_{\gamma\pi}(z=0, E) = \int_{0.1 \text{ GeV}} dEL_{\gamma\pi, \text{MW}}(E) = 2.85 \times 10^{42} \text{ s}^{-1}$. Keeping the shape of the pionic spectrum, we can now normalize Eq. (2.6) (Pfrommer and Enßlin 2004):

$$L_{\gamma\pi}(z=0, E) = 9.52 \times 10^{44} \text{ s}^{-1} \text{ GeV}^{-1} \left[\left(\frac{2\epsilon}{m_{\pi^0}} \right)^{\delta_\gamma} + \left(\frac{2\epsilon}{m_{\pi^0}} \right)^{-\delta_\gamma} \right]^{-\alpha_\gamma/\delta_\gamma}. \quad (3.31)$$

Now we can use Eq. (3.26) to obtain the pionic spectrum which is plotted on the Fig. 3.1 (blue dashed line). We use star formation rate $\psi_{\text{MW}} = 3.2 M_\odot \text{ yr}^{-1}$ (McKee 1989). Finally we find that in this case, when pionic spectrum is normalized to the Milky Way, the GCR ${}^6\text{Li}$ mole fraction that accompanies it is

$$\left(\frac{Y_{6\text{Li}}}{Y_{6\text{Li}_\odot}} \right)_{\text{GCR}} = 0.14$$

which then gives $(\text{Li}/\text{H})_{\text{SFCCR}} = 3.96 \times 10^{-10} = 1.03({}^7\text{Li}/\text{H})_{\text{p,thy}} = 3.22({}^7\text{Li}/\text{H})_{\text{p,obs}}$, which is of course a weaker limit than the maximal pionic case.

We thus see that in a completely model-independent analysis, current observations allow the possibility that SFCCRs are quite a significant source of ${}^6\text{Li}$ and of γ -rays.

Indeed, we cannot exclude that SFCR-produced lithium can be a potentially large contaminant of the pre-Galactic Li component of halo stars, which would exacerbate the already troublesome disagreement with CMB-based estimates of primordial ${}^7\text{Li}$. Consequently, we conclude that models for SFCR acceleration and propagation should include both γ -ray and ${}^6\text{Li}$ production; and more constraints on SFCR, both theoretically (e.g. space and time histories) and observationally (e.g. EGRB and possibly diffuse synchrotron measurement), will clarify the picture we have sketched.

Note that had we also considered the possibility of astration of ${}^6\text{Li}$ (§3.3.2), we would have found a greater ${}^6\text{Li}$ residual, and thus had an even larger SFCR-produced component.

3.5. ${}^6\text{Li}$ AND GAMMA-RAYS FROM COSMOLOGICAL COSMIC RAYS

In this section we turn to the as-yet unobserved cosmological component of cosmic rays, and to the synthesis of lithium by SFCR. This lithium component would be the first made after big bang nucleosynthesis. Any Li which is produced this way prior to the most metal-poor halo stars would amount to a pre-Galactic Li enrichment and thus would be a *non-primordial* Li component, unaccompanied by beryllium and boron production. This structure-formation Li would be an additional “contaminant” to the usual components in halo stars, the ${}^7\text{Li}$ abundance due to primordial nucleosynthesis, and the ${}^6\text{Li}$ and ${}^7\text{Li}$ contribution due to Galactic cosmic rays (Ryan et al. 2000). Moreover, the pre-Galactic but non-primordial component would by itself be indistinguishable from the true primordial component, and thus would lead to an overestimate of the BBN ${}^7\text{Li}$ production.

Our goal in this section is to exploit the γ -ray connection to constrain the structure-formation Li contamination. Unfortunately, we currently lack a detailed understanding of the amount and time-history of the structure formation cosmic rays (and resulting γ -rays and Li). Thus we will make the conservative assumption that *all* structure formation cosmic rays, and the resulting γ s and Li, are generated prior to *any* halo stars. Furthermore, we will assume that the pionic contribution to the EGRB is *entirely* due to structure formation cosmic rays. This allows us to relate observational limits on the pionic EGRB to pre-Galactic Li.

With this assumption and a SFCR composition $\Phi_\alpha^{\text{cr}}/\Phi_p^{\text{cr}} \approx y_\alpha^{\text{cr}} = 0.1$, we can now use the appropriate scaling factor from Table 3.1 to rewrite Eq. (3.13)

$$I_{\gamma_\pi^0}(\epsilon > 0, z) = \frac{\xi_\gamma \zeta_\alpha}{4\pi y_\alpha^{\text{cr}} y_\alpha^{\text{ism}}} \frac{\zeta \sigma_{\pi^0}}{\sigma_{6\text{Li}}^{\alpha\alpha}} \left(\frac{{}^6\text{Li}}{\text{H}} \right) n_b c \quad (3.32)$$

$$= 1.86 \times 10^{-5} \text{ photons cm}^{-2} \text{ s}^{-1} \text{ sr}^{-1} \left(\frac{{}^6\text{Li}}{{}^6\text{Li}_\odot} \right) \quad (3.33)$$

or

$$\left(\frac{{}^6\text{Li}}{{}^6\text{Li}_\odot} \right) = 0.538 \left(\frac{I_{\gamma_\pi^0}(> 0)}{10^{-5} \text{ cm}^{-2} \text{ s}^{-1} \text{ sr}^{-1}} \right) \quad (3.34)$$

where we used the solar lithium mole fraction $Y({}^6\text{Li})_\odot = 1.09 \times 10^{-10}$.

To set up an extreme upper limit on pre-Galactic SFCR ${}^6\text{Li}$, we assume that the *entire* pionic extragalactic γ -ray background came from SFCR-made pions, and was created prior to *any* halo star. As mentioned in the previous section, the method used in subtraction of the Galactic foreground is crucial for obtaining the EGRB spectrum. What is more, the EGRB spectrum is an important input parameter in the procedure described in Chapter 2 (Prodanović and Fields 2004a) where we estimate the maximal pionic γ -ray flux that will be used here. Our results (Fields and Prodanović 2005) for the SFCR lithium upper limits are collected in Table 3.2. The results depend on the choice of the EGRB spectrum as well as the redshift of origin of cosmic-rays according to the single-redshift approximation used in Chapter 2 (Prodanović and Fields 2004a) to obtain the maximal pionic EGRB fraction. Note that we considered only the two most extreme redshifts to illustrate the results. In the Table 3.2, z is the redshift, $I_{\gamma\pi}(> 0)$ is the upper limit for the pionic γ -ray intensity above 0 energy determined from (3.18) as explained in the previous section, $(\text{Li}/\text{H})_{\text{SFCR}}^{\text{max}}$ is the upper limit to total (${}^6\text{Li} + {}^7\text{Li}$) lithium abundance that can be of SFCR origin, while $\text{Li}_p^{\text{theo}}$ and Li_p^{obs} are the theoretical and observational primordial lithium abundances respectively as given in Eqs. (3.20) and (3.19).

Notice that for the case of Keshet et al. (2004) EGRB, since a spectrum was unavailable, the procedure described in Chapter 2 and section §3.3.1 for maximizing the pionic fraction of the EGRB could not be used. Thus, to place an upper limit on SFCR lithium we assumed that the entire EGRB can be attributed to decays of pions, that is, assume $I_\gamma = I_{\gamma\pi}^0$. For the Sreekumar et al. (1998) and Strong et al. (2004b) EGRB spectra, we use the upper limits to $I_{\gamma\pi}^0$ obtained in Chapter 2 (Prodanović and Fields 2004a). Once the $I_{\gamma\pi}^0$ is set we can use (3.34) to find the SFCR ${}^6\text{Li}$ upper limit.

To find the total halo star contribution we must also include ${}^7\text{Li}$, which is in fact produced more than ${}^6\text{Li}$ in $\alpha\alpha$ fusion: as seen in Table 3.1, $({}^7\text{Li}/{}^6\text{Li})_{\text{SFCR}} = \langle\sigma_{7\text{Li}}^{\alpha\alpha}\rangle/\langle\sigma_{6\text{Li}}^{\alpha\alpha}\rangle \approx 2$. The total SFCR elemental Li production appears in Table 3.2, both in terms of the absolute Li/H abundance and its ratio to the different measures of primordial Li (§3.3.2).

From Table 3.2 we see that the maximal possible SFCR contribution to halo star lithium could be quite substantial. If the pre-Galactic SFCR component is dominantly produced at high redshift (i.e. as in the $z \sim 10$ results) then the maximum allowed Li production can exceed the primordial Li production (however it is estimated), in some cases by a factor up to 25! The situation is somewhat better if the pre-Galactic SFCR production is at low redshift, but here it is hard to understand how this would predate the halo star component of our Galaxy. The high-redshift result is thus the more likely one, but also somewhat troubling in that the limit is not constraining. The indirect limits on SFCR Li in the previous section are somewhat stronger, but these also hold the door open for a significant level of pre-Galactic synthesis.

We caution that the lack of a strong constraint on SFCR Li production is not the same as positive evidence that the production was large. Recall that we have made several assumptions which purposely maximize the SFCR contribution; to the extent that these assumptions fail, the contribution falls, perhaps drastically. A more

detailed theoretical and observational understanding of the SFCR history, and of the EGRB, will help to clarify this situation. Moreover, given that the halo star Li is already found to be below the CMB-based ${}^7\text{Li}$ BBN results, we are already strongly biased to believe that the pre-Galactic SFCR component is *not* very large. Thus one might be tempted instead to go the other way and use Li abundances to constrain SFCR activity.

We thus now go the other way and use solar ${}^6\text{Li}$ to constrain the SFCR γ -ray flux. Again, given our incomplete knowledge of SFCRs, we must adopt a simplifying assumption about the degree of ${}^6\text{Li}$ production which is due to SFCR. To be conservative, we make the extreme assumption that *all* of the solar ${}^6\text{Li}$ is produced by SFCR, and thus find via Eq. (3.32) that γ -flux is $I_{\gamma_\pi^0}(> 0 \text{ GeV}) > 1.86 \times 10^{-5} \text{ photons cm}^{-2} \text{ s}^{-1} \text{ sr}^{-1}$. From (3.18) we can determine $I_{\gamma_\pi^0}(> 0.1 \text{ GeV})$ to be $0.23 \times 10^{-5} < I_{\gamma_\pi^0}(> 0.1 \text{ GeV}) < 1.43 \times 10^{-5} \text{ photons cm}^{-2} \text{ s}^{-1} \text{ sr}^{-1}$ depending on the redshift of pionic γ -rays, which is below the observed level as determined by Sreekumar et al. (1998), and a factor of 2-14 lower than the prediction based on GCR. Thus, for a given observed intensity $I_\gamma^{\text{obs}}(> \epsilon_0)$ we can now use (3.18) to constraint the hadronic fraction of EGRB, that is, calculate $f_\pi(> \epsilon_0, z)$ which is also presented in the Table 3.2.

However, since Li probably suffers some level of astration, the use of the solar ${}^6\text{Li}$ abundance does not give us the upper most limit to the required pionic γ -ray flux $I_{\gamma_\pi}(> 0)$. Thus, if one would to compensate for the depletion, the pionic fraction $f_\pi(> \epsilon_0, z)$ would become even larger.

Indeed, this may suggest a solution to the EGRB overproduction by GCRs, seen in the previous section. If ${}^6\text{Li}$ is mostly made by SFCRs, then the associated γ -ray production is in line with the observed background. In this case, ${}^6\text{Li}$ would still be of cosmic-ray origin, but not dominated by GCR production; this situation would be similar to that suggested by Suzuki and Inoue (2002), who found that GCR-created ${}^6\text{Li}$ only becomes comparable to the SFCR component near solar metallicities. Such a scenario faces tests regarding ${}^6\text{Li}$ and other LiBeB abundances and their Galactic evolution.

Chapter 4

IS THERE A SOLAR ${}^6\text{Li}$ PROBLEM?

4.1. OVERVIEW

Cosmic-ray nucleosynthesis is the only known Galactic source of the ${}^6\text{Li}$ (Vangioni-Flam et al. 1999, Fields and Olive 1999b). Thus, it is a standard belief that the observed solar abundance of this isotope was produced by Galactic cosmic-ray (GCR) interactions with the interstellar medium (ISM), where $\alpha\alpha \rightarrow {}^6\text{Li}$ is the dominant channel (Steigman and Walker 1992, Montmerle 1977c). However, in the previous Chapter we have shown that observations of the extragalactic gamma-ray background (EGRB) allow for only $\sim 25\%$ of the solar ${}^6\text{Li}$ abundance to be produced by GCRs. Given the current interest in ${}^6\text{Li}$, this result thus deserves a thorough investigation.

In this Chapter⁸ (Prodanović and Fields 2006) we revisit the problem of lithium- γ -ray consistency with a more precise and realistic calculation. We now employ a carefully propagated cosmic-ray spectrum, as opposed to the standard single-power law spectrum used in Chapter 3 (Fields and Prodanović 2005). Moreover, instead of using a convenient fit for the pionic γ -ray spectrum (Eq. (2.6), Pfrommer and Enßlin 2004) we now calculate it self-consistently from our CR spectrum. We also estimate the spallation $p, \alpha + \text{CNO} \rightarrow {}^6\text{Li}$ contribution to the solar ${}^6\text{Li}$ abundance. These effects slightly reduce but do not eliminate the discrepancy. Moreover, the only remaining effect we expect to be important- ${}^6\text{Li}$ destruction as it is processed through stars-makes the problem more severe. The net effect is that in a realistic calculation, the observed EGRB allows for only $\approx 60\%$ of the solar ${}^6\text{Li}$ abundance to be produced by standard GCRs. Only a conspiracy of extreme assumptions gives GCR production of the solar ${}^6\text{Li}$ that does not at the same time saturate the observed EGRB.

Our result represents a strong hint for the need of a new ${}^6\text{Li}$ source. Recent suggestions such as dark matter and low-energy cosmic rays are discussed in Chapter 7. Upcoming gamma-ray observations by *GLAST* (Gehrels and Michelson 1999) will better constrain (or determine!) the pionic γ -ray fraction of the EGRB and will thus be the key in determining the severity of this problem.

⁸Parts of this were already published in a refereed journal (Prodanović and Fields 2006)

4.2. COSMIC-RAY SPECTRUM

In Eq. (3.13), the Li- γ -ray proportionality depends on the ratio of the mean cross sections $\sigma_\gamma/\sigma_{\alpha\alpha}^i$. These must be properly averaged over the GCR energy spectrum. In previous Chapter, Section 3.4 (Fields and Prodanović 2005), we have adopted a standard propagated cosmic-ray spectrum which is a single power-law in total energy with a spectral index $\alpha = 2.75$ over the entire relevant energy range. While this is a commonly-used rough approximation to the GCR spectrum, it becomes inaccurate at energies $\lesssim 1$ GeV, where ionization energy losses dominate over escape losses. Because $\alpha\alpha \rightarrow {}^6\text{Li}$ threshold energy is at ~ 10 MeV/nucleon, while $pp \rightarrow \pi^0$ threshold is at ~ 280 MeV, the Li- γ connection is particularly sensitive to GCR behavior at very low energies. Note however, that due to stellar wind modulation, interstellar GCR spectrum is not well measured in this low-energy regime. Thus in this Chapter we refine on the analysis presented in Section 3.4 (Fields and Prodanović 2005) by calculating and implementing a carefully propagated CR spectrum for a leaky box model (Meneguzzi et al. 1971).

In the leaky box model CRs propagate freely in a containment volume, but with some constant probability of escape from this volume. Thus, the propagation equation in the leaky box model can be written as

$$\frac{\partial n_i}{\partial t} = Q_i + \frac{\partial(b_i n_i)}{\partial \epsilon} - \frac{1}{\tau_{esc}} n_i = 0 \quad (4.1)$$

where the steady state was assumed. The energy per nucleon is given as ϵ , while n_i is the number density of CR species i in energy interval $d\epsilon$ and Q_i is the source term. Energy losses to the ISM (ionization) are given as $b_i = -(\partial\epsilon/\partial t)_i$ while $1/\tau_{esc}$ accounts for energy losses due to escape. Writing the flux of species i as $\phi_i(\epsilon) = n_i v(\epsilon)$ we can rewrite Eq. (4.1) as

$$\frac{\partial \phi_i(\epsilon)}{\partial \epsilon} = -\frac{1}{b_i \tau_{esc}} \phi_i(\epsilon) + \frac{v}{b_i} Q_i(\epsilon). \quad (4.2)$$

This is the ordinary linear differential equation and thus we find the solution in the form

$$\phi_i(\epsilon) = \frac{1}{w_i(\epsilon)} \int_\epsilon^\infty d\epsilon' q_i(\epsilon') \exp \left[- \int_\epsilon^{\epsilon'} \frac{d\epsilon''}{\Lambda(\epsilon'')} \frac{\partial(v\phi)_i}{\partial \epsilon''} \right] \quad (4.3)$$

where we have introduced $q_i(\epsilon) \equiv Q_i(\epsilon)/\rho_{\text{ISM}}$ and $w_i(\epsilon) \equiv b_i/\rho_{\text{ISM}}$. Energy-dependent escape path-length $\Lambda(\epsilon)$ is given as a function of rigidity $R = cp/Zv$ (Gaisser 1990):

$$\Lambda = v\tau_{esc}\rho_{\text{ISM}} = \begin{cases} 10.8 \text{ g/cm}^2 \beta \left(\frac{4}{R}\right)^{0.6} & R > 4 \text{ GV} \\ 10.8 \text{ g/cm}^2 \beta & R < 4 \text{ GV} \end{cases}. \quad (4.4)$$

We calculate ionization energy losses $d(v\phi)_i/d\epsilon = dX(\epsilon)/d\epsilon$ by adopting a standard Bethe-Bloch formula (Bethe 1930) where $X(\epsilon)$ is the ionization energy loss range of protons in units g/cm^2 (grammage):

$$\frac{d\epsilon}{dX} = \frac{4\pi z Z^2 e^4}{A\langle m \rangle m_e v^2} \left[\ln \left(\frac{2\gamma^2 m_e v^2}{I} \right) - \frac{v^2}{c^2} \right]. \quad (4.5)$$

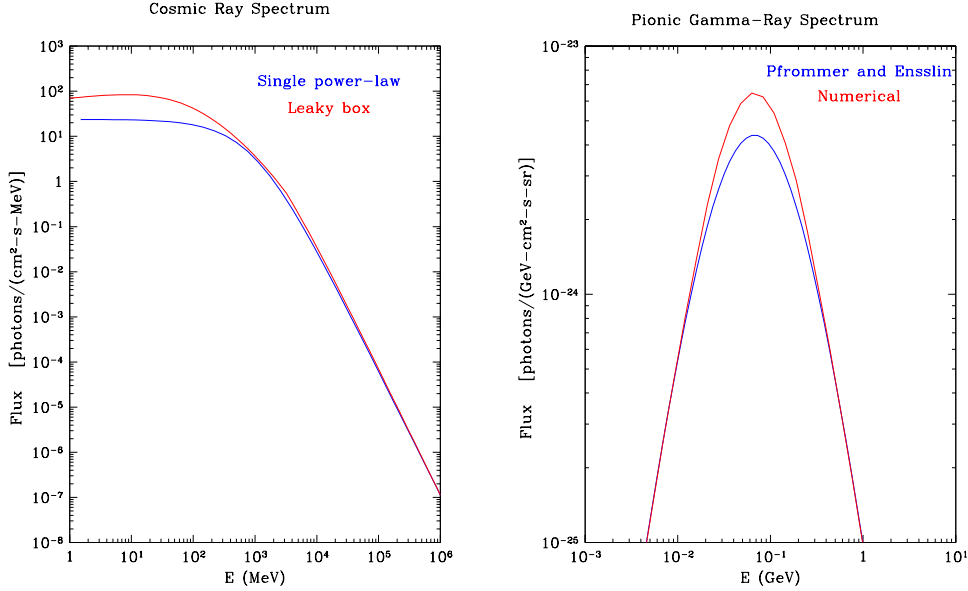


Figure 4.1: On the left panel we compare single power-law cosmic-ray spectrum used in Chapter 3 (Fields and Prodanović 2005) with CR spectrum calculated from the leaky box model and used in this Chapter (Prodanović and Fields 2006). On the right panel we compare Pfrommer and Enßlin (2004) fit for the pionic gamma-ray spectrum (used in Chapters 2, 3 and 5) with the one used in this Chapter, which was numerically calculated from Dermer’s model and using a carefully propagated cosmic-ray spectrum.

Here Z is the projectile charge, A is the nucleon number, z is the number of electrons per atom (≈ 1), $I = 13.6$ eV is the mean excitation potential of hydrogen ionization energy, while the mean target mass is $\langle m \rangle = m_p \sum A_i y_i / \sum y_j \approx 1.4 m_p$. Finally, we assume a standard source spectrum which is a power-law in momentum (e.g. Gaisser 1990) $q_i \propto p^{-2.2} = \phi_i(\epsilon)/\Lambda$ (units $\text{g}^{-1}\text{s}^{-1}\text{MeV}^{-1}$), while we normalize it by using CR observations at higher energies where $\phi_i(\epsilon) \propto \epsilon^{-2.75}$.

As we can see on the left panel of Fig. 4.1 this gives ~ 4 times higher CR flux around $\alpha \rightarrow {}^6\text{Li}$ threshold, compared to the one used in Section 3.4 (Fields and Prodanović 2005) where a single power-law spectrum was assumed, while for energies $\gtrsim 1$ GeV a single-power law spectrum is a good approximation.

4.3. PIONIC GAMMA-RAY SPECTRUM

Pfrommer and Enßlin (2004) provide a useful parametrization of the pionic γ -ray spectrum used in Chapter 2 (Fields and Prodanović 2005). However, here we numerically calculate the pionic γ -ray spectrum in full detail, by adopting Dermer’s isobar+scaling model (Dermer 1986); the pionic spectrum we adopt uses the same cosmic-ray spectrum as the ${}^6\text{Li}$ production, and thus is self-consistent.

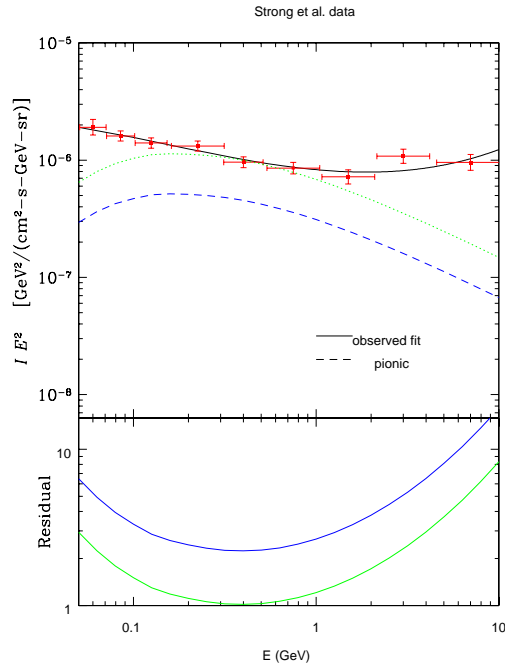


Figure 4.2: In the upper panel of this figure, we plot the pionic spectrum (dotted green line - maximized, dashed blue line - normalized to the Milky Way), compared to the observed EGRB spectrum (solid line, fit to data); we use the Strong et al. (2004b) data points, which are given in red crosses. The bottom panel represents the residual function, that is, $\log[(IE^2)_{\text{obs}}/(IE^2)_{\pi}] = \log(I_{\text{obs}}/I_{\pi})$.

At the lower energy end, Dermer’s model uses the isobar theory (Stecker 1970), where the π^0 meson is produced by the excitation of the $\Delta_{3/2}$ resonance ($pp \rightarrow p\Delta_{3/2} \rightarrow pp\pi^0$). On the other hand, the scaling model (Stephens and Badhwar 1981) is based on the accelerator data of the Lorentz invariant cross section for $pp \rightarrow \pi^0$ production at energies above ~ 12 GeV, and is thus used for the higher energy end in Dermer’s model.

In order to calculate $I_{\gamma\pi}$ one needs to know the history of the CR sources and the targets. Both histories come from cosmic star-formation rate. As described in detail in Chapter 3 (Fields and Prodanović 2005) we can obtain the GCR pionic γ -ray spectrum integrated over the history of the sources (Eq. 3.26, same parameter values used). The cosmic star-formation rate alone fixes the *shape* of the pionic EGRB, but requires a normalization that physically connects the star formation rate to cosmic-ray flux, and which normalizes the present gas fraction in a typical galaxy. In order to place an *upper limit* to the pionic EGRB, we allow this normalization to vary freely to maximize (as described in Chapter 2) the pionic γ -ray flux consistent with present EGRB observations (Fields and Prodanović 2005, Prodanović and Fields 2004a). This is presented in Fig. 4.2 as a dotted green line. The observed EGRB spectrum is that of Strong et al. (2004b) and is plotted as red data points, with a black solid line fit

(Fields and Prodanović 2005). Finally, we find maximal pionic γ -ray fraction to be 58% of the total observed EGRB.

More realistically, we can use the Milky Way to determine both the scaling between star formation rate and cosmic-ray flux, and the present-day gas fraction. We do this again by following Pavlidou and Fields (2002), in the same way as in §3.4.2, adopting the same parameters. The resulting γ -ray spectrum is presented in Fig. 4.2 as a blue dashed line. This corresponds to the pionic γ -ray contribution expected from the normal galaxies. In addition to this guaranteed component to the EGRB, unresolved blazars will also contribute significantly Pavlidou and Fields (2002), presumably comprising much or all of the remaining signal.

Having determined an upper limit and a more realistic estimate to $I_{\gamma\pi}$ one can find the corresponding ${}^6\text{Li}$ abundance, via Eq. (3.13). This is our main goal, to which we now turn.

4.4. ESTIMATES OF GCR-PRODUCED ${}^6\text{Li}$

In this section we calculate limits to and estimates of the ${}^6\text{Li}$ produced by GCRs that are allowed by preset EGRB data. We present our results in the steps of increasing realism. For now we retain the Copernican assumption that the Milky Way cosmic-ray fluence is typical of star-forming galaxies ($F_{\text{MW}}/F_{\text{MW}} = 1$); we will revisit this assumption in the final Chapter.

1. By using Eq. (3.13), *maximal* pionic γ -ray fraction and procedure described in Chapter 3 (Fields and Prodanović 2005), we find the fraction of ${}^6\text{Li}$ abundance produced in $\alpha\alpha \rightarrow {}^6\text{Li}$ reaction to be ${}^6\text{Li}_{\alpha\alpha} = 0.61 {}^6\text{Li}_{\odot}$ (${}^6\text{Li}_{\odot} \equiv {}^6\text{Li}/\text{H} = 1.53 \times 10^{-10}$; Anders and Grevesse 1989). This corresponds to an extreme upper limit for all ${}^6\text{Li}$ produced by the GCR $\alpha\alpha$ reaction.
2. Though the $\alpha\alpha$ reaction with the ISM is the dominant channel for ${}^6\text{Li}$ production, a non-negligible contribution, especially at higher metallicity, comes from spallation reactions $p, \alpha + \text{CNO} \rightarrow {}^6\text{Li}$ (both forward and inverse kinematics, that is fast heavy nuclei, are included). If the fusion and the CNO reaction rates were to be equal the required oxygen abundance should be $(\text{O}/\text{H})_{\text{eq}} = 0.51 (\text{O}/\text{H})_{\odot}$ (the procedure is described in Appendix 3 in detail). This now sets the normalization and allows us to calculate the total ${}^6\text{Li}$ abundance produced from all channels with extreme assumption that ISM was at *solar metallicity* over the Galactic history. We find that ${}^6\text{Li}_{\text{GCR}} = 1.79 {}^6\text{Li}_{\odot}$, which now represents the extreme upper limit for *all* ${}^6\text{Li}$ produced by GCRs.
3. Because cosmic-ray CNO abundance is a direct function of the Galactic supernova rate, a precise calculation introduces a factor of 1/2, that is, instead of assuming solar metallicity through out history one should use an average value of $(\text{O}/\text{H})_{\text{eq}} = 0.5 (\text{O}/\text{H})_{\odot}$. This results in the total allowed GCR-produced ${}^6\text{Li}$ abundance of ${}^6\text{Li}_{\text{GCR}} = 1.20 {}^6\text{Li}_{\odot}$, which is still consistent with the standard picture.

4. So far we have been taking the maximal (Fig. 4.2), dotted green line) pionic γ -ray fraction as allowed by the present EGRB data⁹, where we have (without justification) ignored the normalization and just used the shape of our spectrum. However, it is unrealistic to assume that entire emission is due to GCRs. Indeed, independent of the details of our galactic γ -ray estimate, it is clear that the EGRB must contain a large and perhaps dominant contribution from the unresolved AGNs (blazars) and so the galactic signal must leave room for this and cannot saturate the observed level. An estimate of the normalized GCR pionic γ -ray component of the EGRB (Fig. 4.2, dashed blue line) yields a spectrum that is a factor of 2.1 lower than the maximized value. Thus, in this most honest case, we find ${}^6\text{Li}_{\text{GCR}} = 0.57 {}^6\text{Li}_{\odot}$ which now falls short by about a factor of 2 from a standard picture of cosmic-ray ${}^6\text{Li}$ nucleosynthesis.
5. For inverse CNO kinematics a non-negligible LiBeB production comes from two-step spallation reactions, eg. $\text{O} + \text{H} \rightarrow {}^{11}\text{B} + \text{H} \rightarrow {}^6\text{Li}$ (Kneller et al. 2003). For example, production rate of ${}^6\text{Li}$ from two-step reactions of fast oxygen is $\sim 40\%$ of single-step fast oxygen spallation reactions, for a fixed $\Lambda = 10 \text{ g/cm}^2$ (Kneller 2006). However, when two-step inverse CNO kinematics is taken into account, the overall increase is only slight and the result now becomes

$${}^6\text{Li}_{\text{GCR}} = 0.59 {}^6\text{Li}_{\odot}. \quad (4.6)$$

Even in the most extreme assumption that the two-step rates are equal to the single-step inverse CNO kinematic rates, the resulting ${}^6\text{Li}$ abundance would still be only 63% of the solar.

6. Finally, one has to remember that the observed solar ${}^6\text{Li}$ abundance is not the total lithium abundance produced, due to astration, that is, the fact that some of the gas was already processed by stars. Due to very fragile nature of this isotope, ${}^6\text{Li}_{\odot}$ is only the lower bound on the total ${}^6\text{Li}$ produced. For a rough estimate of the level of astration one can use the deuterium. It has been known that the Big Bang nucleosynthesis is the only important source of D (Epstein et al. 1976, Prodanović and Fields 2003) and that it is easily destroyed in stars due to a similarly fragile nature. Thus by comparing the solar nebula D abundance $D_{\text{presol}} = 2.1 \times 10^{-5}$ (Geiss and Gloeckler 1998) with the abundance determined from 5 best quasar absorption systems $D_{\text{QSO}} = 2.78 \times 10^{-5}$ (Cyburt et al. 2003b), we find that roughly $\sim 25\%$ of the gas has passed through stars. Thus ${}^6\text{Li}_{\odot}$ is about $\sim 75\%$ of ${}^6\text{Li}_{\text{tot}}$, and our calculated GCR ${}^6\text{Li}$ now becomes ${}^6\text{Li}_{\text{GCR}} \sim 0.45 {}^6\text{Li}_{\text{tot}}$.

We see that our result either indicates the need for a new important source of ${}^6\text{Li}$ beyond the standard GCR nucleosynthesis, or it points to a possible failure of the usual assumption that the average interstellar Galactic cosmic-ray flux tracks

⁹Determination of the EGRB relies on the subtraction of the Galactic Plane and is thus model-dependent. Moreover, Keshet et al. (2004) report only a limit to the EGRB. Adopting this limit in our analysis would only strengthen our result.

the instantaneous star formation rate. We will consider each possibility in turn in the Discussion Chapter. However, one of the uncertainties comes from normalizing to the Milky Way. Our calculation is hampered by lack of evidence of the “pion bump” in the Milky Way γ -ray spectrum. Fortunately, we (Prodanović et al. 2007) have recently shown how future GeV–TeV–PeV gamma-ray observations of the diffuse emission from the Galactic Plane can determine the level of pionic γ -ray emission in the Milky Way, which we demonstrate in the next Chapter (Prodanović et al. 2007).

Chapter 5

DIFFUSE TeV GAMMA-RAY OBSERVATIONS

5.1. OVERVIEW

The Milky Way Galactic Plane has long been known to be a strong source of diffuse gamma-ray emission (Kraushaar et al. 1972, Fichtel et al. 1975). The Energetic Gamma Ray Emission Telescope (EGRET) instrument on the Compton Gamma-Ray Observatory satellite measured this emission over the full sky and for energies in the range 0.03 – 10 GeV, with reasonably high resolution in each bin (where the data are reported with angular bins of width 0.5 degree and with several logarithmically-spaced bins per decade in energy (Hunter et al. 1997)). It was expected that a very significant component of the diffuse emission would arise from the decays of neutral pions ($\pi^0 \rightarrow \gamma + \gamma$), arising from the collisions of hadronic cosmic rays with the hadronic component of the interstellar medium (i.e. $p + p \rightarrow p + p + \pi^0$; Stecker 1970, 1971, Dermer 1986). We refer to these throughout this book as “pionic” gamma rays, to distinguish them from gamma rays produced by leptonic processes, e.g. the inverse-Compton upscattering of ambient photons by very high-energy electrons.

The spatial variation of the pionic component of the diffuse Galactic gamma-ray emission should track the column density of the interstellar medium. However, since other sources of gamma rays also depend, though in more complicated ways, on the imprecisely-known distribution of interstellar matter and radiation, it is difficult to extract the pionic component by its spatial dependence alone. As discussed in Chapter 2, the energy spectrum of the pionic gamma-rays has characteristic shape, however observations do not reveal any strong evidence of this “pion bump”. Based on the lack of this feature we found the maximal pionic fraction of the diffuse Galactic Plane emission to be $\sim 50\%$ (Chapter 2; Prodanović and Fields 2004a). This is supported by the very detailed and comprehensive study of the Galactic gamma-ray emission by Strong et al. (2004c). That study indicates that a key second feature of pionic gamma rays is that at high energies (certainly by ~ 1 TeV) they should dominate the total emission and their slope will follow that of the hadronic cosmic rays. (The emission at energies below the bump is expected to be subdominant to the leptonic components.) In the GeV energy range, a significant component of the observed EGRET data is not well explained, and this discrepancy, which is observed in all sky directions, is known as the “GeV excess” (Hunter et al. 1997).

In this Chapter¹⁰ (Prodanović et al. 2007), we consider constraints on the pionic gamma rays from experiments operating at much higher energies than EGRET. There are upper limits on the total gamma-ray emission near both TeV ($= 10^3$ GeV) and PeV ($= 10^6$ GeV) energies. Depending on assumptions about the slope of the hadronic cosmic ray spectrum, these place at least somewhat restrictive limits on the pionic gamma-ray emission. However, the most exciting recent development is the first positive *detection* of diffuse gamma-ray emission from the Galactic Plane, by the Milagro Collaboration (Atkins et al. 2005). They find $\phi_\gamma(> 3.5 \text{ TeV}) = (6.8 \pm 1.5 \pm 2.2) \times 10^{-11}$ photons $\text{cm}^{-2} \text{s}^{-1} \text{sr}^{-1}$ in the Galactic Plane region of longitude $\ell \in (40^\circ, 100^\circ)$ and latitude $|b| < 5^\circ$. The basic question of the present Chapter is “What is the origin of the (apparently) diffuse flux observed by Milagro?”. The Milagro Collaboration argued that their result is consistent with being purely pionic in origin, though they note that some of the flux may arise from unresolved point or extended sources (Atkins et al. 2005). As we will argue in steps of increasing detail, their result appears to be *too large* to be purely pionic, and thus seems to indicate a new mystery of Galactic gamma rays, which we will call the “TeV excess.” Our GeV–TeV–PeV overview perspective is shown in Fig. 5.1. In brief, our arguments are as follows:

1. We can simply extrapolate the last EGRET points to higher energies, and the Milagro result should not exceed this trend – and while it does not, it could not be any larger. This is shown in Fig. 5.1 as the solid line.¹¹ This alone indicates that a strong inverse Compton component at high energies is disfavored (Atkins et al. 2005), in agreement with considerations at lower energies (Strong et al. 2004c). In the PeV range, this extrapolation appears to be at best barely allowed, and is possibly excluded, depending on the choice of the hadronic cosmic ray spectrum.
2. A more sophisticated approach is to only extrapolate the pionic component to high energies, where it should dominate. We first consider a pionic component of maximal normalization (while this is unrealistically high, it is in fact *lower* than the normalization obtained if the GeV EGRET data is effectively assumed to be purely pionic, as above). We allow two choices for the hadronic cosmic ray energy spectrum slope at high energies, as shown by the dashed lines in Fig. 5.1. The first, with index $\alpha = 2.61$ (for $d\phi/dE \sim E^{-\alpha}$), is motivated by the slope chosen by the Milagro Collaboration, which provides a good single-parameter fit joining the highest-energy EGRET points to the Milagro point. We argue below that the physics of pionic emission suggests that this is an unrealistically shallow spectrum if the observed GeV–TeV signal is indeed pionic. When we instead choose $\alpha = 2.75$, in accordance with the locally observed cosmic rays (Asakimori et al. 1998), we find that the Milagro measurement is 5 times *larger*

¹⁰Parts of this were already published in a refereed journal (Prodanović et al. 2007)

¹¹The Milagro Collaboration extrapolated the *integral* energy spectrum, while we use the *differential* energy spectrum (though adopting the same spectral index). While these procedures are in principle equivalent, the smoothness of the integral spectrum comes at the cost of correlations between the points.

than the *maximal* pionic flux allowed at 3.5 TeV. The PeV limits are on the verge of ruling out (or detecting!) the pionic signal, regardless of the choice of α . In addition, when the PeV limits are derived using local cosmic ray spectrum, this rules out the continuation of GeV-TeV $\alpha = 2.61$ gamma-ray power law to PeV energies.

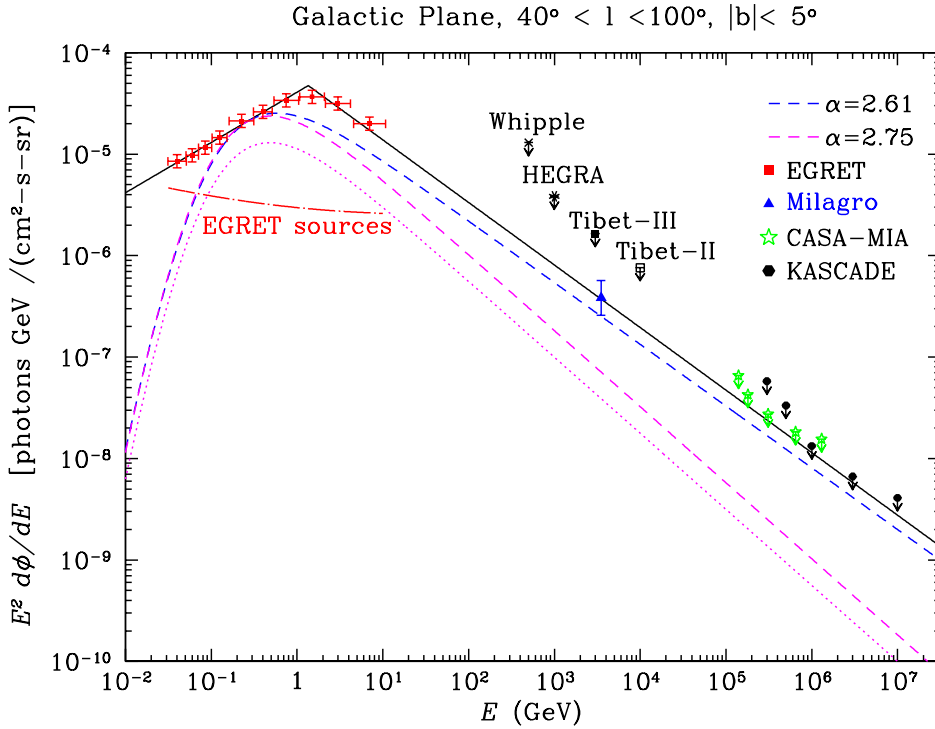


Figure 5.1: The diffuse gamma-ray GeV-TeV-PeV spectrum of the Galactic plane in the region visible to Milagro. The EGRET data points and the Milagro signal are empirically well-fit (solid line) with a spectral index $\alpha = 2.61$. The *maximized* pionic spectrum appears in the dashed lines; we see that pionic emission having the empirical $\alpha = 2.61$ index (dark blue line) signal comes close to (but somewhat undershoots) the Milagro result; on the other hand, the maximal pionic signal generated by cosmic rays with the locally measured $\alpha = 2.75$ spectrum (magenta lines) falls far short of Milagro, leaving a TeV excess. The dotted line represents a pionic spectrum normalized to the one plotted in de Boer et al. (2005) (their Fig. 5, region B) at $E = 1$ GeV. The PeV limits of CASA-MIA and KASCADE are on the verge of being constraining (see also Fig. 5.2). Finally, fluxes of the ten EGRET sources that we have identified were smoothed over the Milagro field of view and then summed, which is plotted with red dash-dotted line; the Milagro result falls below the extrapolation of this trend and thus demands a significant break in some or all of the EGRET source spectra (see also Fig. 5.3).

3. More realistically, the normalization of the pionic component should be even lower, at most $\sim 50\%$ of maximal in the “optimized” model of Strong et al. (2004c) designed to minimize the GeV excess. On the other hand, the “conventional” model of Strong et al. (2004c), which uses the locally observed cosmic-ray spectrum and normalization, comes somewhat closer to the EGRET data near the pionic maximum at $m_\pi/2$, but leaves the GeV excess (thus motivating the non-standard optimized model). The results from the conventional model appear as the dotted line in Fig. 5.1. As noted by de Boer et al. (2005), the GeV excess of the conventional model allows room for a large component of gamma rays from dark matter annihilation products (including pions, though we reserve the word “pionic” to refer to pions produced by cosmic ray collisions with the interstellar medium). These gamma rays from dark matter are claimed to help ameliorate the GeV excess (note that their spectrum abruptly ends below the dark matter mass of 50–100 GeV). We point out here that this interpretation *increases* the TeV excess, making the Milagro measurement about 10 times larger than the pionic component.

Thus, taking a realistic normalization and slope for the pionic component, we find that the Milagro measurement seems to indicate a TeV excess, which would be even more interesting than their conclusion that their result may be consistent with being purely pionic. Our arguments are supported by the gamma-ray flux limits at PeV energies. The diffuse gamma-ray data is summarized in Section 5.2. In Section 5.3 we analyze the consistency of the data with diffuse pionic emission, and explore the possibility of unresolved sources contributing significantly to the Milagro measurement. We go on in Section 5.4 to show how the framework of the GeV–TeV–PeV Galactic gamma-ray emission can be tested in detail. We conclude in Section 5.5 with an observational strategy which uses present and upcoming gamma-ray experiments to disentangle the nature of diffuse Galactic gamma-ray sources, both pionic and otherwise.

The resolution of the outstanding issues has important implications for more than just the pionic gamma rays, and will shed new light on Galactic cosmic rays in numerous ways: it will probably finally detect, and at least strongly constrain, the presence and interactions of hadronic cosmic rays throughout the Galactic interstellar medium; it will constrain the origin, source distribution, and spectra of both hadronic and leptonic cosmic rays; and it will thereby sharpen our account of the Galactic cosmic ray energy budget and thus the efficiency of cosmic ray accelerators. Furthermore, a detailed and quantitative understanding of astrophysical sources of diffuse Galactic gamma-rays will greatly clarify the existence and nature of any other Galactic sources, such as dark matter. And finally, a good understanding of Galactic gamma-rays will allow for this foreground to be better subtracted to obtain the diffuse extragalactic gamma-ray background.

5.2. HIGH-ENERGY GAMMA-RAY DATA

The Milagro Gamma-Ray Observatory is a ground-based water Čerenkov detector in New Mexico that collects air-shower particles created when high-energy particles interact in the atmosphere; showers initiated by gamma-rays and hadrons can be statistically distinguished by how they register in the detector (Atkins et al. 2003, 2004, 2005). The Milagro Collaboration recently reported a diffuse flux $\phi_\gamma(> 3.5 \text{ TeV}) = (6.8 \pm 1.5 \pm 2.2) \times 10^{-11} \text{ photons cm}^{-2} \text{ s}^{-1} \text{ sr}^{-1}$ of gamma rays from the Galactic Plane region $\ell \in (40^\circ, 100^\circ)$ and latitude $|b| < 5^\circ$ (Atkins et al. 2005). Note that this emission is integrated over both higher energies and also the entire angular region, where no resolved sources were detected (Atkins et al. 2005). In fact, to obtain the Galactic Plane diffuse emission Milagro did not directly measure the gamma-ray flux, but rather the ratio of electromagnetic to hadronic showers. Furthermore, their measurement was made by subtracting the off-source and on-source (Galactic Plane) fluxes, in order to cancel the isotropic cosmic-ray component; this also cancels the extragalactic gamma-ray background, which is at the otherwise relatively high level $\sim 10^{-6} \text{ GeV cm}^{-2} \text{ s}^{-1} \text{ sr}^{-1}$ (compare in Fig. 5.1). An independent measurement of the hadronic cosmic-ray flux was then taken to derive the gamma-ray flux, and the result also depends on the assumed spectral indices of each species. We note that for the hadronic cosmic rays, Milagro adopts the conventional observed value $\alpha = 2.75$.

The Milagro Collaboration reports that their result is consistent with the diffuse emission extrapolated from EGRET, assuming a spectral index $\alpha = 2.61$, which is taken from the last four points of the EGRET integral spectrum (Atkins et al. 2005). This single-parameter fit provides a good description of these data. (By extrapolating from the EGRET differential spectrum, our Fig. 5.1 highlights the uncertainty in this procedure, that is, it demonstrates how a small change in the assumed spectral index can be important over a large energy range.) The apparent success of a single power law over this large energy baseline is very suggestive that the emission at these energies is dominated by a single source. In particular, given the understanding of how the various components of the diffuse emission change with energy from Strong et al. (2004c), one sees that this effectively assumes that all of the EGRET GeV data is pionic. However, the Milagro Collaboration is careful to note that their result could have a contribution from unresolved point or extended sources (Atkins et al. 2005, Nemethy 2005).

This first detection of diffuse emission at TeV energies invites a detailed comparison with other data. In our analysis, we will start with the assumption that Milagro detection corresponds to truly diffuse pionic emission, and then investigate the validity and consequences of this.

The EGRET data covers the range 0.03 – 10 GeV and is publicly available from the NASA archives¹² in the form of integral gamma-ray fluxes (in a given energy bin) at a given galactic coordinate where the coordinate step is 0.5° . We have taken those data points that fall into the Milagro region $\ell \in (40^\circ, 100^\circ)$, $|b| < 5^\circ$, and averaged them for each energy bin. Finally, we have determined the EGRET gamma-ray flux at the mean energy for each bin, where the underlying assumption is that the flux is

¹²EGRET data archive: <http://coss.c.gsfc.nasa.gov/docs/cgro/egret/>

energy-independent over the width of a bin. This is presented in Fig. 5.1 with red data points. Following Strong et al. (2004c), we took fixed fractional uncertainties of 15% on the fluxes (since these are predominantly systematic in nature, they do not change when the field of view changes). Below, we additionally consider the EGRET sources detected in this region, taking their spectra from the Third EGRET Catalog (Hartman et al. 1999).

We also consider the upper limits on gamma-ray fluxes from other high-energy experiments. Although these experiments did not observe exactly the same region of the Galactic Plane as Milagro, we argue that their results can be put on a common footing. Especially at and above 1 TeV, it is expected that the diffuse Galactic emission is purely pionic, and hence scales with the column density (Strong et al. 2004c). Then fluxes from different regions of the Galactic Plane, if corrected for differences in column density, can be made *physically equivalent*, even if they are *geographically distinct*. This depends on the common assumption that there are no significant variations in the hadronic cosmic ray fluxes and spectra as a function of position in the Galactic Plane (e.g. Strong and Mattox 1996; but see also Strong et al. 2004a).

To correct for the differences in column density in different regions of the Galactic Plane, we take a simplistic approach and scale from the EGRET diffuse flux at lower energies (even though it is not purely pionic at those energies, this should be a reasonable approach for the relative variations in expected intensity). We calculate the region correction factor by comparing the EGRET diffuse gamma-ray flux averaged over the Milagro region with the one averaged over the region observed by a given experiment. We find that our correction factors do not vary much with energy. Table 5.1 summarizes the input data and the region correction factors f_{rc} . Here, $f_{rc} = F_{EG,reg}/F_{EG,Milagro}$ where $F_{EG,reg}$ and $F_{EG,Milagro}$ are the diffuse gamma-ray flux observed by EGRET and averaged over a given Galactic region and the region observed by Milagro, respectively.

For energies near 1 TeV, we show in Fig. 5.1 the equivalent upper limits on the diffuse Galactic gamma-ray emission from the Whipple 2000, HEGRA (Aharonian et al. 2001) and Tibet-II/III (Amenomori et al. 2006) experiments. For energies near 1 PeV, we also show the similar upper limits from the CASA-MIA (Borione et al. 1998) and KASCADE (Schatz et al. 2003) experiments.

Table 5.1: Diffuse gamma-ray observations used in this Chapter. The flux limits quoted by the various experiments are divided by f_{rc} before being shown in our Fig. 5.1; this compensates for the differences in expectations for different regions.

Experiment	Observation Region		Region Correction f_{rc}	Spectral Index α	Confidence Limit
	ℓ range	$ b $ range			
Milagro	(40°, 100°)	< 5°	$\equiv 1$	2.61	99 %
Whipple	(38.5°, 41.5°)	< 2°	1.6	2.4	99.9 %
HEGRA	(38°, 43°)	< 2°	1.6	2.6	99 %
Tibet II, III	(20°, 55°)	< 2°	1.6	2.5	99 %
CASA-MIA	(50°, 200°)	< 5°	0.7	2.66	90 %
KASCADE	R.A. \in (0°, 360°)	$\delta \in$ (14°, 84°)	0.2	independent	90 %

The diffuse gamma-ray limits reported have an underlying assumption of a spectral index. We present each observational limit as originally reported with their assumed spectral index. For CASA-MIA, only the ratio of gamma-ray to hadronic integrated fluxes was reported in Borione et al. (1998), and we take the spectral index given by Glasmacher et al. (1999). We have to note here that there is a strong dependence of CASA-MIA limits on the assumed spectral index. This point is emphasized in Fig. 5.2 where we plot the CASA-MIA limits for their measured spectral index $\alpha = 2.66$ (Glasmacher et al. 1999), and also for the steeper spectral index of $\alpha = 2.80$ reported by JACEE (Asakimori et al. 1998). On the other hand, the KASCADE limits (Schatz et al. 2003) do not depend on the assumption of the spectral index (Schatz 2006).

5.3. ANALYSIS OF THE DATA

5.3.1. DIFFUSE COMPONENTS

For pionic gamma-ray spectrum ($p_{\text{cr}} + p_{\text{ism}} \rightarrow p + p + \pi^0$, followed by $\pi^0 \rightarrow \gamma + \gamma$) we again adopt (Pfrommer and Enßlin 2004) fit. As we can see from Eq. (2.6), the pionic spectral shape is determined by a single parameter, the cosmic-ray spectral index α . However, we note that there are still uncertainties in this pionic source function; see the discussions in e.g. Blattnig et al. (2000) and Kamae et al. (2005). At the present level of analysis, the uncertainties in the astrophysical inputs, particularly the Galactic cosmic-ray spectrum, are larger.¹³ In Chapter 2, we (Prodanović and Fields 2004a) have shown that the lack of a strong pionic feature at $m_\pi/2$ in the diffuse Galactic gamma-ray data can be used to place a model-independent (i.e. flux-independent) upper limit on the pionic component of $\sim 50\%$.

For better comparison to other data, we assume a spectral index and convert the Milagro energy-integrated flux into a differential flux, also evaluated at 3.5 TeV. If we adopt the Milagro best-fit gamma-ray index of $\alpha = 2.61$, we find a gamma flux of $d\phi/dE = (3.1 \pm 1.2) \times 10^{-14}$ photons $\text{cm}^{-2} \text{s}^{-1} \text{GeV}^{-1} \text{sr}^{-1}$. This point is shown in Fig. 5.1 as a blue triangle. We note here that if the integral flux reported by Milagro is recalculated for a more realistic spectral index of $\alpha = 2.75$ then the variation of the flux is just 6%, which is much smaller than reported uncertainty.

Even when the pionic component is maximized as in Chapter 2 (Prodanović and Fields 2004a), it fails to explain the Milagro result. To appreciate this mismatch, it is important to recall that the physics of the pionic signal demands that above the pion bump, the pionic spectrum is characterized by a single spectral index which is the same as that of the cosmic rays. Thus, if the high-energy EGRET and Milagro points are due to pionic emission, their spectral index must reflect the underlying cosmic ray index along the line of sight. If we adopt the best-fit EGRET/Milagro index $\alpha = 2.61$ as reflecting the average Galactic cosmic ray spectrum towards the Milagro region, the resulting pionic flux at the Milagro energy is 66% of the observed

¹³For example, Kamae et al. (2005) finds that diffractive effects could change the gamma-ray index by about +0.05 units; this is about the level of the uncertainty in the measured local cosmic-ray spectrum, but much smaller than the index shift (≥ 0.2 units) needed to reconcile the EGRET and Milagro data with the pionic signal expected from cosmic rays.

result. For the locally-measured cosmic-ray spectral index of $\alpha = 2.75$, the maximal allowed pionic contribution drops to just 19% of the Milagro flux. Note however that due to large uncertainties in Milagro measurement, the maximal fraction that the pionic gamma-ray component can account for in this case, can be at most about 30%. Were we to raise the pionic prediction to meet the Milagro and high-energy EGRET signals, the result would overshoot the EGRET signal below 1 GeV.

This result on the pionic normalization, supported by the more detailed work of Strong et al. (2004c), indicates that it is not realistic to simply extrapolate the EGRET data into the TeV range, where the pionic component should be dominant. At the very least, the non-pionic components of the GeV data should be subtracted first. Also, as shown by the solid line in Fig. 5.1, when the EGRET data are further extrapolated into the PeV range, the expectations are right on the edge of upper limits from the CASA-MIA and KASCADE experiments. The upper dashed line in Fig. 5.1 shows a line of the same EGRET/Milagro best-fit spectral index ($\alpha = 2.61$), with a maximal pionic normalization. Besides being ~ 2 times larger than favored at low energies, this curve still falls below the Milagro point (with a more realistic normalization, it would fall more significantly below).

While the spectral index fit of $\alpha = 2.61$ is quite suggestive for connecting the EGRET and Milagro observations, it is not consistent with local observations of the hadronic cosmic rays, which instead suggest $\alpha = 2.75$. Over the long lever arm of ~ 1 GeV to ~ 1 TeV, this makes a significant difference. Cosmic-ray experiments such as JACEE fit their measured cosmic-ray spectra with $\alpha = 2.80 \pm 0.04$ (Asakimori et al. 1998). In our analysis we will adopt $\alpha = 2.75$ as a more conventional, locally measured value, consistent with our previous work. In this case, we find that, even for a maximized pionic normalization, the pionic flux at 3.5 TeV is 5 times smaller than the Milagro measurement. For a pionic normalization as low as assumed by de Boer et al. (2005), the pionic flux at 3.5 TeV is about 10 times smaller than the Milagro measurement. In any case, the joint demands of using a realistic cosmic ray spectrum and not exceeding the maximal pionic normalization mean that the expectations fall well below the Milagro observation. We therefore call this problem the “TeV excess.”

Pushing beyond the TeV range to PeV energies further constrains both the TeV and GeV excesses. In Fig. 5.1, we see that the upper limits reported by CASA-MIA (Borione et al. 1998) and KASCADE (Schatz et al. 2003) appear to already rule out the simple single-power-law extrapolation from GeV energies upward. Indeed, the published PeV limits barely permit the maximal pionic emission allowed at an index of at the level of the EGRET/Milagro $\alpha = 2.61$ fit. Thus the PeV data already play a useful role in limiting the level of pionic emission and thus strengthening the case for a non-pionic TeV excess seen by Milagro. Indeed, it is clear that there is no source which can have a single power law spectrum which lies beneath the GeV data and matches the TeV signal, without running afoul of the PeV constraints.

Moreover, as noted above, the PeV data from CASA-MIA were obtained from a gamma-to-hadron shower ratio in concert with an assumed cosmic-ray spectral index of $\alpha = 2.66$. In Fig. 5.2, we zoom into the TeV–PeV region to show the effect of choosing the steeper spectral index $\alpha = 2.80$ measured by Asakimori et al. (1998). Note that because only the ratio of integral fluxes is given, the assumption of a

different spectral index also results in a different normalization need to calculate gamma-ray flux. We then see that the limits can become much stronger in absolute terms. The pionic constraints remain similar, as both the data and predictions move together. On the other hand, the tighter absolute limits now exclude a continuation of the GeV-TeV $\alpha = 2.61$ power-law fit to PeV energies.

Moskalenko et al. (2006) have recently shown that the attenuation of gamma rays by the interstellar radiation field ($\gamma + \gamma \rightarrow e^+ + e^-$) can be significant for energies $\gtrsim 10$ TeV and sightlines near the Galactic Center. This effect would be most prominent around 100 TeV. However, at few hundred TeV attenuation by the CMB takes over and dominates at PeV energies (Moskalenko et al. 2006). As the sensitivity and impact of the PeV data improves, it will be necessary to take these effects into account. In addition, the decreasing flux and heavier composition beyond the cosmic ray knee will also reduce the expected gamma fluxes.

The presence of a TeV excess must be viewed in the light of the well-known GeV excess and its possible explanations. Inverse Compton scattering makes a significant contribution at GeV energies, but in the TeV regime it declines rapidly, and is much smaller than the pionic gamma-ray flux (Strong et al. 2004c). In the de Boer et al. (2005) proposed scenario, the GeV excess originates from the annihilation of dark

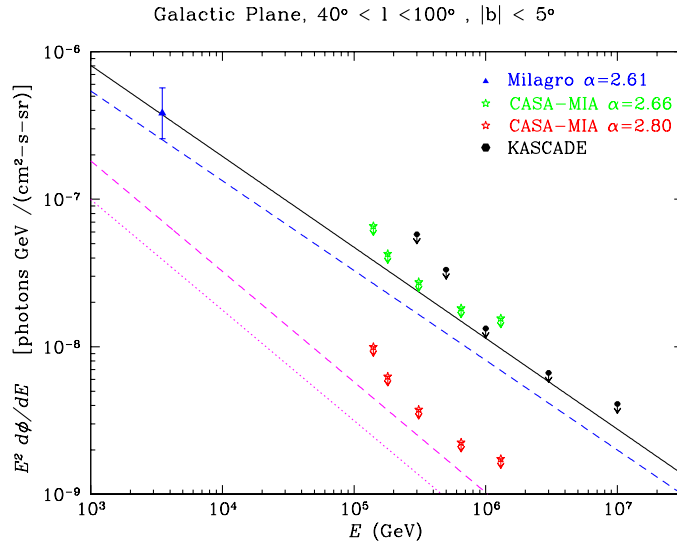


Figure 5.2: In this figure, we zoom in the PeV region of Fig. 5.1 to emphasize the strong dependence of the CASA-MIA limits on the assumed spectral index. The value adopted in this Chapter $\alpha = 2.66$ (Glasmacher et al. 1999) results in limits plotted as green stars. On the other hand, if a steeper spectrum is assumed $\alpha = 2.80$ (i.e. adopting the JACEE cosmic-ray flux; Asakimori et al. 1998) this results in stronger CASA-MIA limits plotted as red stars. As in Fig. 5.1, dashed lines represent the maximal pionic spectrum for $\alpha = 2.61$ (blue) and $\alpha = 2.75$ (magenta), while the pionic spectrum adopted by de Boer et al. (2005) is presented as a dotted magenta line.

matter particles with mass $\simeq 100$ GeV. In this case the dark-matter gamma-ray signal will have a sharp cutoff at the dark matter mass, and again cannot contribute as significantly at TeV energies. (And since we are discussing the Galactic Plane, well away from the center, the contribution of any dark matter component should be greatly reduced.) In order to explain the TeV excess, we require a component which is subdominant at GeV energies, important at TeV energies, and vanishing again at PeV energies. This might arise from unresolved sources with hard ($\alpha \simeq 2$) spectra, cutting off before the PeV range, and we turn to this possibility next.

5.3.2. UNRESOLVED SOURCES

It is possible that unresolved point or extended sources contributed to the total gamma ray flux measured by Milagro (Atkins et al. 2005, Nemethy 2005). While Milagro did not find any resolved sources in this region of the Galactic Plane, there are ten unidentified gamma-ray point sources in this region given in the Third EGRET Catalog (Hartman et al. 1999). (It is worth noting that the definition of these as point sources depends on the degree-scale angular resolution of EGRET; future experiments should be able to measure the energy spectra and angular extent of these sources much more precisely.) The spectra of these sources are described therein by single power law fits, which we extrapolate to the TeV range and consider as contributions to the Milagro diffuse measurement.

In the GeV range, these objects have significantly harder spectra ($\alpha \simeq 2$) than the pionic diffuse component, so in principle, they could become quite important at higher energies. Additionally, we found that the combined extrapolated flux at $E_\gamma = 3.5$ TeV of these ten point sources, spread out over the Milagro region, is $\sum_{i=1}^{10} F_{\text{ps}}^i(E_\gamma = 3.5 \text{ TeV}) \simeq 2.5 \times 10^{-13}$ photons $\text{cm}^{-2} \text{s}^{-1} \text{GeV}^{-1} \text{sr}^{-1}$. Amazingly, this is about a factor of 10 larger than the total diffuse emission for the whole region measured by Milagro, i.e. $F_{\text{diff}}(E_\gamma = 3.5 \text{ TeV}) \approx 3.0 \times 10^{-14}$ photons $\text{cm}^{-2} \text{s}^{-1} \text{GeV}^{-1} \text{sr}^{-1}$. Thus it is obvious that indeed, unresolved point sources could contribute significantly to the TeV excess, even taking into account the uncertainties in the extrapolations in energy. In fact, in order to not grossly overproduce the measured flux, the spectra of these ten objects must be strongly cut off before the TeV range.

Four of these ten EGRET objects have been observed at TeV energies by the Whipple (Fegan et al. 2005, Buckley et al. 1998) and HEGRA (Aharonian et al. 2005a) experiments. In Fig. 5.3, we show the combined GeV and TeV spectral information on these objects. Aharonian et al. (2005a) reported a detection by HEGRA of the source TeV J2032+4130, which, if related to the J2033+4118 EGRET source, would mean a TeV signal that is more than two orders of magnitude lower than what would have been expected based on the EGRET observation. If all of the sources were like this, then these extrapolated unresolved sources would not be able to explain the TeV excess. However, in the other three cases shown, the TeV limits are not yet strong enough to decide if these sources are excluded from contributing significantly to the TeV excess. For example, even when limits for just these four sources are used, the total flux still remains about 3 times above the Milagro diffuse flux; and there are still the other six objects that we don't have information about yet.

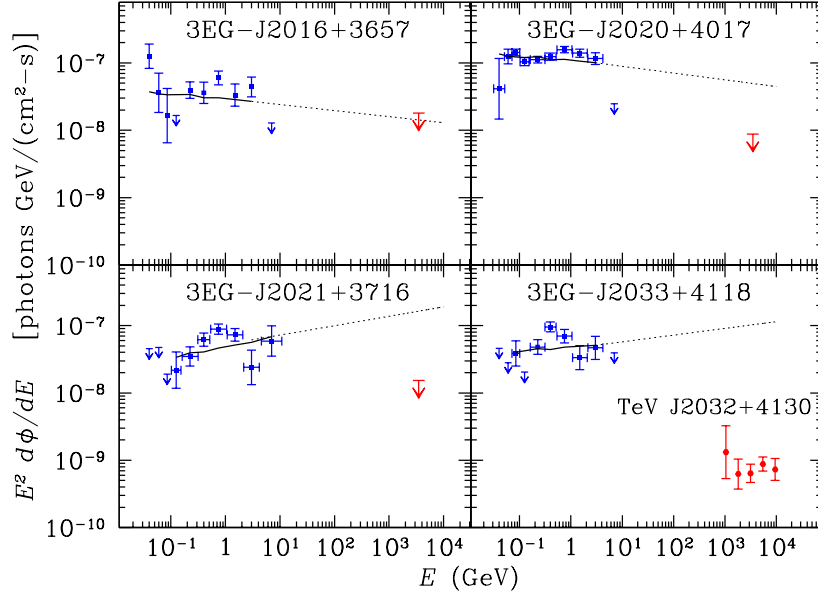


Figure 5.3: In this figure we plot four of the EGRET sources from the Milagro $\ell \in (40^\circ, 100^\circ)$, $|b| < 5^\circ$ region that were observed in TeV range as well; we see here (but also from Fig. 5.1) that the power-law trends at GeV energies must not continue to TeV energies. The EGRET data points (blue) were plotted using publicly available data. The extrapolation slope used for each source is given in Table 5.2 (Hartman et al. 1999). Limits at $E = 3.5$ TeV plotted in red were derived from observations: J2016+3657 and J2021+3716 Whipple (Fegan et al. 2005), J2020+4017 Whipple (Buckley et al. 1998), J2033+4118 HEGRA (Aharonian et al. 2005a).

In addition, sources of comparable TeV intensity to those detected recently by HESS (Aharonian et al. 2005b, 2006a) could contribute significantly to the flux in the Milagro region, if present in this region of the Galactic Plane but not resolved; these sources may be bright at TeV but not GeV energies.

Consequently, it is for now impossible to determine whether the Milagro measurement arises from truly diffuse emission or unresolved sources. Even if the entire flux is due to unresolved sources, it is clear that all of these ten EGRET sources will have to be cut off before 3.5 TeV, or else the extrapolated flux could be much too large. Direct observations of these ten EGRET sources in the TeV range are thus of very high importance for further progress.

Table 5.2: Unidentified EGRET Point Sources in Milagro Region

3EG Catalog Source	Galactic Coords		$F(> 100 \text{ MeV})$ [$10^{-8} \text{ cm}^{-2} \text{ s}^{-1}$]	Spectral Index γ
	ℓ [°]	b [°]		
J1903+0550	39.52	-0.05	62.1 ± 8.9	2.38 ± 0.17
J1928+1733	52.71	0.07	157.0 ± 36.9	2.23 ± 0.32
J1958+2909	66.23	-0.16	26.9 ± 4.8	1.85 ± 0.20
J2016+3657	74.76	0.98	34.7 ± 5.7	2.09 ± 0.11
J2020+4017	78.05	2.08	123.7 ± 6.7	2.08 ± 0.04
J2021+3716	75.58	0.33	59.1 ± 6.2	1.86 ± 0.10
J2022+4317	80.63	3.62	24.7 ± 5.2	2.31 ± 0.19
J2027+3429	74.08	-2.36	25.9 ± 4.7	2.28 ± 0.15
J2033+4118	80.27	0.73	73.0 ± 6.7	1.96 ± 0.10
J2035+4441	83.17	2.50	29.2 ± 5.5	2.8 ± 0.26

5.4. IMPLICATIONS AND OBSERVATIONAL STRATEGY

The pioneering Milagro observation (Atkins et al. 2005) above 3.5 TeV is the first positive detection of a Galactic diffuse component at very high energies. The Milagro result becomes all the more powerful when placed in the context of GeV gamma-ray observations by EGRET (Hunter et al. 1997), and PeV upper limits by CREAMIA (Borione et al. 1998) and KASCADE (Schatz et al. 2003). In particular, the combined GeV–TeV–PeV signal is incompatible with emission from pions created by cosmic rays with the locally measured $\alpha = 2.75$ index. This result follows from the physics of pion production and decay, and is independent of any detailed Galactic model. Moreover, pionic emission is the only conventional source at TeV energies. But the pionic spectral shape and the GeV EGRET data together constrain the pionic emission to fall below the Milagro TeV signal by at least a factor of ~ 5 when using a pionic spectrum arising from cosmic rays as locally observed; even without requiring consistency with the local cosmic-rays, the deficit is at least a factor of ~ 2 . This mismatch constitutes the TeV excess.

The TeV excess takes its place alongside the well-established GeV excess to underscore our present state of ignorance about the sources of diffuse Galactic gamma rays. These data demand an explanation. (1) We are challenged to determine the dominant sources of diffuse Galactic gamma-rays at the highest energies, and to determine what portion of the emission is truly diffuse, and what portion is due to (as yet) unresolved point sources. (2) We are still tasked to search for a pionic signature, since the mere existence of hadronic cosmic rays and of interstellar matter together *guarantee* that this flux must exist at some level in the Galactic gamma-ray sky. (3) Our difficulty in explaining the diffuse Galactic gamma-ray spectrum is all the more galling given that current measurements are consistent with a very simple spectral shape: as seen in Fig. 5.1, the present GeV–TeV–PeV gamma-ray data are all consistent with a piecewise power law having a break at a peak around 0.8 GeV. It would be enormously instructive to determine whether improved spectral resolution and energy coverage confirm this simple form or reveal telltale features. For now, neither the low-energy

or high-energy power law indices, nor the energy scale of the break, can easily be understood in terms of the observed properties of local Galactic cosmic rays.

With these broad questions at hand, we now briefly explore astrophysical consequences of some of the possible solutions, and then review the observational arsenal which can be brought to bear on these problems.

5.4.1. POINT SOURCE SPECTRAL BREAK: IMPLICATIONS

The possibility of a spectral break for at least some Galactic point sources might have important implications. If Galactic point sources (presumably, supernova remnants) are the dominant source of Galactic cosmic-ray protons at TeV energies then the shape of the diffuse pionic gamma-ray spectrum should track that of individual Galactic point sources. That is, if there is a break or a cutoff somewhere between 10 GeV and 1 TeV in gamma-ray spectra of these sources that should carry over to spectra of cosmic rays accelerated in them. In that case the break in the spectrum is a measure of maximal SNR acceleration energy. Moreover, this would imply that another cosmic-ray component (or reacceleration) is required to come in before the ~ 1000 TeV cosmic-ray “knee,” contrary to conventional models.

5.4.2. “GeV EXCESS” EXPLAINED BY DARK MATTER?

In this Chapter (Prodanović et al. 2007) we have tested the consistency of the model proposed by de Boer et al. (2005) with the diffuse Galactic Plane TeV gamma-ray observation of Atkins et al. (2005). This model requires a conventional pionic component in order for the GeV excess to originate from WIMP annihilation. We found that such a pionic component will then be able to account for only $\sim 10\%$ of the Milagro TeV gamma-ray flux. Thus, although the GeV excess could be explained this way, there still will be a potential TeV excess. However, due to large uncertainties regarding point source contribution to Milagro TeV gamma-ray flux of EGRET sources, our model-independent analysis is unable to rule (de Boer et al. 2005) model in or out, on the basis of gamma-rays alone. On the other hand, the recent analysis by Bergstrom et al. (2006) does claim to exclude the de Boer et al. (2005) model on the basis of antiproton fluxes.

Finkbeiner (2004) has proposed that dark matter annihilations may account for both the EGRET GeV excess and the WMAP Galactic haze, through the inverse-Compton and synchrotron energy losses of electrons and positrons produced in the annihilations. Though the mechanism of producing the GeV gamma rays is different from that of de Boer et al. (2005), in both cases the gamma-ray spectrum is cut off at energies above the dark matter mass, presumably ~ 100 GeV.

5.4.3. ANSWERING THE QUESTIONS: OBSERVATIONS

Some of the existing and upcoming gamma-ray experiments will be able to answer the questions we have raised. Namely, the Gamma-ray Large Area Space Telescope (GLAST; Michelson 2001) will make observations in the 10 MeV – 300 GeV energy band, which means that it will go about an order of magnitude higher in energy than EGRET, and will thus have the first view into this “unopened window” in energy. This will give new understanding of how GeV and TeV diffuse Galactic Plane gamma-

ray observations connect. It will tell us more about the nature of the GeV excess and how high it extends in energy. In particular, GLAST observations of diffuse emission could find a break in the diffuse gamma-ray spectrum, which would point to the nature of the GeV excess. Though a potential break could be due to high inverse Compton component (Strong et al. 2004c), it could also have a dark matter origin; the shapes of two spectra may differ enough to make separation possible.

GLAST observations of point sources at such high energies should uncover the break in their spectra implied by the overproduction of TeV gamma-rays when GeV data are extrapolated without a break (Fig. 5.3). A possible break, along with in general a better determination of point source spectra, could place strong constraints and possibly give a definite answer about the existence of the diffuse TeV excess. Discovering a break in the spectra of supernova remnants in particular would immediately have important consequences for the nature of Galactic cosmic rays and thus hadronic gamma-rays. This feature would indicate a maximum cosmic ray energy which then should also limit Galactic cosmic rays accelerated by supernovae. Any cosmic rays above such energies must be accelerated from other sources, Galactic or otherwise.

The Very Energetic Radiation Imaging Telescope Array System (VERITAS; Weekes et al. 2002) will complement and partially overlap with GLAST by observing in the energy range of 50 GeV – 50 TeV. VERITAS enjoys greater flux sensitivity compared to Milagro. Consequently, VERITAS should better determine the intensity of diffuse Galactic Plane gamma-ray emission. At least as important, VERITAS has far better point source sensitivity, which results in far lower contamination by unresolved point sources. All of this will allow VERITAS to place strong constraint on the possible diffuse nature of the TeV excess and in turn constrain the pionic gamma-ray component.

The High-Energy Stereoscopic System (HESS) is already surveying point sources (Aharonian et al. 2006a). Its sensitivity is similar to VERITAS, and thus it is in the position to already answer some of these questions. Although it is located in the southern hemisphere, and does not observe the same region of the Galactic Plane as Milagro, an independent measurement of the diffuse gamma-ray flux would help resolve some of the issues we have presented in this Chapter (Prodanović et al. 2007). A possible diffuse Galactic Plane gamma-ray measurement made by HESS could be used to check for consistency with EGRET observations, in a similar way as presented in this Chapter. The much better angular resolution of HESS compared to Milagro would give a result far less dependent on the unresolved point sources. Thus, a potential discovery of a diffuse TeV excess even in this case would then tell us a lot about the nature of this excess. We also note that the MAGIC telescope, a very large atmospheric imaging Čerenkov telescope, has a very low energy threshold, down to 30 GeV (Baixeras 2003), and will thus also be a powerful probe.

Moreover, very recently, the HESS Collaboration has reported the discovery of an apparently diffuse flux from a very small region at the Galactic Center (Aharonian et al. 2006b). While near 200 GeV, this flux is similar to expectations, it falls off less steeply ($\alpha = 2.3$ instead of 2.75), reaching an excess of at least a factor 10 near 10 TeV. While the spectrum here is falling less steeply than that which would be

required to explain the Milagro TeV excess, the remarkable similarity of the excess suggests that a common origin is possible, e.g. perhaps due to source cosmic rays (Berezhko and Volk 2000, 2004). Note that Milagro has only measured a single point – the flux above 3.5 TeV – and hence cannot yet distinguish between possible new spectra emerging near that energy.

If the enhanced gamma ray flux seen by Milagro indeed arises from neutral pion decays, as in the model of Berezhko and Volk (2000, 2004) with enhanced high-energy cosmic ray fluxes near sources, then it *must* be accompanied by an equally enhanced flux of neutrinos from charged pion decays. (In proton-proton collisions at high energies, neutral and charged pions are produced in comparable numbers; the neutral pions decay to two gamma rays, and the charged pions ultimately decay to three neutrinos and an electron or positron.) The same conclusion would hold if the TeV flux excess is due to dark matter annihilations (Finkbeiner 2004, de Boer et al. 2005) or unresolved sources in which the gamma rays are produced by pion decays. If the excess gamma rays are produced leptonically, by inverse Compton scattering, there will not be accompanying enhanced neutrino fluxes. These considerations may allow new tests of the TeV excess in IceCube and other large neutrino detectors (Beacom and Candia 2004, Candia 2005, Kelley et al. 2005), for which the detection prospects would be enhanced by a factor approaching 10, and more if the excess persists to higher energies.

Finally, as we have emphasized, gamma-ray energy spectra provide the most direct and model-independent probe of pionic production and hence hadronic cosmic rays. However, the sky distribution of course also provides important clues (Strong et al. 2004c), and the warp in the Galactic Plane may be helpful for separating the pionic gamma-ray component. Since the cosmic rays are believed to be isotropic within the Galaxy, the pionic component of the gamma ray flux should be proportional to the column density of gas along the line of sight, whereas the inverse Compton component depends on the radiation density. Three-dimensional models of the Galactic neutral hydrogen density, revealed by the Doppler-shifted 21-cm line emission, show that the Galactic Plane is strongly warped at radii $\gtrsim 10$ kpc (Levine et al. 2006). Some evidence of this warp can be seen in neutral hydrogen column density maps (Kalberla et al. 2005), showing up as an excursion to positive latitudes near Galactic longitude $\ell \sim 100$ and an excursion to negative latitudes near $\ell \sim 260$. In the energy range corresponding to pionic gamma rays, these same features should be seen. While some evidence of this effect was noted earlier (Hunter et al. 1997), it appears to be easiest to see in the new EGRET maps of Cillis and Hartman (2005), which are shown for several energy ranges (note the high-resolution figures are only available online). Here the warp effect can be quite easily seen in several of the maps, which probably implies that the distribution of all gas is similar to that of neutral hydrogen alone. Besides offering some hope to separate the pionic component with spatial information, the non-trivial geometry would allow for the first time some information about distances along the line of sight. While our comments here are only qualitative, we are unaware of any published correlation of the EGRET and 21-cm maps. The future GLAST mission, with significantly better sensitivity and angular resolution, should allow much more detailed studies.

5.5. TeV EXCESS: POSSIBLE OUTCOMES

The nature and origin of the diffuse gamma-ray emission from our Galaxy at GeV energies (Hunter et al. 1997) has become an increasingly pressing problem, with the GeV excess (Strong et al. 2004c) seeming to demand new astrophysics (e.g. high-energy cosmic-ray populations) or new physics (annihilating dark matter). The Milagro detection (Atkins et al. 2005) of a TeV Galactic signal, possibly of diffuse origin, invites us to place the GeV emission in a larger context. In this Chapter (Prodanović et al. 2007), we show that TeV and PeV gamma-ray observations provide a long “lever arm” on the GeV excess and its origin.

In particular, the combined GeV–TeV–PeV observations shed new light on emission due to hadronic cosmic-ray interactions. These hadronic gamma-rays must exist at some level, and appear with a characteristic spectrum fixed by pion decay and the primary cosmic-ray spectrum. Since the “pion bump” at $E_\gamma = m_\pi/2$ is not seen, the evidence for pionic emission must come from the high-energy tail, which should dominate over any leptonic (i.e. inverse Compton) signal at high energies ($\gtrsim 1$ TeV). For this reason, TeV–PeV data offer key new constraints on pionic gamma-rays, which can allow us to determine the hadronic gamma component and thus isolate the residual contribution(s).

Can we arrive at a consistent picture of high-energy Galactic gamma-ray emission? Yes, though present data are insufficient to single out a unique combination of sources. However, some conclusions are already clear: (a) The simplest picture, in which pions are created from cosmic-rays with energy spectra as measured locally, is *inconsistent* with published EGRET and Milagro data. (b) Besides the “GeV excess” identified by EGRET, a “TeV excess” is likely to be present as well. We have shown that one of the main uncertainties in accounting for the Atkins et al. (2005) diffuse TeV gamma-ray observation comes from unresolved sources. (c) As we have pointed out, indications of a possible break in spectra of some point sources can have important consequences for cosmic-ray acceleration. (d) The true picture of Galactic gamma-rays, which might follow several scenarios, can be revealed with further observations.

1. One possibility is that the TeV excess is indeed truly diffuse and due to pionic emission (Atkins et al. 2005). In the simplest picture, this would be a scenario where no break in the diffuse gamma-ray spectrum is observed between the GeV and TeV regimes. This would in turn require a spectral index $\alpha = 2.61$, as pointed out by the Milagro Collaboration, which would indicate that measured local cosmic-ray spectrum is different from, and harder than, the Galactic average. This would also mean that the pionic component is very close to maximal, if not larger, as shown in Fig. 5.1. In this case, the spectrum should follow the same power law out to the PeV region. This PeV signal would lie just below the current limits, awaiting discovery (or falsification!) with modest improvements in sensitivity.

Such a hard pionic spectrum would greatly reduce the GeV excess, lessening the motivation for a large inverse Compton or dark matter component. For a more realistic pionic spectrum, there is the well-known problem of the GeV excess.

We are noting here that models which explain the GeV excess with a low pionic normalization and new component at GeV energies must now be confronted with the TeV excess that they create.

2. Another possibility is that the TeV excess is truly diffuse, but not due to interstellar pionic emission. This would be the case if there is a “hard electron component,” i.e. with a spectrum not observed locally (see e.g. Aharonian and Atoyan 2000, Pohl and Esposito 1998). Such an anomalous component could create an inverse Compton signal which composes the GeV excess, but also extends to TeV energies where it dominates over the pionic component. This scenario would result in a gamma-ray spectral break at a few tens of GeV. Having a definite handle on the inverse Compton component would in turn determine the pionic gamma-ray component. Moreover, because the hard electron spectrum model explains a large fraction of the GeV excess, it thus excludes dark matter explanation. However, if the TeV excess cannot be explained with the inverse Compton component, then this would indicate a more exotic solution.
3. Just as the GeV excess raises the exciting prospect of a dark matter signal (de Boer et al. 2005), so too does the TeV excess. This scenario is testable. If the TeV excess is due to annihilations, one expects a strict cutoff above the mass of the dark matter particle (which necessarily must be rather heavy, $m_{\text{DM}} \gtrsim E_{\gamma, \text{Milagro}} \geq 3.5 \text{ TeV}$); this should appear as a break or perhaps even a peak in the gamma-ray spectrum. Also, the evidence for the TeV excess comes from the Milagro region which lies $\ell > 40^\circ$ from the Galactic center, and thus probes rather peripheral Galactocentric radii $R > R_\odot \sin \ell \simeq 5 \text{ kpc}$. Given that dark matter densities (and the resulting annihilation rate $\propto n_{\text{DM}}^2$) are expected to peak at the center, one would expect a rapid increase in the diffuse signal as one scans from the Milagro region to the Galactic center. And a dark matter interpretation of either or both gamma-ray signals faces similar challenges from other high-energy particle observations (e.g. Bergstrom et al. 2006).
4. Finally, the TeV excess could result from unresolved isolated sources such as supernova remnants. This scenario could easily be checked by surveying for TeV point sources in the Galactic region observed by Milagro. Indeed, the EGRET sources in the Milagro region appear as “hot spots” on the Milagro map, though it is unclear how significant this may be. Also, another observation of the diffuse Galactic Plane TeV gamma-rays could yield a flux that does not require a TeV excess, but is instead consistent with a diffuse pionic emission with a more conventional spectral index. Thus it is crucial that VERITAS TeV telescope surveys the EGRET sources, especially the ones in the region observed by Milagro.

A measurement of the diffuse Galactic Plane TeV gamma-ray flux with better resolution telescopes like VERITAS and HESS would not only confirm the Milagro detection, but also would provide much sharper angular resolution of the signal. These additional data could significantly tighten the constraints based on gamma-ray spec-

tra, and open up the possibility of distinguishing the diffuse TeV sources based on the sky distribution.

Thus, existing diffuse gamma-ray observations of the Galactic plane are consistent with an energy spectrum that is at once empirically simple (a broken power law) yet stubbornly resistant to theoretical explanation. Fortunately, upcoming observations across the GeV-TeV-PeV range will add qualitative and quantitative detail that will distinguish among and/or exclude the possible sources of the highest energy photons in our Galaxy.

Chapter 6

PROBING PRIMORDIAL AND PRE-GALACTIC LITHIUM WITH HIGH VELOCITY CLOUDS

6.1. OVERVIEW

The primordial lithium abundance currently presents a pressing cosmological conundrum. The recent *Wilkinson Microwave Anisotropy Probe (WMAP)* determination of the cosmic baryon density (Spergel et al. 2003), combined with big bang nucleosynthesis theory (BBN), tightly predicts the primordial ${}^7\text{Li}$ abundance (Cyburt et al. 2003b), but Li measurements in halo stars give values lower than this by factors of $\gtrsim 2$. Moreover, the ${}^7\text{Li}$ problem becomes even worse when one realizes that there is likely to be an *additional pre-Galactic source of lithium*, which would have arisen during the formation of the Local Group, namely, from the structure formation cosmic rays (SFCRs). However, the limits are still weak, and as we have shown in Chapter 3 (Fields and Prodanović 2005) EGRB observation still allows a significant fraction of the pre-Galactic Li to be produced by SFCRs.

To date, halo stars are the only sites suitable for observations of pre-Galactic Li and have proven to be a very powerful tool for studies both of cosmology and of cosmic rays. But given that the observations are dominated by systematic errors (Ryan et al. 2000, Bonifacio et al. 2002), it is critical to identify other independent sites in which pre-Galactic Li can be measured. Recently, Zaldarriaga and Loeb (2002) pointed out that observations of highly redshifted ($z \sim 500$) lines from cosmic Li recombination can be used to probe the Li abundance at these very early epochs. This method could prove very powerful but is not yet available. In the meantime, in this Chapter¹⁴ (Prodanović and Fields 2004b), we propose a new site that is currently accessible.

A way to independently test the pre-Galactic Li abundance is to look at high-velocity clouds (HVCs). These are gas that is falling onto our Galaxy, and the lowest metallicity clouds have a metallicity of about 10% of solar. These low-metallicity HVCs thus should have a mostly pre-Galactic composition, with a small contamination from the Galaxy. Moreover, these cold clouds are free of the possibility of thermonuclear depletion, which complicates the interpretation of halo star Li abundances.

¹⁴Parts of this were already published in a refereed journal (Prodanović and Fields 2004b)

Thus, measuring Li in HVCs would provide an important test of the Li problem: if the measurement is consistent with the *WMAP*+BBN Li abundance (i.e. at that level or above), it would indicate that low Li measured in halo stars is a convection problem, or if measurement is below the *WMAP* result it would indicate that the Li problem is more severe and requires more radical solutions. Also, the measurement of Li in HVCs would test the significance of the SFCR contribution to Li production.

6.2. HIGH-VELOCITY CLOUDS

Clouds of neutral hydrogen HI that significantly depart from the normal Galactic rotation, i.e. that have velocities with respect to the local standard of rest $|v_{\text{LSR}}| \gtrsim 90$ km/s, are called HVCs (Wakker and van Woerden 1997). Both positive and negative velocities are observed; however, the sign of their radial velocity does not directly imply that their full space motion is either away or toward the Galactic plane. Although determination of their distances is very uncertain, the limits can go up to tens of kiloparsecs (Wakker 2001). HVCs contain heavy elements and exhibit a wide range of metallicities, which in some clouds can be as low as 1/10 of solar (Wakker 2001).

A few models for their nature have been proposed. Some HVCs may be of Galactic origin, e.g. in the Galactic fountain model (Shapiro and Field 1976, Bregman 1980), while others may be extragalactic (Oort 1970, Blitz et al. 1999, Braun and Burton 1999), resulting from the accretion of gas that was left over from the formation of the Galaxy. HVCs consistent with Galactic origin would have normal metallicities as opposed to those with extragalactic origin, which are expected to have lower metallicities (Wakker and van Woerden 1997). There is also another type of object, like the Magellanic Stream, which represents material that was stripped from satellite galaxies.

When measuring abundances, it is crucial to know the dust content of the HVC, in order to correct for the depletion onto dust; this effect is known to be very large for local interstellar abundances (Stecker and Salamon 1996). The effect of dust is such that it “hides” some fraction of the present abundance and thus introduces non negligible upward corrections to the observations of gas-phase abundances. In particular, a gas-phase observation of Li is always a lower bound to the true abundance. Searches for the dust in HVCs (Waxman and Bahcall 1999, Bates et al. 1988, Fong et al. 1987) give negative results, indicating either a dust content much lower than in low-velocity HI clouds or that the dust is very cold (Wakker and van Woerden 1997). Also, Tripp et al. (2003) found recently that HVC Complex C has little or no dust, based on the iron abundance. We note that in another class of low-metallicity objects, the QSO absorption systems, there is also evidence that dust depletion is small, at least in some systems (Lopez et al. 2002).

Thus, HVCs with low metallicities and little dust, like Complex C (Tripp et al. 2003), are very promising sites for testing the pre-Galactic lithium. Complex C would be particularly suitable for this measurement since (Sembach 2004) have already measured the deuterium abundance there and found it to be consistent with the primordial abundance inferred from the *WMAP*. Complex C is observed to have low metallicity,

although there are also indications that its origin might be from the material that was tidally stripped from a satellite galaxy, like in the case of the Magellanic Stream (Tripp et al. 2003). In that case, Complex C might not be as pristine as one would want it to be in order to test the pre-Galactic lithium; however, it is still the most promising candidate for such a task.

6.3. LITHIUM IN HVC: EXPECTATIONS

We will take the point of view that low-metallicity HVCs consist of infalling extragalactic (i.e. intragroup) matter, with some admixture of Galactic material responsible for the nonzero metallicity. We thus expect the HVC lithium to consist of at least two components: (1) primordial ${}^7\text{Li}$ plus (2) some amount of ${}^6\text{Li}$ and ${}^7\text{Li}$ from Galactic processes; it is also likely that there is a third component due to SFCRs. The Galactic Li sources are Galactic cosmic rays (which make ${}^7\text{Li}$ and are the only Galactic source of ${}^6\text{Li}$; see Steigman and Walker 1992, Vangioni-Flam et al. 1999, Fields and Olive 1999a) and other sources of ${}^7\text{Li}$: the supernova neutrino process (e.g. Woosley et al. 1990) and low-mass giant stars (Sackmann and Boothroyd 1999). In models of the Galactic chemical evolution of Li, both the Galactic cosmic-ray Li components and the supernova component scale linearly with metallicity (Ryan et al. 2000). The evolution of stellar Li is more complex (Romano et al. 2001) but is only important at the highest metallicities ($\gtrsim 10^{-0.8}$ solar) and to a rough approximation also scales linearly with metallicity. Of course, it is unclear whether the Galactic contribution to HVC Li should be taken as a diluted form of the solar component or as the predicted value at the HVC metallicity, but as long as the Galactic component scales linearly with metal content, these two results should be the same.

Thus, the total (pre-Galactic plus Galactic) Li content in an HVC would depend on the cloud metallicity, and the pre-Galactic component should be more dominant the lower the metallicity. One would thus expect to find

$$\begin{aligned} \text{Li}_{\text{HVC}} &\gtrsim {}^7\text{Li}_p + \frac{Z}{Z_\odot} [({}^7\text{Li}_\odot - {}^7\text{Li}_p) + {}^6\text{Li}_\odot] & (6.1) \\ &\gtrsim 7 \times 10^{-10} & (6.2) \end{aligned}$$

where the notation $\text{Li} \equiv \text{Li}/\text{H} = n_{\text{Li}}/n_{\text{H}}$ represents the lithium abundance. The primordial lithium abundance is given as ${}^7\text{Li}_p$ (Cyburt et al. 2003b), while the solar abundances were taken from Anders and Grevesse (1989). The final, numerical value is that appropriate for the HVC Complex C (Sembach 2004), which has $Z = Z_\odot/6$ as determined from the oxygen abundance, as described in the next section.

Measuring at or above this limit would be consistent with the BBN prediction of primordial Li abundance and would thus indicate that the solution to the lithium problem should be found in stellar modeling. Moreover, this measurement would also be a valuable test of additional sources of pre-Galactic lithium, like SFCRs. Since the Galactic contribution in Eq. (6.2) is about the same as primordial, a measurement above this level would indicate the presence of an additional source of Li (from the presence of dust, it always follows that $\text{Li}_{\text{HVC}} \geq \text{Li}_{\text{obs}}$). The value in Eq. (6.2) includes the Galactic contribution, which is essentially “guaranteed”. In addition,

SFCRs should provide an additional Li source, particularly if the HVCs really are intragroup gas that has been exposed to the Local Group SFCR flux. In Chapter 3 we (Fields and Prodanović 2005) have used a model-independent way to constrain the SFCR-Li abundance range, which by using (6.2) comes to be about 0.4 – 5.6 of the Galactic HVC lithium component. Thus, if Li in HVCs was found to be sufficiently above the primordial level, the excess over the Galactic contribution could be attributed to SFCRs, which would then give us more insight into this cosmic-ray population. This way, we could limit the level of contamination of ISM-Li with SFCR-made Li, which could possibly find its way into our Galaxy through the in falling HVCs.

However, we stress that measuring lithium below the level in Eq. (6.2) is also not excluded, in which case the already existing lithium problem would become more severe. Granted, one would then be able to argue that this just indicates that there is more dust than it was assumed at first; however, one would then have to explain why lithium would be more affected by dust than some other elements that indicate a low presence of dust (Tripp et al. 2003).

6.4. LITHIUM IN HVC: OBSERVABILITY

Although measuring lithium in the HVCs would be a way to test (and possibly resolve!) the lithium problem and SFCRs, the question is whether this measurement can realistically be made. Lithium measurements in diffuse gas are particularly difficult because of the low abundance and hence small column density. For example, local interstellar medium (ISM) observations typically find an Li column of order $\sim 10^9 \text{ cm}^{-2}$ (Knauth et al. 2003). Thus, to compensate for the low column density and make a successful Li observation in a cloud of gas, one needs to look toward a very bright background object. In the case of the local ISM, Knauth et al. (2003) exploited bright stars ($m_V \sim 1 - 6$) to successfully observe diffuse Li and even to resolve isotopic lithium abundances using high-dispersion spectra.

Lithium measurements in the HVCs would resemble the ISM measurements in the sense that both systems contain diffuse, gas-phase Li. However, the observed HI column in, e.g. the HVC Complex C (toward the QSO PG 1259+593) is $N(\text{HI}) \approx 10^{20} \text{ cm}^{-2}$ (Sembach 2004). This indicates that the Li column can be $\gtrsim 10^{10} \text{ cm}^{-2}$; indeed, Eq. (6.2) gives $N(\text{Li}) = 7 \times 10^{10} \text{ cm}^{-2}$ for a hydrogen column of $N(\text{HI}) = 10^{20} \text{ cm}^{-2}$. Thus, with respect to the column density, HVCs are more favorable sites for measuring Li than the ISM. On the other hand, local ISM Li measurements can exploit nearby bright stars, while for HVC measurements, one would have to observe toward an extragalactic object. In that case, the brightest candidates are QSOs, of which the brightest are $m_V \sim 15$, about 10^4 times dimmer than stars used in the ISM measurements. Finally, one would have to worry about the presence of dust in the HVCs, but Tripp et al. (2003) found elemental abundances that imply that Complex C contains little or no dust. On the other hand, depletion onto dust is a significant effect for the ISM Li measurements. This is the main reason why the expected Li column in HVC Complex C ($\sim 10^{10} \text{ cm}^{-2}$) is so much bigger than the ones reported by Knauth et al. (2003).

Thus, we see that observing Li in an HVC is more challenging than in the ISM, but the measurement is an important one and is not beyond the reach of current instruments. Although it would be very interesting and important to resolve isotopic lithium abundances in the HVCs using a high-dispersion spectrum, the first step should more realistically be to obtain an *elemental* Li abundance, using a low-dispersion spectrum. An elemental Li abundance would still provide important answers about the lithium problem and possibly give a valuable insight into the population of cosmic rays that originate from the large-scale structure formation.

To get the sense of the observability of elemental Li, consider the Knauth et al. (2003) observations of the ISM lithium, where *isotopic* lithium abundances were successfully measured and resolved. For example, the Li column density toward the Per X star ($m_{v,*} \approx 6$) is $N(\text{Li}) \sim 5 \times 10^9 \text{ cm}^{-2}$, which is about 10 times lower than the expected column of the elemental Li in Complex C toward QSO PG 1259+593 ($m_{v,\text{QSO}} \approx 15$). However, the star used in the ISM Li measurement has about 4000 times larger flux than the quasar that could be used in the HVC Li measurement. Thus, for the same exposure time and spectral resolution that was used in the Knauth et al. (2003) ISM measurement of ^6Li , the HVC Li observability would be about 300 times lower; that is, a similar *isotopic* measurement would require that much larger an exposure time. The ISM Li isotopes were measured with an exposure time of about 100 ks, so measuring Li isotopes in HVCs does not seem feasible at present.

However, Knauth et al. (2003) used a 2.7 m telescope for their ISM-Li observation. Thus, if one were to use a 10 m telescope to observe Li in HVC Complex C, this would increase the observability by a factor of about 14; i.e. the HVC Li exposure time would now be about 20 times higher compared to the Knauth et al. (2003) ISM-Li measurement. This is still quite a challenge in terms of a reasonable exposure time. It is important to note that the Knauth et al. (2003) measurements were made with impressive spectral resolution. However, much lower resolution would be quite sufficient for measuring the *elemental* lithium abundance, as in the first measurements of elemental Li in the local ISM (Traub and Carleton 1973, vanden Bout et al. 1978). Thus, by having a spectral resolution that is about a factor of 6 lower than the one obtained by Knauth et al. (2003), the exposure time needed for the elemental lithium measurement in Complex C would be about 300 ks. Therefore, even though this is just a crude estimate, we believe that, although challenging, elemental lithium is reasonably observable in a suitable HVC sight line, such as that toward QSO PG 1259+593.

Thus, we strongly urge that Li be measured in one or more low-metallicity HVCs, since any detection, at or above the level given in Eq. (6.2), would be of profound importance, especially for BBN.

Chapter 7

DISCUSSION

In this book we have shown that, because both lithium and hadronic gamma-rays are produced in cosmic-ray interactions, there is an intimate link between them, which can be utilized as a powerful probe of lithium nucleosynthesis, the diffuse gamma-ray sky and cosmic-ray populations.

We have used the Li–gamma-ray connection to test, in a model-independent way, the still-putative population of structure formation cosmic-rays, which adds to the severity of the already existing ${}^7\text{Li}$ problem. Namely, using the EGRB we use two different lines of argument to place an upper limit on the SFCR contribution to pre-Galactic lithium in halo stars. Such a component of lithium would be confused with the true primordial abundance and thus would exacerbate the existing deficit in halo star Li relative to the CMB-based expectations of BBN theory. Unfortunately, current EGRB data are such that our model-independent upper limit (which assumes, among other things, that *all* SFCRs are created prior to *any* halo stars) is very weak. In particular, we cannot exclude the possibility that a significant portion of pre-Galactic lithium is due to SFCRs. We thus find that the nucleosynthesis aspects of SFCRs are important and deserve further more detailed study. However, we have pointed out that a possible observation of lithium in high-velocity clouds could be a powerful, and much needed, probe of both, the ${}^7\text{Li}$ problem and the SFCR population.

Applying our tool on the fiducial case of ${}^6\text{Li}$ originating from Galactic cosmic-ray interactions, potentially revealed yet another lithium problem. Namely, with a simplified approach, we found that the observed extragalactic gamma-ray background allows for only $\sim 25\%$ of the solar ${}^6\text{Li}$ abundance to be produced by GCRs. Refinement of this result in a rigorous way revealed that the solar ${}^6\text{Li}$ problem still persists, although it is now less severe. More specifically, a realistic, detailed calculation that includes ${}^6\text{Li}$ production from both fusion reaction with the ISM and spallation CNO channels (2-step inverse kinematics also included), yields a ${}^6\text{Li}$ abundance that is only $\approx 60\%$ of the total ${}^6\text{Li}$ produced, if standard GCRs are the only relevant source. Correcting for astration will result in even lower ${}^6\text{Li}_{\text{GCR}}$ abundance at the level of $\sim 45\% {}^6\text{Li}_{\text{tot}}$.

Additional sources of ${}^6\text{Li}$ are of considerable current interest, because of the recent report of a ${}^6\text{Li}$ plateau in metal-poor halo stars (Asplund et al. 2006). As with the familiar ${}^7\text{Li}$ Spite plateau, an analogous ${}^6\text{Li}$ feature would suggest a pre-Galactic source of ${}^6\text{Li}$. And indeed, recently two very different cosmological sources of ${}^6\text{Li}$ have

been proposed: (1) production in the early universe, stimulated by supersymmetric dark matter particle decays during big bang nucleosynthesis (Dimopoulos et al. 1988, Kawasaki et al. 2005, Jedamzik 2000, Ellis et al. 2005, Kusakabe et al. 2006); and (2) production during the virialization and baryonic accretion of large-scale structures, which generates cosmological shocks (Miniati et al. 2000) that can in turn accelerate a population of cosmological cosmic rays (Blasi 2004, Suzuki and Inoue 2002; but see Prantzos 2006 for constraints).

However, the ${}^6\text{Li}$ plateau is at $\lesssim 10\%$ level of the ${}^6\text{Li}_\odot$, and thus whatever its source is, it will not be able to account for the factor $\gtrsim 2$ discrepancy between ${}^6\text{Li}_\odot$ and ${}^6\text{Li}_{\text{GCR}}$ we have found. On the other hand, the existence of the ${}^6\text{Li}$ plateau at the 10% level of the solar abundance for metallicities $[\text{Fe}/\text{H}] \lesssim -1$, can be used as a constraint to any non-standard ${}^6\text{Li}$ source that is expected to account for the potentially missing $\approx 40\%$ of ${}^6\text{Li}_\odot$. Moreover, ${}^6\text{Li}$ plateau would indicate that such a source would have to become important only at late times, and near-solar metallicities.

We note that another additional source of ${}^6\text{Li}$ could come from a population of cosmic rays having low energies ($\lesssim 100$ MeV). Such particles are excluded from the solar system and hence not directly constrained observationally. A large flux of such particles, well above the extrapolated observed high-energy trends, could produce large additional amounts of ${}^6\text{Li}$ but no pions and hence no pionic γ -rays. Indeed, recent observations of H_3^+ in molecular clouds (McCall et al. 2003) seems to demand a large low-energy cosmic-ray flux in the neighborhood of these clouds. On the other hand, low-energy cosmic rays widespread enough to participate significantly in LiBeB nucleosynthesis on Galactic scales face strong constraints that come from energetics (Ramaty and Lingenfelter 1999) and from LiBeB abundance ratios (Vangioni-Flam et al. 1998). These limits are evaded if the solar ${}^6\text{Li}$ reflects a localized low-energy cosmic ray enhancement, either due to a hypernova-like Type Ic supernova (Fields et al. 2002, Nakamura and Shigeyama 2004), or to solar cosmic-ray production in the protosolar nebula (e.g. Gounelle et al. 2006). In either case, the other ${}^7\text{LiBeB}$ will be produced and constrain the allowable ${}^6\text{Li}$ contribution.

Throughout this work we have assumed that the Milky Way CR fluence can be approximated with the cosmic mean. Therefore, our result might indicate that more ${}^6\text{Li}$ was being produced than γ -rays would suggest, which would be the case if the Milky Way CR flux was at some time(s) a factor of ~ 2 (on average) higher than the typical CR flux in a normal galaxy.

If indeed our finding of an unexplained component to solar ${}^6\text{Li}$ points to enhanced cosmic-ray activity, this in turn would point to anomalies in Milky Way star formation and/or cosmic-ray properties. We have assumed that the cosmic ray fluence here is typical of the mean star-forming galaxy ($F_{\text{MW}}/F_{\text{avg}} = 1$). If instead our Galaxy had a more vigorous cosmic-ray history, this could account for the difference. Also, we have in our most realistic assessment normalized to the Milky Way pionic gamma-ray luminosity. Of course, being that pionic signature has not been observed in the diffuse Galactic Plane gamma-ray sky, this normalization is model dependent. However, we have demonstrated how, by using observations over a wide energy range GeV–TeV–PeV, answering the question of the diffuse pionic gamma-ray fraction will be in the reach of upcoming experiments. Moreover, such long lever arm also reveals a potential

“TeV excess” which can have important consequences for GCR acceleration theory.

Thus, as we have shown, Li–gamma-ray connection provides a powerful tool even when there are only limits to the diffuse pionic gamma-ray emission. Upcoming gamma-ray experiments will go far to clarify the nature of Galactic and extragalactic pionic gamma-rays, and hence ${}^6\text{Li}$ and pre-Galactic ${}^7\text{Li}$ production. *GLAST* could detect the pionic γ -ray signature from diffuse Galactic emission as well as in the EGRB; this would remove the need to estimate these components, and give a deeper insight into existing lithium problems.

Appendix 1. NOTATION AND NORMALIZATION CONVENTIONS

The interactions of cosmic-ray species i with target nucleus j produces species k at a rate per target particle of

$$\Gamma_k = \int_{E_{\text{th},k}} dE \sigma_{ij \rightarrow k}(E) \phi_i \equiv \sigma_{ij \rightarrow k} \Phi_i. \quad (1.1)$$

Here E is the cosmic-ray energy per nucleon, $\sigma_{ij \rightarrow k}$ is the energy-dependent production cross section, with threshold $E_{\text{th},k}$, and ϕ_i is the cosmic-ray flux. The rate per unit volume for $i + j \rightarrow k$ is thus $q_k = \Gamma_k n_j$.

Note that the flux in Eq. (1.1) is position- and time-dependent. To isolate this dependence, it is useful to define a total, energy-integrated, flux

$$\Phi_i = \int_{E_{\text{th},\text{min}}} dE \phi_i \quad (1.2)$$

where we choose the lower integration limit to always be the *minimum* threshold $E_{\text{th},\text{min}}$ for all reactions considered; in our case this is the $\alpha + \alpha \rightarrow {}^7\text{Li}$ threshold of 8.7 MeV/nucleon. From Eqs. (1.1) and (1.2) it follows that

$$\sigma_{ij \rightarrow k} = \Gamma_k / \Phi_i \quad (1.3)$$

represents a flux-averaged cross section. Also note that if the spectral *shape* of ϕ_i is constant (as we always assume), then so is $\sigma_{ij \rightarrow k}$, and the flux Φ_i contains all of the time and space variation of Γ_k .

Finally, two conventions are useful for quantifying abundances. Species i , with number density n_i , has a ‘‘mole fraction’’ (or baryon fraction) $Y_i = n_i/n_{\text{b}}$. It is also convenient to introduce the ‘‘hydrogen ratio’’ $y_i = n_i/n_{\text{H}} = Y_i/Y_{\text{H}}$.

Appendix 2.

COSMIC GAMMA-RADIATION TRANSFER

The expression for γ -ray intensity in a Friedmann universe is well-known (Stecker 1969), but usually expressed in redshift space. For our purposes, the result expressed in the time domain is critical, and indeed is more fundamental, so we give a derivation based on the Boltzmann equation. For this section we adopt units in which $c = 1$.

The differential photon (number) intensity I is directly related via

$$I(\vec{p}, \vec{x}, t) = p^2 f(\vec{p}, \vec{x}, t) \quad (2.1)$$

to the γ -ray distribution function $f(\vec{p}, \vec{x}, t) = d^3 N / d^3 \vec{p} d^3 \vec{x}$. Here \vec{p} and \vec{x} , as well as the volume elements, are physical quantities (and thus subject to change with cosmic expansion). The distribution function is related to the photon sources via the relativistic Boltzmann equation

$$p^\mu \partial_\mu f - \Gamma_{\mu}^{\alpha\beta} p^\alpha p^\beta f = E \frac{dq}{d^3 \vec{p}} \quad (2.2)$$

where gravitational effects enter through the Affine connection Γ , where $E = p = |\vec{p}|$, and where the source function (number of photons created per unit volume per unit time) is q .

For an isotropic FRW universe we have $f = f(E, t)$, and thus

$$\partial_t f - \frac{\dot{a}}{a} E \partial_E f = \frac{q(E)}{4\pi E^2} \quad (2.3)$$

where $q(E) = dq/dE$ and where we neglect photon scattering and absorption.

We now note that a given photon's energy E drops due to redshifting as a^{-1} . It is thus useful to define a comoving energy $\epsilon = aE$; with $a(t_0) = 1$, we see that ϵ is also the *present-day (observed) photon energy*. Changing variables from $f(E, t)$ to $f(\epsilon, t)$, and similarly for q , the energy-dependent ∂_ϵ term drops out; this is physically reasonable since we do not allow for scattering processes, and thus a photon's energy can only change due to redshifting. We then have

$$\partial_t f = a^2 \frac{q(\epsilon/a)}{4\pi \epsilon^2} \quad (2.4)$$

which, for any fixed comoving energy ϵ , integrates to

$$f(\epsilon, t) = \frac{1}{4\pi \epsilon^2} \int_0^t dt' a^2 q(\epsilon/a). \quad (2.5)$$

Eq. 2.1 then gives the intensity

$$I(\epsilon, t) = \frac{1}{4\pi a(t)^2} \int_0^t dt' \frac{1}{a(t')} q_{\text{com}}[\epsilon/a(t')] \quad (2.6)$$

where $q_{\text{com}} = a^3 q$ is the comoving source rate. Eq. 2.6 is the usual expression (which is often then expressed in terms of an integral over redshift). Finally, if we integrate over the entire energy spectrum, and evaluate at the present epoch t_0 (when $a_0 = 1$), we have

$$I(> 0, t_0) = \int_0^\infty d\epsilon I(\epsilon, t_0) = \frac{1}{4\pi} \int_0^{t_0} dt' q_{\text{com}}(> 0) \quad (2.7)$$

where $q_{\text{com}}(> 0) = \int_0^\infty du q(u)$ is the total source rate, integrated over energy.

We see from Eq. 2.7 that the energy-integrated intensity is the same as one would find from uniform sources in a non-expanding universe (which have been “switched on” for a duration t). This result is physically sensible, because the two effects of cosmic expansion are to introduce a particle horizon and redshifting. The energy integration removes the effect of redshifting, so that the only effect is that of the particle horizon, which acts to set the integration timescale.

Appendix 3. CNO REACTION RATES

The reaction rate for production of species k from $i + j \rightarrow k + \dots$ where i is the projectile and j is the target can be expressed as (in units of $\text{cm}^{-3}\text{s}^{-1}\text{GeV}^{-1}$)

$$q_k \equiv n_j \int_{\epsilon_{\text{th}}} d\epsilon \sigma_{ij}^k \phi_i. \quad (3.1)$$

We can express the flux of cosmic-ray species i as $\phi_i = y_i \phi_{i,p}$ where y_i is the abundance. The flux of species i , $\phi_{i,p}$, is equal to the cosmic-ray proton flux at high energies where losses are dominated by the escape in the leaky box model. At energies $\lesssim 1$ GeV the ionization losses become important and thus the spectra of different CR species have strong dependence on the charge and nucleon number (see Eq. 4.5). Writing n_j as $y_j n_p$ we can now rewrite Eq. (3.1) in the form

$$q_k \equiv n_p y_i y_j \int_{\epsilon_{\text{th}}} d\epsilon \sigma \phi_{i,p}. \quad (3.2)$$

In order to calculate the contribution of spallation reaction to ${}^6\text{Li}$ production compared to the fusion channel, we will set the normalization by determining eg. the oxygen abundance (we will express C and N in terms of oxygen abundance) for which the two rates (CNO spallation and $\alpha\alpha$ fusion) would be equal. That is, we want $q_{\text{CNO}} = q_{\alpha\alpha}$. We can write this as

$$n_p^{\text{ism}} y_\alpha^{\text{ism}} y_\alpha^{\text{cr}} \int_{\epsilon_{\text{th}}} d\epsilon \sigma_{\alpha\alpha} \phi_{\alpha,p} = n_p^{\text{ism}} \sum_{i=\text{C,N,O}} y_i^{\text{ism}} \left(y_\alpha^{\text{cr}} \int_{\epsilon_{\text{th}}} d\epsilon \sigma_{\alpha i} \phi_{\alpha,p} + \int_{\epsilon_{\text{th}}} d\epsilon \sigma_{pi} \phi_p \right) \quad (3.3)$$

$$+ y_i^{\text{cr}} \left(y_\alpha^{\text{ism}} \int_{\epsilon_{\text{th}}} d\epsilon \sigma_{i\alpha} \phi_{i,p} + \int_{\epsilon_{\text{th}}} d\epsilon \sigma_{ip} \phi_{i,p} \right)$$

where we include both forward and inverse (i.e. fast heavy nuclei) kinematics. Setting

$$\hat{\sigma} \equiv \int_{\epsilon_{\text{th}}} d\epsilon \sigma \phi \quad (3.4)$$

and adopting the abundances (Anders and Grevesse 1989) $y_{\text{C}}/y_{\text{O}} = (y_{\text{C}}/y_{\text{O}})_{\odot} = 0.42$, $y_{\text{N}}/y_{\text{O}} = (y_{\text{N}}/y_{\text{O}})_{\odot} = 0.13$ and $y_\alpha^{\text{cr}} = y_\alpha^{\text{ism}} = 0.1$ we can now solve Eq. (3.3) for the

oxygen abundance to find

$$\begin{aligned} \hat{\sigma}_{\text{CNO}} \equiv & 0.42[0.1(\hat{\sigma}_{\alpha\text{C}} + \hat{\sigma}_{\text{C}\alpha}) + (\hat{\sigma}_{\text{pC}} + \hat{\sigma}_{\text{Cp}})] & (3.5) \\ & + 0.13[0.1(\hat{\sigma}_{\alpha\text{N}} + \hat{\sigma}_{\text{N}\alpha}) + (\hat{\sigma}_{\text{pN}} + \hat{\sigma}_{\text{Np}})] \\ & + 0.1(\hat{\sigma}_{\alpha\text{O}} + \hat{\sigma}_{\text{O}\alpha}) + (\hat{\sigma}_{\text{pO}} + \hat{\sigma}_{\text{Op}}) \end{aligned}$$

$$y_{\text{O}} = \frac{10^{-2}\hat{\sigma}_{\alpha\alpha}}{\hat{\sigma}_{\text{CNO}}}. \quad (3.6)$$

This now sets the normalization and allows us to estimate how CNO and $\alpha\alpha$ reaction rates compare. That is, if we assume the solar metallicity throughout the history, we find that

$$q_{\text{CNO}} = \frac{\hat{\sigma}_{\text{CNO}}}{10^{-2}\hat{\sigma}_{\alpha\alpha}} y_{\odot} q_{\alpha\alpha}. \quad (3.7)$$

References

- Aharonian, F. and Atoyan, A. M.: 2000, *Astron. Astrophys.*, **362**, 937.
- Aharonian, F. et al. [HEGRA Collaboration]: 2001, *Astron. Astrophys.*, **375**, 1008.
- Aharonian, F. et al. [HESS Collaboration]: 2005a, *Astron. Astrophys.*, **431**, 197.
- Aharonian, F. et al. [HESS Collaboration]: 2005b, *Astron. Astrophys.*, **437**, L7.
- Aharonian, F. et al. [HESS Collaboration]: 2006a, *Astrophys. J.*, **636**, 777.
- Aharonian, F. et al.: 2006b, *Nature*, **439**, 695.
- Alcaraz, J. et al.: 2000, *Phys. Letter B*, **490**, 27.
- Amenomori, M. et al. [Tibet AS Gamma Collaboration]: 2006, *Advance in Space Research*, **37**, 1932.
- Anders, E. and Grevesse, N.: 1989, *GeCoA*, **53**, 197.
- Asakimori, K. et al. [JACEE Collaboration]: 1998, *Astrophys. J.*, **502**, 278.
- Asplund, M., Lambert, D. L., Nissen, P. E., Primas, F. and Smith, V. V.: 2006, *Astrophys. J.*, **644**, 229.
- Atkins, R. W. et al. [Milagro Collaboration]: 2003, *Astrophys. J.*, **595**, 803.
- Atkins, R. W. et al. [Milagro Collaboration]: 2004, *Astrophys. J.*, **608**, 680.
- Atkins, R. W. et al. [Milagro Collaboration]: 2005, *PRL*, **95**, 251103.
- Baade, W. and Zwicky, F.: 1934, *Proceedings of the National Academy of Science*, **20**, 259.
- Baixeras, C.: 2003, *Nucl. Phys. B Proceedings Supplements*, **114**, 247.
- Bates, B., Catney, M. G. and Keenan, F. P.: 1988, *Ap&SS*, **146**, 195.
- Beacom, J. F. and Candia, J.: 2004, *Journal of Cosmology and Astro-Particle Physics*, **11**, 9.
- Berezhko, E. G. and Volk, H. J.: 2000, *Astrophys. J.*, **540**, 923.
- Berezhko, E. G. and Volk, H. J.: 2004, *Astrophys. J.*, **611**, 12.
- Bergstrom, L., Edsjo, J., Gustafsson, M. and Salati, P.: 2006, *Journal of Cosmology and Astroparticle Physics*, **05**, 006.
- Berrington, R. C. and Dermer, C. D.: 2003, *Astrophys. J.*, **594**, 709.
- Bethe, H. A.: 1930, *Annalen der Physik*, **5**, 325.
- Bird, D. J. et al.: 1994, *Astrophys. J.*, **424**, 491.
- Blandford, R. and Eichler, D.: 1987, *Phys. Rep.*, **154**, 1.
- Blasi, P.: 2004, *Astroparticle Physics*, **21**, 45.
- Blattnig, S. R., Swaminathan, S. R., Kruger, A. T., Ngom, M. and Norbury, J. W.: 2000, *Phys. Rev. D*, **62**, 094030.
- Blitz, L., Spergel, D. N., Teuben, P. J., Hartmann, D. and Burton, W. B.: 1999, *Astrophys. J.*, **514**, 818.
- Boezio, M. et al.: 2003, *Astroparticle Physics*, **19**, 583.
- Bonifacio, P. et al.: 2002, *Astron. Astrophys.*, **390**, 91.
- Borione, A. et al. [CASA-MIA Collaboration]: 1998, *Astrophys. J.*, **493**, 175.
- Bothe, W. and Kolhorster, W.: 1929, *Zeitschrift fur Physik*, **56**, 751.
- Braun, R. and Burton, W. B.: 1999, *Astron. Astrophys.*, **341**, 437.
- Bregman, J. N.: 1980, *Astrophys. J.*, **236**, 577.

- Buckley, J. H. et al. [Whipple Collaboration]: 1998, *Astron. Astrophys.*, **329**, 639.
- Burbidge, E. M., Burbidge, G. R., Fowler, W. A. and Hoyle, F.: 1957, *Reviews of modern Physics*, **29**, 547.
- Candia, J. : 2005, *Journal of Cosmology and Astro-Particle Physics*, **11**, 2.
- Cassé, M., Vangioni-Flam, E. and Audouze, J.: 2001, Cosmic Evolution, World Scientific.
- Cillis, A. N. and Hartman, R. C.: 2005, *Astrophys. J.*, **621**, 291.
- Cole, S. et al.: 2001, *Mon. Not. R. Astron. Soc.*, **326**, 255.
- Cyburrt, R. H., Ellis, J., Fields, B. D. and Olive, K. A.: 2003a, *Phys. Rev. D*, **67**, 103521.
- Cyburrt, R. H., Fields, B. D. and Olive, K. A.: 2003b, *Phys. Letters B*, **567**, 227.
- Cyburrt, R. H., Fields, B. D. and Olive, K. A.: 2004, *Phys. Rev. D*, **69**, 123519.
- de Boer, W., Sander, C., Zhukov, V., Gladyshev, A. V. and Kazakov, D. I.: 2005, *Astron. Astrophys.*, **444**, 51.
- Dermer, C. D.: 1986, *Astron. Astrophys.*, **157**, 223.
- Dimopoulos, S. , Esmailzadeh, R. , Starkman, G. D. and Hall, L. J.: 1988, *Astrophys. J.*, **330**, 545.
- Ellis, J. , Olive, K. A., and Vangioni, E.: 2005, *Phys. Letters B*, **619**, 30.
- Epstein, R. I., Lattimer, J. M. and Schramm, D. N.: 1976, *Nature*, **263**, 198.
- Fegan, S. J. et al. [Whipple Collaboration]: 2005, *Astrophys. J.*, **624**, 638.
- Fichtel, C. E., Kniffen, D. A. and Hartman, R. C.: 1973, *Astrophys. J.L.*, **186**, L99.
- Fichtel, C. E., Hartman, R. C., Kniffen, D. A., Thompson, D. J., Ogelman, H., Ozel, M. E., Tumer, T. and Bignami, G. F.: 1975, *Astrophys. J.*, **198**, 163.
- Fields, B. D. and Olive, K. A.: 1999a, *Astrophys. J.*, **516**, 797.
- Fields, B. D. and Olive, K. A.: 1999b, *New Astronomy*, **4**, 255.
- Fields, B. D. and Prodanović, T.: 2005, *Astrophys. J.*, **623**, 877.
- Fields, B. D., Olive, K. A., Cassé, M. and Vangioni-Flam, E.: 2001, *Astron. Astrophys.*, **370**, 623.
- Fields, B. D., Daigne, F., Cassé, M. and Vangioni-Flam, E.: 2002, *Astrophys. J.*, **581**, 389.
- Finkbeiner, D. P.: 2004, arXiv:astro-ph/0409027.
- Fong, R., Jones, L. R., Shanks, T., Stevenson, P. R. F., and Strong, A. W.: 1987, *Mon. Not. R. Astron. Soc.*, **224**, 1059.
- Furlanetto, S. and Loeb, A.: 2004, *Astrophys. J.*, **611**, 642.
- Gabici, S. and Blasi, P.: 2003a, *Astrophys. J.*, **583**, 695.
- Gabici, S. and Blasi, P.: 2003b, *Astroparticle Physics*, **19**, 679.
- Gaisser, T. K.: 1990, Cosmic Rays and Particle Physics, Cambridge University Press.
- Gehrels, N. and Michelson, P.: 1999, *Astroparticle Physics*, **11**, 277.
- Geiss, J. and Gloeckler, G.: 1998, *Sp. Sci. Rev.*, **84**, 239.
- Glasmacher, M. A. K. et al. [CASA-MIA Collaboration]: 1999, *Astroparticle Physics*, **10**, 291.
- Gounelle, M., Shu, F. H., Shang, H., Glassgold, A. E., Rehm, K. E. and Lee, T.: 2006, *Astrophys. J.*, **640**, 1163.
- Hartman, R. C. et al. [EGRET Collaboration]: 1999, *Astrophys. J.S.*, **123**, 79.
- Hess, V. F.: 1912, *Phys. Zeitschr.*, **13**, 1084.
- Hunter, S. D. et al.: 1997, *Astrophys. J.*, **481**, 205.
- Jedamzik, K.: 2000, *Phys. Rev. Letters*, **84**, 3248.
- Jones, F. C. and Ellison, D. C.: 1991, *Sp. Sci. Rev.*, **58**, 259.
- Kalberla, P. M. W., Burton, W. B., Hartmann, D., Arnal, E. M., Bajaja, E., Morras, R. P. and Poppel, W. G. L.: 2005, *Astron. Astrophys.*, **440**, 775.
- Kamae, T., Abe, T. and Koi, T.: 2005, *Astrophys. J.*, **620**, 244.
- Kang, H. and Jones, T. W.: 2002, *Journal of Korean Astronomical Society*, **35**, 159.
- Kang, H., Jones, T. W. and Gieseler, U. D.: 2002, *Astrophys. J.*, **579**, 337.
- Kawasaki, M., Kohri, K. and Moroi, T.: 2001, *Phys. Rev. D*, **63**, 103502.
- Kawasaki, M., Kohri, K. and Moroi, T.: 2005, *Phys. Letters B*, **625**, 7.
- Kelley, J. L. et al. [IceCube Collaboration]: 2005, *International Cosmic Ray Conference*, **5**, 127.

- Keshet, U. et al.: 2003, *Astrophys. J.*, **585**, 128.
- Keshet, U., Waxman, E. and Loeb, A.: 2004, *Journal of Cosmology and Astroparticle Physics*, **04**, 006.
- Knauth, D. C., Federman, S. R. and Lambert, D. L.: 2003, *Astrophys. J.*, **586**, 268.
- Kneller, J. P.: 2006, private communication.
- Kneller, J. P., Phillips, J. R. and Walker, T. P.: 2003, *Astrophys. J.*, **589**, 217.
- Kniffen, D. A.: 1996, *A&AS*, **120**, 615.
- Kraushaar, W. L., Clark, G. W., Garmire, G. P., Borken, R., Higbie, P., Leong, V. and Thorsos, T.: 1972, *Astrophys. J.*, **177**, 341.
- Kusakabe, M., Kajino, T. and Mathews, G. J.: 2006, *Phys. Rev. D*, **74**, 023526.
- LeBohec, S. et al. [Whipple Collaboration]: 2000, *Astrophys. J.*, **539**, 209.
- Levine, E. S., Blitz, L. and Heiles, C.: 2006, *Astrophys. J.*, **643**, 881.
- Loeb, A. and Waxman, E.: 2000, *Nature*, **405**, 156.
- Lopez, S., Reimers, D., D'Odorico, S. and Prochaska, J. X.: 2002, *Astron. Astrophys.*, **385**, 778.
- Madau, P. and Phinney, E. S.: 1996, *Astrophys. J.*, **456**, 124.
- McCall, B. J. et al.: 2003, *Nature*, **422**, 500.
- McKee, C. F.: 1989, *Astrophys. J.*, **345**, 782.
- Meneguzzi, M., Audouze, J. and Reeves, H.: 1971, *Astron. Astrophys.*, **15**, 337.
- Mercer, D. J. et al.: 2001, *Phys. Rev. C*, **63**, 65805.
- Michelson, P. F.: 2001, *AIP Conference Proceedings*, **587**, 713.
- Miniati, F.: 2002, *Mon. Not. R. Astron. Soc.*, **337**, 199.
- Miniati, F. et al.: 2000, *Astrophys. J.*, **542**, 608.
- Montmerle, T.: 1977a, *Astrophys. J.*, **216**, 177.
- Montmerle, T.: 1977b, *Astrophys. J.*, **216**, 620.
- Montmerle, T.: 1977c, *Astrophys. J.*, **217**, 878.
- Moskalenko, I. V., Porter, T. A. and Strong, A. W.: 2006, *Astrophys. J.*, **640**, 155L.
- Mukherjee, R. and Chiang, J.: 1999, *Astroparticle Physics*, **11**, 213.
- Nakamura, K. and Shigeyama, T.: 2004, *Astrophys. J.*, **610**, 888.
- Nemethy, P.: 2005, private communication.
- Olive, K. A., Steigman, G. and Walker, T. P.: 2000, *Phys. Rep.*, **333**, 389.
- Oort, J. H.: 1970, *Astron. Astrophys.*, **7**, 381.
- Pavlidou, V. and Fields, B. D.: 2002, *Astrophys. J.L.*, **575**, L5.
- Pfrommer, C. and Enßlin, T. A.: 2004, *Astron. Astrophys.*, **413**, 17.
- Pohl, M. and Esposito, J. A.: 1998, *Astrophys. J.*, **507**, 327.
- Prantzos, N.: 2006, *Astron. Astrophys.*, **448**, 665.
- Prodanović, T. and Fields, B. D.: 2003, *Astrophys. J.*, **597**, 48.
- Prodanović, T. and Fields, B. D.: 2004a, *Astroparticle Physics*, **21**, 627.
- Prodanović, T. and Fields, B. D.: 2004b, *Astrophys. J.L.*, **616**, L115.
- Prodanović, T. and Fields, B. D.: 2006, *Astrophys. J.L.*, **645**, L125.
- Prodanović, T., Fields, B. D. and Beacom, J. F.: 2007, *Astroparticle Physics*, **27**, 10.
- Ramaty, R. and Lingenfelter, R. E.: 1999, *LiBeB Cosmic Rays, and Related X- and Gamma-Rays*, **171**, 104.
- Ramaty, R., Scully, S. T., Lingenfelter, R. E. and Kozlovsky, B.: 2000, *Astrophys. J.*, **534**, 747.
- Reeves, H., Fowler, W. A. and Hoyle, F.: 1970, *Nature*, **226**, 727.
- Romano, D., Matteucci, F., Ventura, P. and D'Antona, F.: 2001, *Astron. Astrophys.*, **374**, 646.
- Ryan, S. G. et al.: 2000, *Astrophys. J.L.*, **530**, L57.
- Ryu, D., Kang, H., Hallman, E. and Jones, T. W.: 2003, *Astrophys. J.*, **593**, 599.
- Sackmann, I. J. and Boothroyd, A. I.: 1999, *Astrophys. J.*, **510**, 217.
- Salamon, M. H. and Stecker, F. W.: 1998, *Astrophys. J.*, **493**, 547.
- Sanuki, T. et al.: 2000, *Astrophys. J.*, **545**, 1135.
- Schatz, G.: 2006, private communication.

- Schatz, G. et al. [KASCADE Collaboration]: 2003, *International Cosmic Ray Conference*, **4**, 2293.
- Sembach, C. R.: 2004, *Astrophys. J.S.*, **150**, 387.
- Shapiro, P. R. and Field, G. B.: 1976, *Astrophys. J.*, **205**, 762.
- Spiegel, D. N. et al.: 2003, *Astrophys. J.S.*, **148**, 175.
- Spite, M. and Spite, F.: 1982, *Nature*, **297**, 483.
- Sreekumar, P. et al.: 1998, *Astrophys. J.*, **494**, 523.
- Stecker, F. W.: 1969, *Astrophys. J.*, **157**, 507.
- Stecker, F. W.: 1970, *Ap&SS*, **6**, 377.
- Stecker, F. W.: 1971, Cosmic Gamma Rays, NASA SP-249, Washington D. C.
- Stecker, F. W. and Salamon, M. H.: 1996, *Astrophys. J.*, **464**, 600.
- Steigman, G. and Walker, T. P.: 1992, *Astrophys. J.L.*, **385**, L13.
- Stephens, S. A. and Badhwar, G. D.: 1981, *Ap&SS*, **76**, 213.
- Strong, A. W. and Mattox, J. R.: 1996, *Astron. Astrophys.*, **308**, L21.
- Strong, A. W., Moskalenko, I. V. and Reimer, O.: 2000, *Astrophys. J.*, **537**, 763.
- Strong, A. W., Moskalenko, I. V. and Reimer, O.: 2003, *International Cosmic ray Conference*, **5**, 2687.
- Strong, A. W., Moskalenko, I. V., Reimer, O., Digel, S. and Diehl, R.: 2004a, *Astron. Astrophys.*, **422**, L47.
- Strong, A. W., Moskalenko, I. V. and Reimer, O.: 2004b, *Astrophys. J.*, **613**, 956.
- Strong, A. W., Moskalenko, I. V. and Reimer, O.: 2004c, *Astrophys. J.*, **613**, 962.
- Suzuki, T. K. and Inoue, S.: 2002, *Astrophys. J.*, **573**, 168.
- Totani, T. and Inoue, S.: 2002, *Astroparticle Physics*, **17**, 79.
- Traub, W. A. and Carleton, N. P.: 1973, *Astrophys. J.L.*, **184**, L11.
- Tripp, T. M. et al.: 2003, *Astron. J.*, **125**, 3122.
- vanden Bout, P. A., Snell, R. L., Vogt, S. S. and Tull, R. G.: 1978, *Astrophys. J.*, **221**, 598.
- Vangioni-Flam, E. and Cassé, M.: 2001, *New Astronomy Review*, **45**, 583.
- Vangioni-Flam, E., Ramaty, R., Olive, K. A. and Cassé, M.: 1998, *Astron. Astrophys.*, **337**, 714.
- Vangioni-Flam, E., Cassé, M., R. Cayrel, M. S., Audouze, J. and Spite, F.: 1999, *New Astronomy*, **4**, 245.
- Wakker, B. P.: 2001, *Astrophys. J.S.*, **136**, 463.
- Wakker, B. P. and vanWoerden, H.: 1997, *Annu. Rev. Astron. Astrophys.*, **35**, 217.
- Waxman, E. and Bahcall, J.: 1999, *Phys. Rev. D*, **59**, 023002.
- Weekes, T. C. et al. [VERITAS Collaboration]: 2002, *Astroparticle Physics*, **17**, 221.
- Woodsley, S. E., Hartmann, D. H., Hoffman, R. D. and Haxton, W. C.: 1990, *Astrophys. J.*, **356**, 272.
- Yoshida, T., Terasawa, M., Kajino, T. and Sumiyoshi, K.: 2004, *Astrophys. J.*, **600**, 204.
- Zalzarriaga, M. and Loeb, A.: 2002, *Astrophys. J.*, **564**, 52.